European Heart Journal – Cardiovascular Imaging
doi:10.1093/ehjci/jew025

REVIEW

Recommendations for the imaging assessment of prosthetic heart valves: a report from the European Association of Cardiovascular Imaging endorsed by the Chinese Society of Echocardiography, the Inter-American Society of Echocardiography, and the Brazilian Department of Cardiovascular Imaging†

Patrizio Lancellotti[1,2]*, Philippe Pibarot[3,4], John Chambers[5], Thor Edvardsen[6], Victoria Delgado[7], Raluca Dulgheru[1], Mauro Pepi[8], Bernard Cosyns[9], Mark R. Dweck[10], Madalina Garbi[11], Julien Magne[12,13], Koen Nieman[14,15], Raphael Rosenhek[16], Anne Bernard[17,18], Jorge Lowenstein[19], Marcelo Luiz Campos Vieira[20,21], Arnaldo Rabischoffsky[22], Rodrigo Hernández Vyhmeister[23], Xiao Zhou[24], Yun Zhang[25], Jose-Luis Zamorano[26], and Gilbert Habib[27,28]

[1]Department of Cardiology, GIGA-Cardiovascular Sciences, University of Liège Hospital, Liège, Belgium; [2]Gruppo Villa Maria Care and Research, Anthea Hospital, Bari, Italy; [3]Québec Heart and Lung Institute/Institut Universitaire de Cardiology et de Pneumologie de Québec, Québec, Canada; [4]Department of Cardiology, Laval University and Canada Research Chair in Valvular Heart Disease, Québec, Canada; [5]Guy's and St Thomas' Hospitals, London, UK; [6]Department of Cardiology, Oslo University Hospital, Rikshospitalet and University of Oslo, Oslo, Norway; [7]Department of Cardiology, Heart Lung Center Leiden University Medical Center, Leiden, The Netherlands; [8]Centro Cardiologico Monzino, IRCCS, Milan, Italy; [9]Cardiology, Centrum voor Hart en Vaatziekten, UZ Brussel, Bruxelles, Belgium; [10]BHF/University Centre for Cardiovascular Science, University of Edinburgh, Edinburgh, UK; [11]King's Health Partners, King's College Hospital NHS Foundation Trust, London, UK; [12]CHU Limoges, Hôpital Dupuytren, Service Cardiologie, Limoges F-87042, France; [13]INSERM 1094, Faculté de médecine de Limoges, 2, rue Marcland, 87000 Limoges, France; [14]Department of Cardiology, Erasmus MC, Rotterdam, The Netherlands; [15]Department of Radiology, Erasmus MC, Rotterdam, The Netherlands; [16]Department of Cardiology, Medical University of Vienna, Vienna, Austria; [17]Cardiology department, CHRU de Tours, F-37000 Tours, France; [18]François Rabelais University, Faculty of Medicine, F-37000 Tours, France; [19]Servicio Cardiodiagnostico Investigaciones Médicas de Buenos Aires, Argentina; [20]Heart Institute (InCor), São Paulo University Medical School, São Paulo, Brazil; [21]Hospital Israelita Albert Einstein, São Paulo, Brazil; [22]Hospital Pro Cardíaco Echocardiography Department Coordinator, Rio de Janeiro, Brazil; [23]Hospital Fuerza Aérea de Chile, Cardiología Clínica Las Condes, Valparaíso University, Valparaíso, Chile; [24]Cardiology, Chinese PLA General Hospital in Beijing, China; [25]Shandong University Qilu Hospital in Jinan, Shandong, China; [26]University Alcala de Henares, Hospital Ramon y Cajal, Madrid, Spain; [27]Aix-Marseille Université, 13005 - Marseille, France; and [28]Cardiology Department, APHM, La Timone Hospital, 13005 - Marseille, France

Received 6 January 2016; accepted after revision 7 January 2016

Prosthetic heart valve (PHV) dysfunction is rare but potentially life-threatening. Although often challenging, establishing the exact cause of PHV dysfunction is essential to determine the appropriate treatment strategy. In clinical practice, a comprehensive approach that integrates several parameters of valve morphology and function assessed with 2D/3D transthoracic and transoesophageal echocardiography is a key to appropriately detect and quantitate PHV dysfunction. Cinefluoroscopy, multidetector computed tomography, cardiac magnetic resonance imaging, and to a lesser extent, nuclear imaging are complementary tools for the diagnosis and management of PHV complications. The present document provides recommendations for the use of multimodality imaging in the assessment of PHVs.

Keywords echocardiography • cardiac magnetic resonance • cinefluoroscopy • computed tomography • nuclear imaging • prosthetic heart valve

* Corresponding author. Tel: +32 4 366 71 94; Fax: +32 4 366 71 95. E-mail: plancellotti@chu.ulg.ac.be

† Endorsed by the Chinese Society of Echocardiography, the Inter-American Society of Echocardiography, and the Brazilian Department of Cardiovascular Imaging.

EACVI Documents Reviewers: Nuno Cardim (Portugal), Erwan Donal (France), Maurizio Galderisi (Italy), Kristina H. Haugaa (Norway), Philipp A. Kaufmann (Switzerland), Denisa Muraru (Italy).

Table of contents

Introduction

Valvular heart disease affects >100 million people worldwide and represents a growing problem because of the increasing burden of degenerative valve disease in the ageing population and of the still high incidence of rheumatic heart disease in developing countries.[1] About 4 million prosthetic heart valve (PHV) replacements have been performed over the past 50 years, and this remains the only definitive treatment for most patients with severe valvular heart disease.[2] The total number of replacements is projected to be 850 000 per year by 2050.[3]

PHV dysfunction is rare but potentially life-threatening. Although often challenging, establishing the exact cause of PHV dysfunction is essential to determine the appropriate treatment strategy.[4,5] In clinical practice, a comprehensive approach that integrates several parameters of valve morphology and function assessed with 2D/3D transthoracic (TTE) and transoesophageal (TOE) echocardiography is a key to appropriately detect and quantitate PHV dysfunction. Cinefluoroscopy, multidetector computed tomography (CT), cardiac magnetic resonance imaging (CMR), and to a lesser extent, nuclear imaging are complementary tools for the diagnosis and management of PHV complications.[4,5] The present document provides recommendations for the use of multimodality imaging in the assessment of PHVs.

Types of PHVs

A number of valve designs have been withdrawn or are currently implanted only rarely. However, these may still require imaging either as routine or on the suspicion of malfunction. Replacement valves are broadly grouped as biological or mechanical (*Table 1*).[6,7]

Table 1 Types of prosthetic heart valves

Biological
Stented
Porcine bioprosthesis
Pericardial bioprosthesis
Stentless
Porcine bioprosthesis
Pericardial bioprosthesis
Aortic homograft
Pulmonary autograft (Ross procedure)
Sutureless
Transcatheter
Mechanical
Bileaflet
Single tilting disk
Caged ball

Table 2 Designs and models of biological replacement heart valve

Stented porcine replacement valve
- Hancock standard and Hancock II
- Medtronic Mosaic[a]
- Carpentier-Edwards standard and supra-annular
- St Jude Medical Biocor, Bioimplant, Epic
- AorTech Aspire
- Labcor
- Carbomedics Synergy

Stentless valve Porcine
- St Jude Medical Toronto[a]
- Medtronic Freestyle
- Cryolife-O'Brien[a]
- Cryolife-Ross Stentless porcine pulmonary
- Edwards Prima Plus
- AorTech Aspire
- St Jude Biocor
- Labcor
- St Jude Quattro stentless mitral
- Shelhigh Skeletorized Super-Stentless aortic porcine and pulmonic
- Medtronic-Venpro Contegra pulmonary valve conduit

Stented pericardial replacement valve
- Carpentier-Edwards Perimount
- Carpentier Edwards Magna
- Mitroflow Synergy
- St Jude Biocor pericardia
- St Jude Trifecta
- Labcor pericardial
- Sorin Pericarbon MORE[a]

Stentless pericardial
- Sorin Pericarbon
- 3F-SAVR
- Freedom Solo

Sutureless
- Perceval S (Sorin)
- Edwards Intuity (Edwards Lifesciences)
- 3F Enable (ATS Medical)
- Trilogy (Arbor Surgical Technologies)

[a]Indicates withdrawn from market.

The most frequently implanted biological valve is a stented bioprosthesis. These are composed of fabric-covered polymer or wire stents with a sewing ring outside and the valve inside. The valve may be a whole porcine valve (*Table 2*) (e.g. Carpentier-Edwards standard or Hancock standard). However, there is a muscle bar at the base of the porcine right coronary cusp, which can make it relatively obstructive. This cusp may therefore be excised and replaced by a single cusp from another pig (e.g. Hancock Modified Orifice), or more frequently, each cusp may be taken from three different pigs to produce a tricomposite valve (e.g. Medtronic Mosaic, St Jude Epic or Carbomedics Synergy). Stented pericardial bioprostheses have cusps made from pericardium (*Table 2*) or a sheet of pericardium cut using a template and sewn inside the stent posts or occasionally to the outside of the stent posts (e.g. Mitroflow, Trifecta). Usually the pericardium is bovine, but occasionally porcine and, experimentally, from kangaroos. The bioprostheses also differ in the method of preservation of the valve cusps, the use of anticalcification regimes, and the composition and design of the stents and sewing ring.

Stentless bioprosthetic valves usually consist of a preparation of porcine aorta. The aorta may be relatively long (e.g., Medtronic Freestyle) or may be sculpted to fit under the coronary arteries (e.g., St Jude Medical Toronto). Some are tricomposite (e.g. Cryolife-O'Brien, Biocor) or made from bovine pericardium (e.g. Sorin Freedom) (*Table 2*). Homograft valves consist of human aortic or occasionally pulmonary valves, which are usually cryopreserved. They have good durability if harvested early after death and do not need anticoagulation. For this reason, they may be used as an alternative to a mechanical valve in the young. They may also be used for choice in the presence of endocarditis since they allow wide clearance of infection with replacement of the aortic root and valve and the possibility of using the attached flap of donor mitral leaflet to repair perforations in the base of the recipient's anterior mitral leaflet. The stentless valves were introduced to increase the orifice area available for flow. It was also hoped that stresses on the cusps might be lessened leading to better durability and that some stent-related complications such as valve thrombosis might be less frequent.

The Ross Procedure consists of substituting the patient's diseased aortic valve by his own pulmonary valve.[8] Usually a homograft is then implanted in the pulmonary position. It is an infrequently performed operation requiring extensive training. It is justified because a living valve is placed in the systemic side allowing good durability. It is therefore an alternative in younger patients who do not wish to take regular anticoagulation. The autograft may grow which makes it particularly appropriate for children to reduce the need for repeat operations during growth. It is likely to resist infection better than valves, which include non-biological material and may also be used for preference in patients with infective endocarditis.

Sutureless valves (*Table 2*) were developed in the hope of reducing bypass times in patients at high risk from conventional surgery and to facilitate a minimally invasive approach.[9]

Transcatheter valves are a relatively new technology for patients at high risk for conventional valve replacement or in whom thoracotomy is not feasible or appropriate for technical reasons: e.g. porcelain aorta or when there is a left internal mammary graft crossing the midline.[10] These are the subjects of separate guidelines.[11]

The most frequently implanted mechanical valves are now the bileaflet mechanical valves (*Table 3*). The various designs differ in the composition and purity of the pyrolytic carbon, in the shape and opening angle of the leaflets, the design of the pivots, the size and shape of the housing, and the design of the sewing ring. For example, the St Jude Medical valve has a deep housing with pivots contained on flanges, which may sometimes obscure the leaflets on echocardiography, while the Carbomedics standard valve has a shorter housing allowing the leaflet tips to be imaged more clearly. Single tilting disk valves and occasionally the Starr-Edwards caged-ball valve are also used.

Table 3 Designs and models of mechanical replacement heart valve

Bileaflet mechanical replacement valves	Tilting disk replacement valves
• St Jude Medical: standard, HP, Masters, and Regent	• Bjork-Shiley monostrut[a]
• Carbomedics: standard, reduced cuff, Optiform, Orbis, and supra-annular (Top Hat) Carboseal includes a woven aortic graft	• Sorin Monoleaflet Allcarbon
• Edwards Tekna	• Medtronic-Hall
• Sorin Bicarbon	• Omnicarbon
• Edwards Mira	• Ultracor
• ATS	Caged ball
• On-X	• Starr-Edwards
• Medtronic Advantage	• Smeloff-Cutter
• Jyros	

[a]Indicates withdrawn from market.

These valve types differ, mainly for the aortic site, by implantation position relative to the annulus. Valves are intra-annular, partially supra-annular or entirely supra-annular. The partially supra-annular valves have a supra-annular sewing ring, but part of the housing within the annulus (e.g. On-X, St Jude HP). Wholly supra-annular valves have all parts of their mechanism above the annulus in the aortic site (e.g. Carbomedics 'Top Hat', Medtronic Mosaic) and occasionally in the mitral position (e.g. Carbomedics Optiform). The supra-annular position is designed to lift as much of the replacement valve above the annulus to maximize the orifice area available for flow. The maximum label size implantable may then be limited by the diameter of the aortic root or the position of the ostium of the right coronary artery.

Comparison of the different valve types is difficult because of major variations in sizing convention.[12] This means that for a given patient tissue annulus, there may be major differences in the label size. In a study[13] comparing valve label size against a modelled tissue annulus provided by machined polypropylene blocks, the 'tissue annulus' diameter ranged from 3.5 mm smaller to 3.0 mm larger than the labelled size.

Table 4 Essential parameters in the comprehensive evaluation of prosthetic valve function

	Parameters
Clinical information	• Date of valve replacement • Type and size of the prosthetic valve • Height, weight, body surface area, and body mass index • Symptoms and related clinical findings • Blood pressure and heart rate
Imaging of the valves	• Motion of cusps, leaflets, or occluder • Presence of calcification or abnormal structures on the various components of the prosthesis • Valve sewing ring integrity and motion
Doppler assessment of the valve	• Spectral Doppler envelope • Peak velocity and gradient • Mean pressure gradient • Doppler signal velocity time integral (VTI) • Doppler velocity index (DVI) • Pressure half time in mitral and tricuspid valve • Effective orifice area (EOA) • Presence, location, and severity of regurgitation
Other imaging data	• LV and RV size, function, and hypertrophy • LA and RA size • Co-existent valvular disease • Estimation of pulmonary artery pressure
Previous post-operative studies, when available	• Comparison of above parameters in suspected prosthetic valvular dysfunction

EOA, effective orifice area; LA, left atrial; LV, left ventricle; RA, right atrial. Adapted from Zoghbi *et al.*[14]

Echocardiographic assessment

2D and Doppler echocardiography are essential for initial and longitudinal assessment of patients with PHV.[14] Although such evaluation follows the same principles as for native heart valves, the echocardiographic examination of PHV is more challenging. At the time of echocardiography, it is essential to know and document (i) the reason for the echo study; (ii) the patient's symptoms; (iii) the type and size of the PHV; (iv) the date of surgery; (v) the blood pressure and heart rate; and (vi) the patient's height, weight, and body surface area (*Table 4*). A comprehensive echocardiographic study is indicated in case of new murmur or any symptoms possibly related to PHV. When obtained early after hospital discharge, it can serve to define baseline PHV characteristics ('fingerprint').

2D echocardiographic examination

2D TTE is recommended as first-line imaging in PHV.[7,14] A 2D TOE is more likely to be needed for the evaluation of PHV structure and associated complications.[15] It is advocated in all cases of PHV dysfunction.[16,17]

The complete echocardiographic imaging of the PHV includes the use of multiple views (conventional parasternal and apical TTE views or mid-oesophageal 2-3-4-chamber, commissural, and transgastric TOE views and off-axis views) with attention to determine the type of prosthesis, confirm the adequate valve leaflet/occluder morphology and mobility, check the integrity and stability of the sewing ring (any rocking motion), identify the presence of calcification or abnormal structures on any of the various components of the PHV, assess the size of cardiac chambers, the LV wall thickness and mass, the indices of LV systolic and diastolic function, and the systolic pulmonary arterial pressure (SPAP). Additional findings such as the aortic root and ascending aorta should be evaluated in case of aortic PHV (*Table 5*).

Magnification of real-time 2D images is often necessary for optimal visualization. M-mode enables better evaluation of valve movements (assessment of the brisk opening and closing and the degree

Table 5 Imaging modalities: advantages and limitations

	Technical considerations	Advantages	Limitations
2D TTE	• Multiple views • Careful probe angulation (alignment) for accurate leaflet motion display	• First-line imaging • Ease of use • Assessment of LV function and size and pulmonary pressure	• Limited by acoustic window and body habitus • Acoustic shadowing by prosthetic material • Angle dependent on accuracy of Doppler data
2D TOE	• Multiple views • Careful probe angulation (alignment) for accurate leaflet motion display	• Higher resolution than TTE • Proximity of the oesophagus with the heart • Better visualization of the atrial side of mitral PHV and posterior part of aortic PHV • Better visualization of peri-annular complications	• Acoustic shadowing by prosthetic material • Angle dependent on accuracy of Doppler data
3D TOE	• Multiple cropping planes • Narrow angle mode/Oblique views • Full-volume dataset • Zoom mode	• Ease of use • Excellent spatial imaging • Enable enface viewing (surgical view) • Add on to 2D echo imaging	• Poor visualization of anterior cardiac structure • Poor temporal resolution • Tissue dropout • Lack of tissue characterization • Artefacts due to an oblique (rather than horizontal) orientation of PHVs in mitral position
Cinefluoroscopy	• Postero-anterior (0°) and lateral (90°) projections • '*in profile*' projection (beam parallel to both the valve ring plane and the tilting axis of discs) • '*en face*' projection (beam parallel to the valve outflow tract)	• Ease of use • Evaluation of PHV functioning • Detection of calcium on the leaflets	• No haemodynamic assessment • No clues about the aetiology of limited disc motion
Cardiac CT	• Wider exposure windows and multiphasic reconstructions for assessment of valve mobility • Double oblique planes (short- and long-axis views)	• 3D data set • Not limited by body habitus • Good for aortic pathology • High sensitivity for detection of calcification • Allows visualization/differentiation of thrombus and pannus • Excellent spatial imaging	• Radiation exposure • Potentially nephrotoxic contrast • Contrast allergies • Artefacts from metallic objects
CMR	• T_1-weighted spin echo and gradient echo sequences (steady-state free-precession and fast gradient echo) • Phase-contrast sequences	• Good for aortic pathology (even without contrast) • No ionizing radiation • Myocardial characterization	• Artefacts from metallic objects • Limited data in prosthetic valves • Limited spatial and temporal resolution
Nuclear imaging	• Different tracers to image inflammation, calcification, or metabolism	• Extent of local infectious/metabolic activity • Identify extracardiac infection/ metabolic activity	• Radiation exposure • Limited data in prosthetic valves, except in infective endocarditis

of excursion of the occluder) and corresponding time intervals and recognition of quick movements. Prosthetic disc motion is better evaluated in the mitral position since opening and closing angles can be identified in 77 and 100% of patients by TTE and TOE, respectively.[18] On the contrary, in the aortic position, the opening angles (not closing angles) of single disc prostheses are identified in only 40 and 77% of patients by TTE and TOE, respectively, and for bileaflet mechanical prostheses in 13 and 35%, respectively.[18] Since intermittent cyclic or non-cyclic dysfunction of mechanical prostheses can occur (intermittent increase in transprosthetic gradients), careful examination of the gradients and disc motion during several consecutive beats is recommended.

Doppler echocardiography

The principles of flow assessment through PHVs are similar to those used in evaluating native valve, including interrogation from multiple windows and proper alignment of the Doppler beam with flow direction.[19–21] Doppler recordings should be performed at a sweep speed of 100 mm/s. Measurements should be taken over one to three cycles in sinus rhythm. In atrial fibrillation, Doppler measurements should be performed during periods of physiologic heart rate (65–85 bpm), whenever possible; an average of five cycles is recommended. For calculations of valve effective orifice area (EOA) and Doppler velocity index (DVI), which require measurements from

different cardiac cycles, matching the respective cycles lengths to 10% is recommended.[14] Doppler recordings should be obtained in quiet respiration or in mid-expiratory apnoea. TTE is the method of choice for Doppler signal recordings. However, when technically difficult, TOE is indicated.

Colour Doppler echocardiography

Colour Doppler assessment should be performed in multiple windows with appropriate colour Doppler settings (Nyquist limit around 50–60 cm/s). Colour Doppler evaluation enables discriminating physiologic from pathologic flows and between intra- and/or paraprosthetic regurgitation. The origin and direction of the jets should be evaluated. Localization of paravalvular regurgitation may be difficult and the use of multiple transthoracic transducer positions, including off-axis views, is recommended.[20] In this regard, TOE is often necessary, particularly in mitral and tricuspid valves for which it is superior to TTE. TOE remains essential for assessing paravalvular regurgitation.[11,14,15] Regurgitant jets may be occulted by acoustic shadowing.

3D echocardiography

Real-time 3D echocardiography, particularly during TOE, is suitable for the evaluation of PHVs and provides incremental advantage over 2D imaging.[22,23] The 3D 'en-face' surgical view of the valve is extremely helpful for determining PHV function and defining the presence, origin, direction, and extension of regurgitant jets.[11,24–27] Leaks are defined by 3D echocardiography as echo dropout areas outside the sewing ring confirmed by colour Doppler. 3D echocardiography allows advantageous visualization of PHV components such as the leaflets, rings, and struts (leaflets or disc material support), irrespective of the position. The presence and localization of thrombus formation, pannus, and prosthetic valve dehiscence can be evaluated by 3D echocardiography.[28–33] This is especially useful for the assessment of mechanical mitral and aortic valves where 2D images are often of poor quality due to acoustic shadowing. With 3D imaging, the ventricular side of mitral prosthetic valves, which is consistently prevented with 2D imaging, can be often visualized.[27]

After locating the best plane for imaging the PHV by standard 2D images, narrow-angled acquisition mode, 3D zoom mode, full-volume acquisition (single or multi-beat with ECG gating) with and without colour Doppler can be performed. Once the 3D data sets are acquired, they can be cropped to optimally visualize cardiac structures. By convention, the mitral valve image, as viewed from the left atrial perspective, is rotated to position the aortic valve at 12 and the left atrial appendage at 9 o'clock.[11,26] A 5 o'clock is assigned to the commissure between the left and right coronary sinuses, and 8 o'clock to the commissure between the non-coronary and left coronary sinuses. Aortic paravalvular leaks are more commonly located between the right and non-coronary cusps.[34]

There are a few limitations to 3D imaging such as poor visualization of anterior cardiac structures, poor temporal resolution, suboptimal images due to poor ECG triggering in patients with arrhythmias, and tissue dropout. Traditionally, 3D zoom mode provides images of high spatial resolution at the expense of temporal resolution with frame rates typically <10 Hz. This may hamper the ability to visualize fast moving structures such as vegetations and the dynamic behaviour of mitral rings. Anterior cardiac structures such as the aortic and tricuspid leaflets due to their increased distance from the TOE probe cannot be visualized as well as posterior structures such as the posterior mitral valve leaflet.[11,26]

Stress echocardiography

Stress echocardiography is a valuable tool for the evaluation of PHVs haemodynamic function, especially when there is discordance between the patient's symptomatic status and the PHVs haemodynamics.[4,5,11,35] In patients with no, mild, or equivocal symptoms, the preferred modality is exercise stress echocardiography. Semi-supine bicycle exercise test is technically easier than upright bicycle or post-treadmill, especially when multiple stress parameters are assessed at the peak level of exercise. A low dose (up to 20 μg/kg/min) dobutamine stress echocardiography can be used in patients with moderate or severe symptoms or when an exercise test is impossible. Details about stress echocardiography protocols are provided elsewhere.[36,37]

Key points

2D TTE is recommended as first-line imaging in PHV. TTE is also the method of choice for Doppler signal recordings. Both TTE and TOE are needed for complete evaluation in a patient with suspected PHV dysfunction. 3D echocardiography, especially with TOE, can provide additional information and is increasingly used. For both TTE and TOE, it is essential to obtain images in multiple views and multiple planes to ensure complete visualization of the valvular and paravalvular region. TTE/TOE has higher sensitivity in mitral than aortic position for examining disc valve motion. For the evaluation of PHV regurgitation, TOE is superior in mitral/tricuspid position while TTE is better in aortic position. TOE, especially when completed by 3D evaluation, remains superior for assessing paravalvular regurgitation.

Additional imaging modalities

Cinefluoroscopy

Fluoroscopy is an easy and readily available non-invasive technique for evaluating mechanical PHVs. It is mainly indicated in case of abnormally high gradients. The method allows correct identification of the type of implanted prosthesis and evaluation of its functioning.[38–40] Through appropriate projections, valve leaflet mobility, valvular ring motion, or even rupture and/or migration of parts of the valve can be evaluated. Abnormal tilting or rocking of the base ring is indicative of extensive valve dehiscence. This exam does not, however, allow haemodynamic assessment or provide clues about the aetiology of reduced disc mobility.

Generally, cinefluoroscopic study is carried out with the patient in the supine position. PHVs are viewed in three main projections: (i) the postero-anterior (0°) and lateral (90°) projections to identify the '*in situ*' orientation of the valve; (ii) the '*in profile*' projection (with the radiographic beam parallel to both the valve ring plane and the tilting axis of discs), allowing calculation of opening and closing angles and; (iii) the '*en face*' projection (with the radiographic beam

parallel to the valve outflow tract) which is utilized only for mitral prostheses. For all views, due to variability in surgical prosthesis orientation, careful patient positioning and the use of cranio-caudal angulation are frequently required. Of note, cinefluoroscopy provides a better evaluation of the motion of discs in the aortic position than echocardiography.[41]

A short (~10 beats) cinefluoroscopic film in each projection is acquired, from which frames are selected to evaluate and measure the disc motion radius. The opening and closing angles are calculated as the distance between the two leaflets in the fully open and closed positions (*Figure 1A*, *Panel A* and *B*). For single disc prostheses, the opening angle is defined as the distance between the housing and the disc at its fully open position, and for bileaflet disc prostheses as the distance between the leaflets in the fully open position (*Figure 1B*). The method is usually feasible despite poor radio-opacity of some mechanical valves.

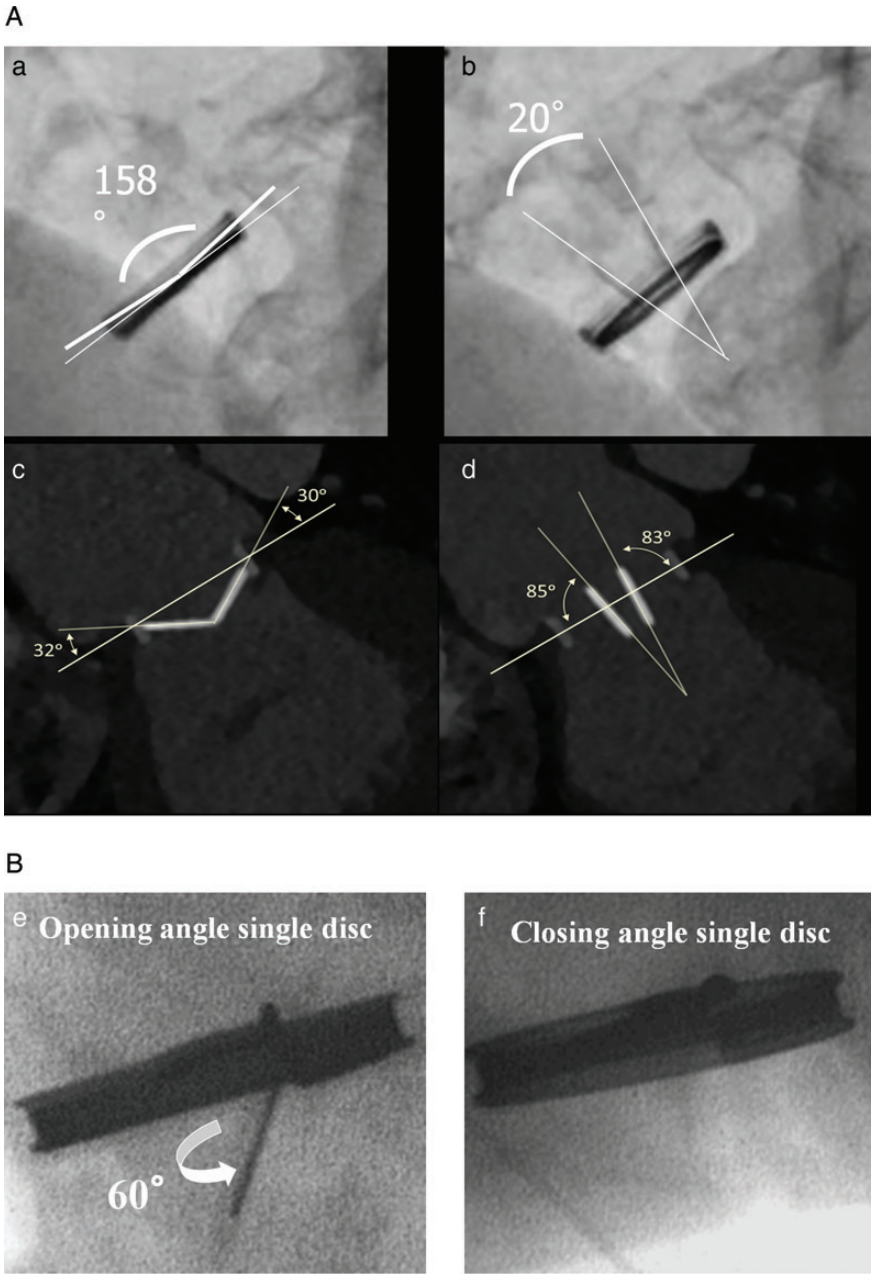

Figure 1 (*A*) Evaluation of closing (*Panels a* and *c*) and opening angles (angle between discs in the fully open and closed positions) (*Panels b* and *d*) of mechanical bileaflet valves as performed using cinefluoroscopy (*Panels a* and *b*) and cardiac computed tomography (Leaflet angles relative to the plane of the orifice ring) (*Panels c* and *d*). (*B*) Evaluation of opening (*Panel e*) and closing angles (*Panel f*) of mechanical tilting disk valve as performed using cinefluoroscopy.

Of note, detection of calcium on the leaflets of a tissue valve is diagnostic of degeneration but does not allow assessment of its hemodynamic impact.

Cardiac computed tomography

Cardiac CT is generally not performed for routine evaluation, but rather when valvular dysfunction or other complications are suspected. It can provide incremental information on valvular mobility, integrity, and (para) valvular pathology (e.g. endocarditis, aneurysmal dilatation, or other involvement of the surrounding tissues).[42,43] CT can be used as an alternative to fluoroscopy for mechanical PHV to measure the opening/closing angles (*Figure 1A*, *Panel C* and *D*) and could be considered for imaging the cusps of biological valves (leaflet thickening, visualization of calcification, or thrombus) if TOE is inconclusive.[44–47] Malcoaptation may be visible, allowing in some cases planimetric quantification of the regurgitant valve orifice. Paravalvular regurgitation may be identified, depending on the size of the defect and the radiopacity of the valve ring.[48,49] Ring dehiscence may be appreciated by a rocking displacement of the valve ring on dynamic CT reconstructions. CT can distinguish thrombus from pannus.[50–54] CT can be used to quantify the severity of stenosis in a bioprosthesis by planimetry of the anatomic orifice area (geometric orifice area, GOA).[45] The morphological consequences of obstructive or regurgitant valve dysfunction can be observed in the form of ventricular or atrial dilatation or stasis of contrast medium suggesting congestion. In preparation for redo surgery, cardiac CT can also be of use to assess the coronary status or the patency of bypass grafts, particularly in younger patients with non-degenerative valvular heart disease.[55,56] To avoid unintended trauma during sternotomy, CT can assess the space between the sternum and the right ventricle. Impingement or injury of the left circumflex coronary artery, though rare, may occur because of its proximity to the annulus, and can be assessed by CT angiography.[57]

Using ECG-synchronized acquisition or reconstruction of data nearly motion-free images (depending on the temporal resolution) with a sub-millimetre isotropic spatial resolution can be acquired and reconstructed in any imaginary cross-sectional plane. If data are acquired throughout the cardiac cycle, then images can be reconstructed representing consecutive cardiac phases, which subsequently allows for assessment of structural displacement. Contrary to real-time echocardiography, dynamic CT reconstructions (repeatedly) display only a single heart cycle. Dynamic assessment of radiopaque mechanical valves does not require injection of contrast medium, similar to cinefluoroscopy. Similarly to coronary CT angiography, pharmacological heart rate modulation may be used.[58] PHVs are visualized best in the fully open or closed positions. Nominal opening angles depend on the type of PHV and sometimes also on its implanted location (*Table 6*).[6,49–51,59] Contrast-enhanced imaging of right-sided valves, particularly the tricuspid valve, is complicated by non-homogeneous opacification when contrast arrives selectively from the superior cava vein. Either the image is acquired during recirculation or contrast is injected at an appropriate timing and proportion simultaneously via an upper and lower limb vessel to improve contrast homogeneity in the right heart.

Disadvantages of cardiac CT are the use of iodine contrast medium and the need for ionizing radiation. Depending on the type of scanner, the selected scan protocol, and the requirement for single- or multiphasic images, the radiation dose varies between ~1 and 20 mSv.[60] Cardiac CT is further limited by its inability to assess flow and haemodynamics. Pledget material adjacent to the valve ring may also be misinterpreted as regurgitation, although the density is often slightly higher than the contrast-enhanced blood.[61]

Cardiovascular magnetic resonance

CMR has been demonstrated to be safe in patients with PHV, in whom it is commonly used to assess concomitant aortic pathology.[62] CMR is an excellent technique for volumetric assessment of cardiac chambers and flows and may be of value for assessing the function of the PHV itself, especially as a complementary method when TTE is non-diagnostic and TOE undesirable.[63–66] CMR can thus be used for valve analysis using steady-state free precession (SSFP) sequences, which precisely discriminate blood from tissue.[67] Turbulent flow through a regurgitant orifice is easily visible with SSFP (visualization of signal voids due to spin dephasing in moving protons).[63,64] PHV anatomy can be imaged by acquisition of standard short-axis, two-, three-, and four-chamber long-axis views in combination with oblique long-axis cines orthogonal to the line of coaptation.[68] Leaflet motion restriction may be identified. GOA may also be measured in bioprosthetic valves.[69] No study has reported on the evaluation of pannus or thrombus using CMR. In some circumstances, assessing the anatomic regurgitant orifice area by planimetry of the regurgitant orifice in a slice parallel to the valvular plane and perpendicular to the regurgitant jet is feasible using SSFP CMR.[70] Furthermore, blood flow and velocity might also be obtained by phase-contrast velocity mapping.[71–73] CMR is thus a useful tool for assessing regurgitation, especially in the follow-up of replacement pulmonary valves. Even though its value has been increasingly proved for the quantitation of regurgitation in native valves and to a lesser degree after transcatheter aortic valve implantation, there are very limited data in patients with surgically implanted PHVs. CMR may also potentially demonstrate abnormal asymmetrical flow patterns in PHV obstruction, although leaflet angle measurements may not always be possible. Late gadolinium enhancement CMR (images obtained 10–20 min after injection of contrast) is widely used to assess cardiac fibrosis in various cardiomyopathies.[74] In patients with PHVs, CMR might serve to evaluate the impact of valve replacement on the myocardial structure. To date, for the heart valves that have been tested, CMR-related heating has not been shown to reach substantial levels.[75–77] Moreover, although CMR provides information on PHV-related flow patterns and velocities, more studies are required to provide diagnostic reference values to allow discrimination of normal from pathological conditions.

Nuclear cardiology

The use of nuclear imaging modalities in the assessment of PHVs is limited. However, recent interest has surrounded the use of 18F-fluorodeoxyglucose positron emission tomography (PET) in the detection of PHV endocarditis,[78] which is not the scope of the present document. Other recent studies suggest that 18F-sodium fluoride PET/CT is able to identify active tissue calcification and predict disease progression in patients with native aortic

Table 6 Mechanical valves: opacification and opening angles

	Prosthesis materials		Open (Degrees)	Closed (Degrees)
	Housing	Occluder		
Caged-ball valves				
Starr-Edwards	Three (aortic) or four-strut (mitral) cobalt-chrome alloy cage	Silicone rubber	N/A	N/A
Tilting disc valves				
Björk–Shiley	Cobalt-chrome alloy	Silicon alloyed pyrolytic carbon on graphite substrate with radio-opaque tantalum marker	60 (<1981) 70 (>1981)	0
Medtronic-Hall	Titanium alloy	Silicon alloyed pyrolytic carbon on tungsten-loaded graphite substrate	75 (aortic) 70 (mitral)	0
Omniscience	Titanium alloy	Silicon alloyed pyrolytic carbon on tungsten-loaded graphite substrate	80	12
Omnicarbon	Pyrolytic carbon over graphite substrate	Silicon alloyed pyrolytic carbon on tungsten-loaded graphite substrate	80	12
Sorin Allcarbon	Cobalt-chromium alloy coated with a thin layer of pyrolytic carbon	Silicon alloyed pyrolytic carbon on tungsten-loaded graphite substrate	60	0
Bileaflet valves				
ATS Medical	Pyrolytic carbon over graphite substrate with metallic band	Silicon alloyed pyrolytic carbon on tungsten-loaded graphite substrate	85	25
Carbomedics	Solid pyrolytic carbon with titanium stiffening ring metallic band	Silicon alloyed pyrolytic carbon on tungsten-loaded graphite substrate	78–80	15
Edwards Tekna (previously Duromedics)	Solid pyrolytic carbon with titanium stiffening ring	Silicon alloyed pyrolytic carbon on tungsten-loaded graphite substrate	73–77	15
St Jude Medical	Pyrolytic carbon over graphite substrate with metallic band	Silicon alloyed pyrolytic carbon on tungsten-loaded graphite substrate	85	30 (19–25 mm) 25 (27–31 mm)
On-X	Pyrolytic carbon with graphite substrate with titanium alloy bands	Pure pyrolytic carbon on tungsten-loaded graphite substrate	85–90	40
Bicarbon	Cobalt-chromium alloy coated with a thin layer of pyrolytic carbon	Silicon alloyed pyrolytic carbon on tungsten-loaded graphite substrate	80	20

Leaflet angles relative to the plane of the orifice ring as provided by the manufacturers. Note that the angles are measured using the same approach by cardiac computed tomography. Conversely, on cinefluoroscopy, opening and closing angle in bileaflet PHVs are defined as the angle between discs in the fully open and closed positions, respectively. This means that the opening angle is the angle between the two discs (generally <30° and in the majority of valves <20°). The closing angle is usually >120°–130°.

stenosis.[79] Further studies are needed to determine whether this technique would be able to identify active mineralization of bioprosthetic valve tissues and thereby predict the risk of structural valve degeneration.

Key points

Non-echo imaging modalities are generally not performed for routine evaluation of PHV, but rather when valvular dysfunction or other complications are suspected. They can provide incremental information on valvular integrity and valvular/paravalvular pathology. Cinefluoroscopy has a complementary role in evaluating disc mobility of mechanical PHVs and valve ring structure. Cardiac CT is also an important adjuvant imaging technique that permits visualization of calcification and degenerative changes of biological prosthesis, pannus formation, the presence of thrombus, and assessment of movement of occluders in mechanical valves. The use of CMR is not yet routine practice but is increasing. Nuclear imaging currently has very limited application in the evaluation of PHV other than in the setting of suspected infective endocarditis.

PHV function and characteristics

Morphologic and functional characteristics

Leaflet motion and occluder mobility

Mechanical PHVs have specific patterns of echoes that can help identify the type of prosthesis.[7,14,80–82] In normal PHVs, the motion is brisk and consistent with each beat. Nominal opening angles depend on the type of PHV and sometimes also on its location (*Table 6*).[39,40,49–51,59]

A 'ball-caged mechanical valve' displays a cage and the moving echo of the ball on the ventricular side. In 2D echo, the metallic struts provide highly reflective echoes. Conversely, the proximal surface of the valve provides less intense echoes. In real time, the poppet moves forward and backward in the cage. For a replacement valve in the mitral position, the poppet is seated in the sewing ring in systole. On M-mode, the cage, the sewing ring, and the ball provide four distinct echoes.

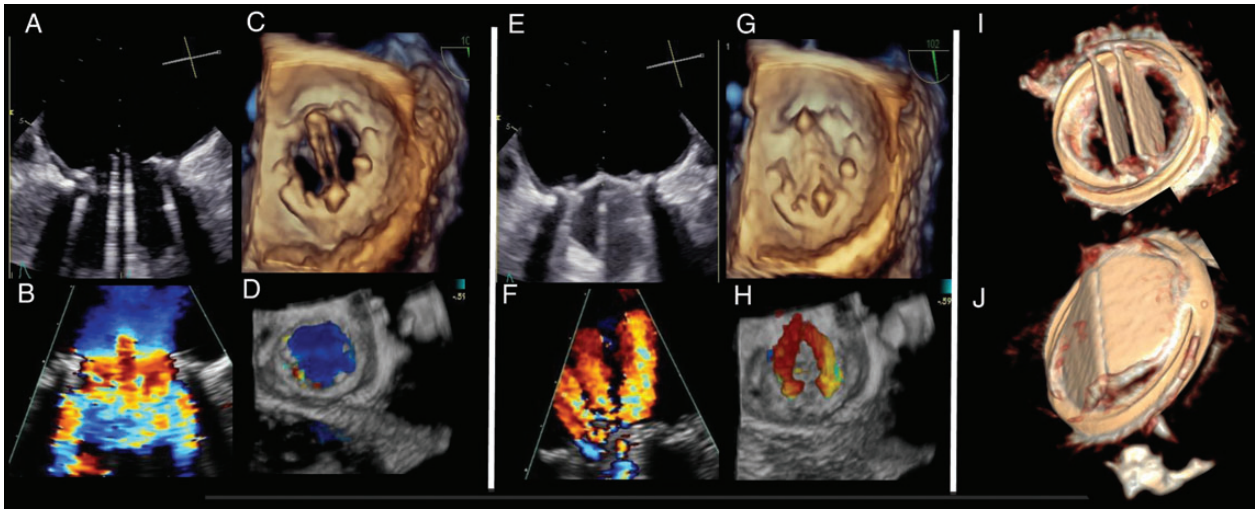

Figure 2 Mechanical valve in mitral position: normal appearance. 2D and 3D transoesophageal echocardiographic (TOE) appearance of a normally functioning mechanical valve in mitral position. (*A*–*D*) 2D and 3D as well as 2D and 3D colour flow appearance of a bileaflet mechanical valve in the opened position from the atrial perspective. Note the two lateral semi-circular orifices and the central slit-like orifice both visible in 2D and 3D TOE. Note the normal anterograde colour flow Doppler and the flow acceleration at the level of the three orifices in 2D TOE (*B*). (*E*–*H*) 2D and 3D as well as 2D and 3D colour flow appearance of a bileaflet mechanical valve in the closed position from the atrial perspective. Note the normal appearance of the retrograde colour flow Doppler showing physiologic 'washing jets' for this type of prosthesis in 2D (*F*) and 3D colour flow imaging (*H*). The volumetric reconstructed cardiac computed tomography scan of the bileaflet valve from the atrial (open, *I*) and ventricular (close, *J*) perspective.

A single echo movement up and down on the ventricular side can be seen with 'tilting disc valve (monoleaflet)'. The opening angle of the disc relative to the valve annulus ranges from 60° to 80° resulting in two orifices of different size. On M-mode, the opening of the valve forms an intense echo with multiple reverberations.

Two separate disks can be visualized in 'bileaflet PHV'; they open and close almost in synchrony. The opening angle of the leaflets relative to the annulus plane ranges from 75° to 90°, with the open valve consisting of three orifices: a smaller, slit-like central orifice between the leaflets, and two larger semi-circular orifices laterally (*Figure 2*).

'Biological valves' have a trileaflet structure, which normally appears thin (1–2 mm) with unrestricted motion and no evidence of prolapse.[1,7,9,83] Their 2D and M-mode appearances reveal a box-like opening in systole in the aortic position and in diastole in mitral or tricuspid position, similar to that of native valves. The sewing ring and the struts (the three struts are shown in the short-axis view in *Figure 3*) are however more echogenic, which can limit the visualization of the leaflets (*Figure 3A* and *B*). Stentless aortic bioprostheses or aortic homografts have a similar appearance to that of native aortic valves, except for an increased thickness in the LV outflow tract and the ascending aorta. Early after implantation, a stentless valve inserted as an inclusion can be surrounded by haematoma and oedema. Sutures are defined as linear, thick, bright, multiple, evenly spaced, usually immobile echoes seen at the periphery of the sewing ring of a PHV; they may be mobile when loose or unusually long. The 3D appearance of biological valve, in any anatomical position, is always similar with the appearance of a native aortic valve, with three cusps, with a larger diameter when used in mitral or tricuspid position and with a smaller diameter when used in aortic or pulmonary position.

Acoustic shadowing

Prosthetic materials, particularly in mechanical models, cause numerous ultrasound artefacts, including acoustic shadowing, reverberations, refraction, and mirror artefacts (*Figure 4*, *Panel A*–*E*).[14,84] This often affects imaging quality and is even more pronounced in case of double PHVs. Multiple and sometimes off-axis views must be used to overcome these problems and interrogate areas around the prostheses. At lower gain settings, the valves are generally better visualized.

Generally, the left/right atrial (LA/RA) side of a prosthetic mitral/tricuspid valve is obscured by acoustic shadowing from the TTE approach, resulting in a low sensitivity for detection of prosthetic mitral or tricuspid regurgitation (MR, TR), thrombus, pannus, or vegetation (*Figure 5*, *Panel A* and *B*). TOE provides superior images of the LA/RA side of the mitral/tricuspid prosthesis (*Figure 5*, *Panel C* and *D*). In the aortic position, the posterior aspect of the valve appears shadowed on TTE (*Figure 4*, *Panel A*) while the anterior aspect of the valve is shadowed on TOE (*Figure 4*, *Panel C* to *E*).[85,86]

For stented valves, the ultrasound beam should be carefully aligned parallel to the flow to avoid shadowing effects of the stents and sewing ring.[87]

Artefacts created by mechanical valves are different for cardiac CT compared with echocardiography or CMR. Partial volume combined with interpolation effects created during image reconstruction causes metal (-coated) structures to appear larger (hyperdense artefact, blooming, and bright streak), while beam-hardening effects create dark shadows (hypodense artefact). These artefacts are most severe during phases of rapid displacement.[31,36,40] Valves with cobalt-chrome rings (Björk–Shiley valve) suffer most severe beam-hardening artefacts. Prospective ECG

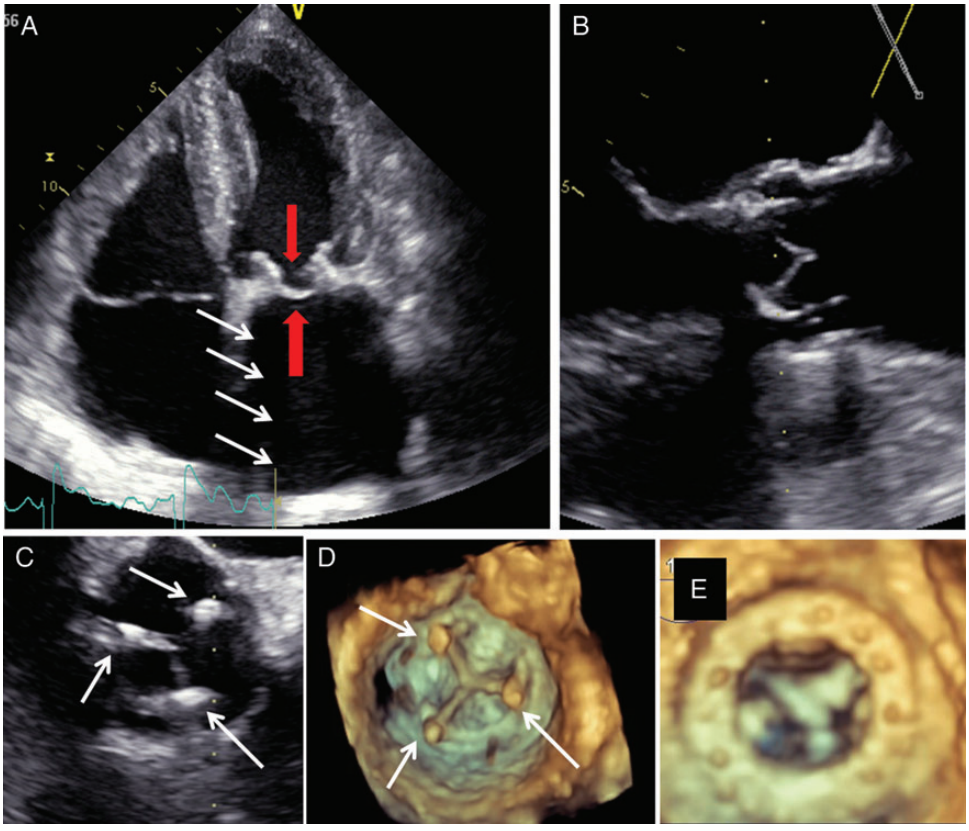

Figure 3 Bioprostheses: normal appearance. 2D and 3D transthoracic (TTE) and transoesophageal (TOE) echocardiography appearance of bioprosthetic replacement valves. (*A*) 2D TTE appearance of a normal bioprosthesis in mitral position; the frame on which the leaflets are attached is a strong echo-reflector leading to acoustic shadowing (white arrows). However, this phenomenon is of lesser magnitude than in mechanical valves. The ventricular and atrial sides of one of the leaflets are nicely delineated (red arrows). (*B*) 2D TOE at 120° appearance of a normal bioprosthesis in aortic position as seen in diastole: the frame of the valve is nicely seen leading to discrete acoustic shadowing; the aortic and ventricular sides of two of the leaflets are clearly seen in the long-axis view. (*C*) 2D TOE at 45° appearance of a normal bioprosthesis in aortic position, as seen in diastole, from the aortic side. The three pillars of the metallic frame on which the leaflets are mounted are seen at 1, 5, and 10 o'clock (arrows), as well as the coaptation lines of the leaflets. (*D*) Same image as in *C* but from a 3D perspective. (*E*) The atrial aspect of a normal bioprosthetic valve in mitral position in diastole from a 3D perspective. The ring of the prosthesis as well as the atrial surface of the three leaflets in systole are seen in detail

triggering can reduce PHV-induced artefacts compared with retrospective ECG gating.

PHVs also produce artefacts with CMR signal loss relative to distortion of the magnetic field by the metal mechanical valves hold.[75] Artefacts are less with biological valve. Artefacts are more pronounced with gradient-echo cines and less on spin-echo images.[65]

Microbubbles

Microbubbles are characterized by a discontinuous stream of rounded, strongly echogenic, fast-moving transient echoes.[88] Microbubbles occur at the LV inflow zone of the valve when flow velocity and pressure suddenly drop at the time of prosthetic valve closing, but may also be seen during valve opening. The cavitation potential is likely correlated with valve design, occluding material, and the velocity of the leaflet closure.[89] Microbubbles are common in the mitral position (*Figure 6*, *Panel A*). They are probably due to carbon dioxide degassing and linked to hypercoagulability of blood near the valve though of doubtful significance. They might be at the origin of high-intensity transient signals in the cerebral circulation, which can be detected using transcranial Doppler examination of the middle cerebral artery.[90] They can be observed in both normal and dysfunctional mechanical PHVs. Microbubbles are not found in bioprosthetic valves.

Spontaneous echo contrast

Spontaneous echo contrast (SEC) is defined as smoke-like echoes.[84] The prevalence of SEC is 7 to 53%. SEC is caused by increased red cell aggregation that occurs in slow flow (e.g. low cardiac output, severe LA dilatation, atrial fibrillation, and pathologic obstruction of a mitral prosthesis).

Strands

Strands are thin, mildly echogenic, filamentous structures that are several millimetre long (often <1 mm thick and >2 mm up to 30 mm length) and move independently from the PHV (*Figure 6*, *Panel B*).[91–93] They

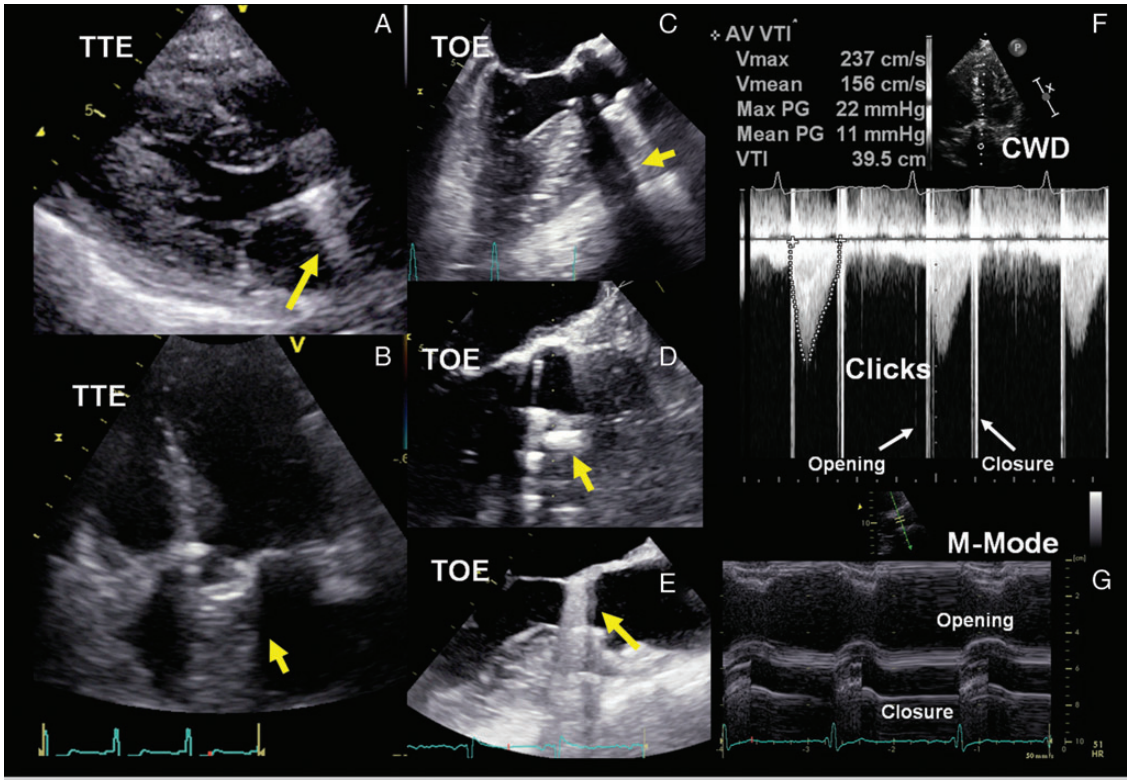

Figure 4 Mechanical valve in aortic position: normal appearance. Acoustic shadowing and reverberations seen with 2D transthoracic and transoesophageal echocardiography when imaging a mechanical valve in aortic position depending on the acoustic view used (*A*–*E*, yellow arrows). (*F*) Continuous wave Doppler (CWD) signal showing the opening and closing clicks (white arrows) of a normally functioning aortic valve, an early peak velocity and a normal mean and peak pressure gradient across the prosthesis. (*G*) M-mode showing normal opening and closure of the discs.

are often visible intermittently during the cardiac cycle but recur at the same site. They are usually located at the LV inflow side of the PHV (i.e. the atrial side of a mitral prosthesis or the ventricular side of an aortic prosthesis). They can be observed on both mechanical and biological PHVs. Strands are found in 6 to 45% of patients.[93] Prosthetic valve-associated strands are likely to have multiple causes; they may have a fibrinous or a collagenous composition. Strands have been found to be more common in patients undergoing TOE for evaluation of the source of embolism than in patients examined for other reasons.[93] Although this association may imply an embolic potential, their meanings and therapeutic implications remain unclear.

Key points

Mechanical PHVs have specific patterns of echoes that can help identify the type of prosthesis. The echocardiographic assessment of PHVs can be limited by the shadowing effect particularly for the mitral prosthesis from the TTE approach and partially for the aortic prosthesis from the TOE views.

Haemodynamic characteristics

All normal functioning mechanical PHVs cause some degree of obstruction to blood flow, closure backflow (necessary to close the valve), and leakage backflow (after valve closure).[87,94]

Flow patterns (anterograde flows) and clicks

Blood flow through normally functioning PHVs differs from flow through native valves. The pattern of anterograde flow is unique to each valve and depends on the shape and number of orifices through which forward flows occurs.[7,14,80–82,94–96] Double-envelope spectral Doppler profiles may often be seen in mechanical PHVs. Spectral Doppler recordings of PHV flow also include brief, intense, high-velocity signals referred to as clicks due to the opening and closing of the occluder mechanism (*Figure 4F* and *5E*). The colour map should entirely fill the orifice in all views (*Figure 2B*).

In the setting of a 'single disc', the large major orifice (semicircular jet in cross-section) may create a dense and typically lower velocity jet arising from the major orifice, and a faint (could be also two or three jets depending on the number of struts), higher-velocity jet from the minor orifice.

Similarly, 'bileaflet mechanical valves' generate a dense, lower velocity jet arising from the two lateral orifices, with a faint higher velocity jet arising from the central orifice. (*Figure 2*, *Panel F*). Three separate jets thus characterize the pattern of the anterograde transvalvular flow (*Figure 2*, *Panel B*).

With 'caged-ball PHVs', blood flows goes around the entire circumference of the ball and gives two curved side jets and a large wake in the central part.

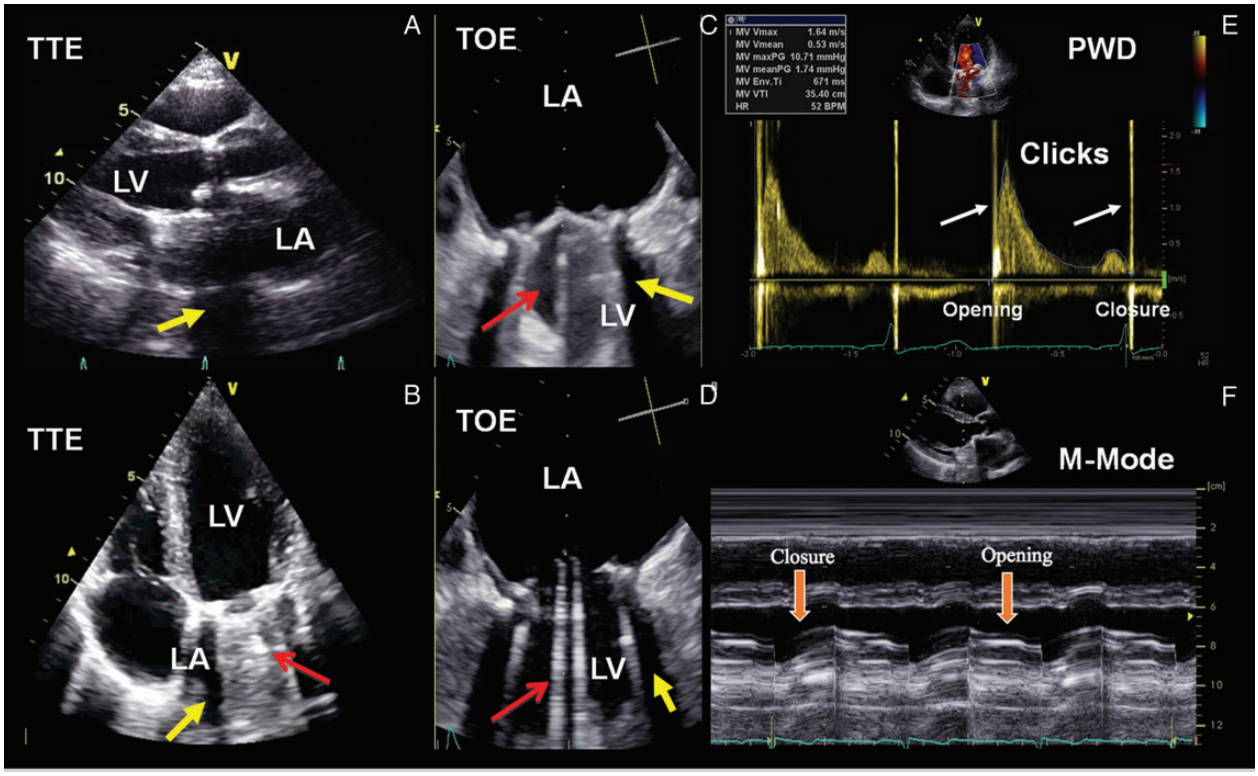

Figure 5 Mechanical valve in mitral position: normal appearance. Acoustic shadowing and reverberations seen with 2D transthoracic and transoesophageal echocardiography when imaging a mechanical valve in mitral position depending on the acoustic view used (*A* and *B*, acoustic shadowing and reverberations on the atrial side (LA) vs. *C* and *D* on the ventricular (LV) side. (*F*) Pulsed wave Doppler (PWD) signal showing the opening and closing clicks (white arrows) of a normally functioning mitral valve. M-mode showing normal opening and closure of the discs.

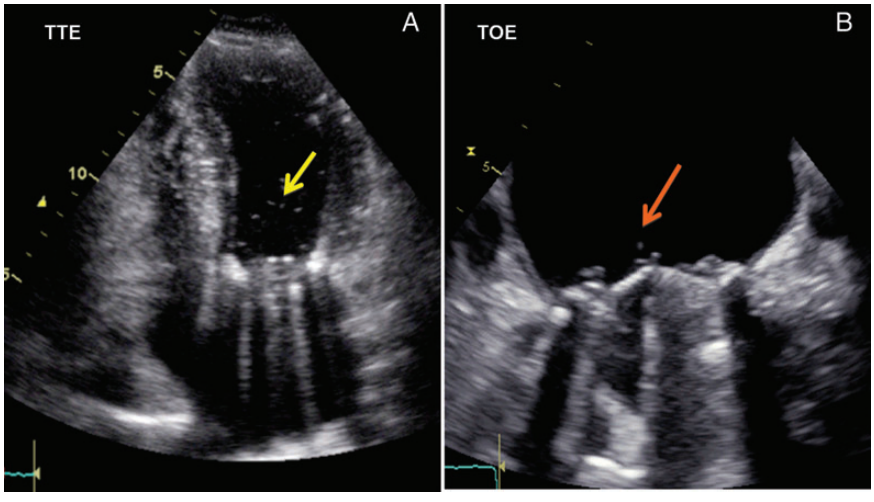

Figure 6 Mechanical valve in mitral position: cavitation and strands. (*A*) Cavitation (yellow arrow) inside the left ventricular cavity related to the presence of a mechanical valve in mitral position, as seen from the apical transthoracic approach. (*B*) Fibrin strands (orange arrow) seen as fine filamentous masses attached to the atrial side of a mechanical valve in mitral position as seen from the transoesophageal approach.

With 'bioprosthesis', a single central anterograde flow pattern is observed.

Pressure gradients and EOA

The haemodynamic performance of most PHVs is inferior to that of the normal native valve.[7,12–14,96,97] Hence, PHVs often cause some degree of obstruction to blood flow, which may vary depending on the model and size of prosthesis as well as the patient's body size.[2,14] Quantitative parameters of PHV function include transprosthetic flow velocity (highest velocity signal in PHVs) and pressure gradients, effective orifice area (EOA), and DVI (*Tables 1* and *2*).

Transprosthetic flow velocity and gradients

Doppler echocardiography takes advantage of the relationship defined by the Bernoulli equation between velocity and pressure, to assess gradients.[98] Using the Bernoulli equation, the difference in pressure across a restrictive orifice is defined as:

$$\Delta P = P1 - P2 = 4(V_2^2 - V_1^2)$$

where $P1$ and $V1$ are the pressure and velocity, respectively, proximal to the restrictive orifice; and $P2$ and $V2$ are the pressure and velocity, respectively, distal to the orifice. The peak difference between pressures is the peak instantaneous gradient, and the average difference over the duration of flow is the mean gradient. Since $V_2 >> V_1$ and the vicious friction are ignored, the energy balance through the orifice simplifies to:

$$\Delta P = 4(V_2^2)$$

which is the simplified Bernoulli equation used to translate the velocity from echocardiography to a pressure drop. However, especially in normally functioning bioprostheses, V_2 values may be low (often <2 m/s), so the use of the simplified Bernoulli equation (default setting on the echo machine) can cause significant overestimation of pressure gradients.[99] This overestimation may be negligible in obstructive PHVs (often seen with mechanical valves) with high V_2 values (from $+3$ to $+5$%), but it may be clinically significant in normally functioning biosprostheses (from $+13$ to $+19$%).[99] In these situations, estimation of the pressure gradient is more accurately determined by integrating the velocity proximal to the prosthesis into the Bernoulli equation ($\Delta P = 4(V_2^2 - V_1^2)$). The peak velocity across the prosthesis is to some extent related to valve size with the small prostheses having higher velocities, but since velocities are determined by cardiac output and systemic vascular resistance, there may be overlap between different valve sizes of a particular type of prosthesis.[7] In patients with aortic prostheses and high cardiac output or narrow LV outflow tract (LVOT), the velocity proximal to the prosthesis may be elevated and therefore not negligible (proximal velocity >1.5 m/s).[100,101]

Because of the inherent risks related to crossing a prosthetic valve with a catheter, invasive assessment of prosthetic valve haemodynamics is rarely used. There is generally a good correlation between peak and mean pressure gradients determined invasively and non-invasively.[14,100–103] However, if significant pressure recovery is present, such as in patients with a small aorta, the pressure gradients measured by left heart catheterization are lower than those measured by Doppler echocardiography. The peak-to-peak pressure gradient measured by catheter is substantially lower than the peak instantaneous gradient measured by catheter or Doppler. Given that the aortic and LV pressure peaks do not occur at the same time, the peak-to-peak pressure gradient has no physiological meaning.[19,95] Furthermore, it is highly influenced by aortic compliance. Hence, this parameter should not be used for the assessment of native or prosthetic aortic valves. Underestimation of the gradients can be observed in the presence of (i) failure to align the Doppler beam parallel with the highest velocity jet (ideal angle $<20^\circ$), (ii) any low flow state (gradients are known to be sensitive to flow), (iii) elevated systemic blood pressure. Overestimation of the gradients can be observed in the presence of (i) any high flow state, (ii) mistaking MR flow signal for transaortic flow signal (MR starts earlier and lasts longer than aortic flow), (iii) angle correction of Doppler interrogation relative to the direction of blood flow (this is not recommended), (iv) the pressure recovery phenomenon (Doppler gradient substantially higher than the invasively determined pressure gradient, particularly in patients with a small aorta).

Effective orifice area

The EOA is not the same parameter as the GOA (the internal valve area theoretically available for the bloodstream to pass through).[104] The EOA is always smaller and describes the functional area.[105] The EOA indeed corresponds to the smallest area of the jet passing through the prosthesis as it exits the valve (vena contracta). Both the shape of the inlet and the size of the orifice affect the ratio between GOA and EOA (coefficient of flow contraction). Clinically, the coefficient of contraction varies from 0.90 to 0.71, which may result in up to a 29% difference between the EOA and GOA.[106] The theoretical GOA can be calculated from the internal orifice diameter of the prosthesis stent provided by the valve manufacturers. In bioprosthetic valves, the GOA can be measured by planimetry from echocardiographic, CT or CMR images.[45,65] The theoretical GOA grossly overestimates the planimetered GOA, because it assumes that the whole internal area of the prosthesis stent is available for blood flow, which is not the case. The valve leaflets indeed occupy a substantial proportion of the stent orifice. Furthermore, the planimetered GOA overestimates the EOA due to the flow contraction phenomenon described above.[45,65] It is important to underline that, from a pathophysiologic standpoint, the transvalvular pressure gradients are essentially determined by the EOA.[107] Hence, the gradients correlate better with EOA than with GOA.

The prosthetic valve EOA is less flow dependent than the transprosthetic velocity or gradient, and is thus often a better index of intrinsic valve haemodynamic performance (*Tables 1* and *2*).[19] However, this parameter is more prone to technical pitfalls and measurement errors. For both aortic and mitral prosthetic valves, the EOA should be calculated by the continuity equation method using the stroke volume measured in the LVOT or rarely the right ventricular outflow tract (RVOT) (*Figures 7* and *8*).[103,108,109] EOA is a reflection of the minimal cross-sectional area (CSA) of the transprosthetic flow jet (the vena contracta), and it is calculated as:

$$\begin{aligned} \text{EOA} &= \text{CSA} \times \text{VTI}_{\text{LVOT}}/\text{VTI}_{\text{PrV}} \\ &= 0.785 \times (D_{\text{LVOT}})^2 \times \text{VTI}_{\text{LVOT}}/\text{VTI}_{\text{PrV}} \end{aligned}$$

$$\text{EOA} = \frac{\text{Stroke volume}}{\text{VTI}_{\text{PrV}}}$$

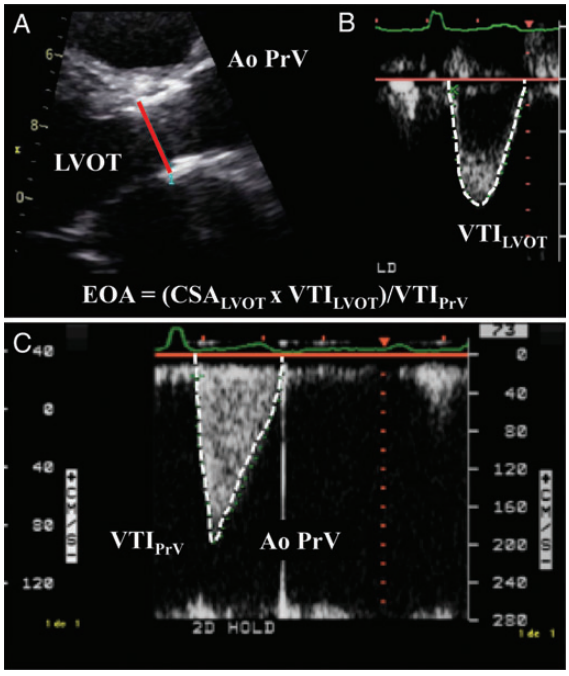

Figure 7 Aortic prosthesis EOA calculation using the continuity equation. The LVOT diameter is measured in mid-systole from the parasternal long-axis view in a zoomed mode, from inner-edge to inner-edge (*A*). The cross-sectional area (CSA) of the LVOT is calculated from the LVOT diameter assuming that the LVOT is circular ($CSA = \Pi \times LVOTd^2/4$). The stroke volume across the prosthesis is computed from multiplying the CSA of the LVOT with the velocity-time integral (VTI) of the LVOT (*B*). The EOA of the prosthesis is then calculated by dividing the stroke volume by the VTI_{PrV} of the transprosthetic flow obtained with continuous wave Doppler (*C*).

where the VTI_{LVOT} is the velocity time integral of blood flow in the LVOT, measured with pulsed wave (PW) Doppler in the LVOT just proximal from the aortic valve (apical views) or rarely the pulmonic valve (short-axis view); and the VTI_{PrV} is the velocity time integral through the prosthetic valve determined by continuous wave (CW) Doppler. The pulmonic site to calculate the stroke volume is rarely used but useful if the LVOT cannot be evaluated.[19]

The continuity method requires that the velocity utilized for the stroke volume calculation is the spatial mean velocity, which is obtained by moving the sample volume approximately 0.5 cm away from the prosthesis sewing ring towards the LV apex.[19] The principle is that the LVOT diameter and velocity derive from almost the same anatomic location. The sample volume position is optimal if the signal contains a nice spectral envelope and the closing click of the prosthesis (in case of aortic prosthesis). The VTI is obtained by tracing the contour of the Doppler flow signal. The peak velocity may be used instead of the VTI in the continuity equation.[19] The VTI_{PrV} is recorded from the same transducer position (apical five- or three-chamber, right parasternal, or suprasternal window with TTE or transgastric position at 90° to 120° or a deep transgastric 'upside-down view' at 0° to 20° with TOE). The measurement of the LVOT diameter (parasternal long-axis zoomed view with TTE or 120° view with TOE) is often challenging in the presence of an aortic prosthesis because of the reverberations and shadowing caused by the prosthesis components. Particular attention should be paid not to mistake the inner border of the prosthesis stent/ring for the inner edge of the LVOT. Any error in the measurement of LVOT diameter will be squared in the calculation of the EOA. For an LVOT diameter of 2.0 cm, a 10% error in measurement (1.8 cm) results in a 19% error in calculated EOA. It is important to emphasize that the substitution of the LVOT diameter by the labelled prosthesis size in the continuity equation is not a valid method to determine the EOA of aortic prostheses.[109] For aortic prostheses, this method is also valid in the presence of concomitant prosthetic regurgitation. However, for mitral prostheses, the continuity equation method cannot be applied when there is >mild concomitant mitral (MR) or aortic regurgitation (AR). In some cases, volumetric method can be used when the conventional 2D-Doppler method is not feasible/reliable. In 'normally functioning' prostheses, the EOA should fall into in the normal reference for that prosthetic valve type and size (*Tables 7* and *8*).

The pressure half time (PHT) method is not valid for estimating the EOA of mitral prostheses.[103] The time for the initial transprosthetic gradient to decline to half of its initial value is not only related to the prosthetic valve area but also to the pressure gradient at the start of diastole and to LV and left atrial compliance.[19] Nonetheless, the PHT may be useful if it is significantly delayed or shows significant lengthening from one follow-up visit to the other despite similar heart rates.[14]

Doppler velocity index

The DVI can be helpful to screen for prosthetic valve stenosis, particularly when reliable measure of the LVOT diameter cannot be obtained to calculate the EOA by the continuity equation method.[110] This index is less dependent on valve size because of the linear relationship of the implanted valve size to the size of the LVOT. For aortic prostheses, the DVI is calculated as the ratio of the proximal peak flow velocity (or VTI) in the LVOT to the transprosthetic peak flow velocity (or VTI). For a normally functioning aortic prosthesis, the DVI is typically >0.30–0.35.[14]

$$DVI = \frac{\text{peak } V_{LVOT}}{\text{peak } V_{PrV}} \quad \text{or} \quad \frac{VTI_{LVOT}}{VTI_{PrV}}$$

For prosthetic mitral valves, DVI is calculated as:

$$DVI = \frac{VTI_{PrV}}{VTI_{LVOT}}$$

It is normally <2.2 for mechanical mitral valves.

Parameters of flow ejection dynamics

Parameters of flow ejection dynamics measured on the CW Doppler signal of the transprosthetic flow velocity (*Figure 7*, *Panel C*) are angle-independent parameters that can also help to distinguish between normal PHV function [with or without patient-prosthesis mismatch (PPM)] vs. acquired PHV stenosis.[111] In a normal aortic native or prosthetic valve, the contour of the CW flow velocity

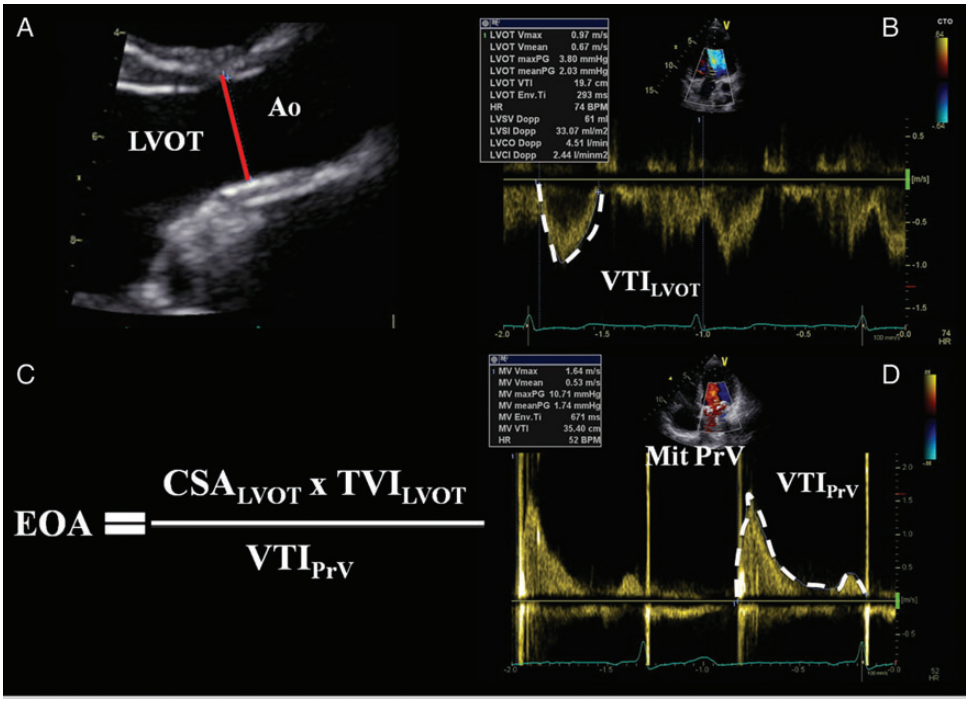

Figure 8 Mitral prosthesis EOA calculation using the continuity equation. The stroke volume across the aortic valve is calculated as described in *Figure 7*, *Panels* (*A*) and (*B*). The EOA of the mitral prosthesis is calculated by dividing the left ventricle stroke volume by the VTI_{PrV} of the trans-prosthetic flow obtained with continuous wave Doppler (*C* and *D*).

Table 7 Normal reference values of effective orifice areas for the prosthetic aortic valves

Prosthetic valve size (mm)	19	21	23	25	27	29
Stented bioprosthetic valves						
Mosaic	1.1 ± 0.2	1.2 ± 0.3	1.4 ± 0.3	1.7 ± 0.4	1.8 ± 0.4	2.0 ± 0.4
Hancock II	–	1.2 ± 0.2	1.3 ± 0.2	1.5 ± 0.2	1.6 ± 0.2	1.6 ± 0.2
Carpentier-Edwards Perimount	1.1 ± 0.3	1.3 ± 0.4	1.5 ± 0.4	1.8 ± 0.4	2.1 ± 0.4	2.2 ± 0.4
Carpentier-Edwards Magna	1.3 ± 0.3	1.5 ± 0.3	1.8 ± 0.4	2.1 ± 0.5	–	–
Biocor (Epic)	1.0 ± 0.3	1.3 ± 0.5	1.4 ± 0.5	1.9 ± 0.7	–	–
Mitroflow	1.1 ± 0.2	1.2 ± 0.3	1.4 ± 0.3	1.6 ± 0.3	1.8 ± 0.3	–
Trifecta	1.4	1.6	1.8	2.0	2.2	2.4
Stentless bioprosthetic valves						
Medtronic Freestyle	1.2 ± 0.2	1.4 ± 0.2	1.5 ± 0.3	2.0 ± 0.4	2.3 ± 0.5	–
St Jude Medical Toronto SPV	–	1.3 ± 0.3	1.5 ± 0.5	1.7 ± 0.8	2.1 ± 0.7	2.7 ± 1.0
Prima Edwards	–	1.3 ± 0.3	1.6 ± 0.3	1.9 ± 0.4	–	–
Mechanical valves						
Medtronic-Hall	1.2 ± 0.2	1.3 ± 0.2	–	–	–	–
St Jude Medical Standard	1.0 ± 0.2	1.4 ± 0.2	1.5 ± 0.5	2.1 ± 0.4	2.7 ± 0.6	3.2 ± 0.3
St Jude Medical Regent	1.6 ± 0.4	2.0 ± 0.7	2.2 ± 0.9	2.5 ± 0.9	3.6 ± 1.3	4.4 ± 0.6
MCRI On-X	1.5 ± 0.2	1.7 ± 0.4	2.0 ± 0.6	2.4 ± 0.8	3.2 ± 0.6	3.2 ± 0.6
Carbomedics Standard and Top Hat	1.0 ± 0.4	1.5 ± 0.3	1.7 ± 0.3	2.0 ± 0.4	2.5 ± 0.4	2.6 ± 0.4
ATS Medical[a]	1.1 ± 0.3	1.6 ± 0.4	1.8 ± 0.5	1.9 ± 0.3	2.3 ± 0.8	–

Effective orifice area is expressed as mean values available in the literature. Further studies are needed to validate these reference values.
[a]For the ATS medical valve, the label valve sizes are 18, 20, 22, 24, and 26 mm. High velocities are common in size 19 or 21 prostheses. Adapted with permission from Ref. 7.

Table 8 Normal reference values of effective orifice areas for the prosthetic mitral valves

Prosthetic valve size (mm)	25	27	29	31	33
Stented bioprosthetic valves					
Medtronic Mosaic	1.5 ± 0.4	1.7 ± 0.5	1.9 ± 0.5	1.9 ± 0.5	–
Hancock II	1.5 ± 0.4	1.8 ± 0.5	1.9 ± 0.5	2.6 ± 0.5	2.6 ± 0.7
Carpentier-Edwards Perimount	1.6 ± 0.4	1.8 ± 0.4	2.1 ± 0.5	–	–
Mechanical valves					
St Jude Medical Standard	1.5 ± 0.3	1.7 ± 0.4	1.8 ± 0.4	2.0 ± 0.5	2.0 ± 0.5
MCRI On-X[a]	2.2 ± 0.9	2.2 ± 0.9	2.2 ± 0.9	2.2 ± 0.9	2.2 ± 0.9

Effective orifice area is expressed as mean values available in the literature. Further studies are needed to validate these reference values.
[a]The On-X valve has just 1 size for 27 to 29 and 31 to 33 mm prostheses. In addition, the strut and leaflets are identical for all sizes (25 to 33 mm); only the size of the sewing cuff is different. Adapted with permission from Ref. 7.

through the prosthesis generally has a triangular shape, with early peaking of the velocity and a short (<100 ms) acceleration time (AT) (i.e. the time from the onset of flow to maximal velocity, *Figure 7*, *Panel C*). However, the acceleration time is highly dependent on heart rate. To overcome this limitation, it is recommended to index the AT to the LV ejection time.

Pressure recovery and localized high gradient

Several studies have reported that Doppler may overestimate the gradient across native, mechanical, or bioprosthetic aortic valves compared with catheter measurements.[100,112–115] As blood flow velocity decelerates between the aortic valve and the ascending aorta, part of the kinetic energy is reconverted back to static pressure energy. This phenomenon is called pressure recovery. Most of the kinetic energy is dissipated in heat as a result of turbulence. Hence the net gradient between the LV and the ascending aorta (i.e. the gradient measured by catheter) is less than the maximum pressure gradient measured by Doppler at the level of the vena contracta. The ratio between the valve EOA and the cross-sectional area of the downstream chamber, i.e. the ascending aorta in the case of native or prosthetic aortic valves, determines the extent of pressure recovery. Hence, pressure recovery generally becomes clinically relevant in patients with smaller aortas, i.e. with an aorta diameter at the sino-tubular junction ≤30 mm.[100,112–115] In these patients, it is thus appropriate to account for pressure recovery by using the simple formula proposed by Garcia *et al.*[112] to calculate the energy loss coefficient: ELC=(EOA × AA/AA − EOA), where AA is the cross-sectional area of the aorta measured at ∼1 cm downstream of the sino-tubular junction. The energy loss coefficient should be indexed for body surface area (i.e. energy loss index) to account for the change in cardiac output related to body size. Pressure recovery generally does not occur in the case of mitral prostheses, because the size of the downstream chamber (i.e. the LV) is large relative to the EOA of the prosthesis.

The downstream pressure recovery phenomenon is distinct from another mechanism responsible for localized high gradients within the central orifice of bileaflet mechanical valves.[100,113,116,117] This may yield to overestimation of gradient (average of 4 to 11% compared with catheterization) and underestimation of EOA regardless of the position (aortic or mitral) of the prosthesis. Because the central orifice is smaller than the lateral orifices, the blood flow velocity may be locally higher within the inflow aspect of the central orifice and continuous-wave Doppler may record this high velocity. The prevalence, magnitude, and predictors of this phenomenon are not fully understood, but it is probably related to PHV size (smaller size, higher velocity) and design (ratio of the size of the central orifice to that of lateral orifices) and flow conditions (higher flow, higher velocity).[100,113,116,117] Given that localized high-velocity region is very small and located at the inflow of the central orifice, the recording of this velocity is highly inconsistent and may vary from one patient to the other and even from one visit to the other in a given patient, depending on the direction and angulation of the Doppler beam.

Physiologic regurgitation (retrograde flows)

Mechanical valves have a normal regurgitant volume that may include either a backflow related to the backward motion of the occluder(s) (i.e. the closing volume), a leakage backflow through the components of the prosthesis (leakage volume) or both.[7,14,80–82,94–96] This 'built-in' regurgitation theoretically prevents blood stasis and thrombus formation by a washing effect. Minor regurgitation is thus normal in virtually all mechanical valves. As opposed to pathologic regurgitant jets, the normal leakage backflow jets are characterized by being narrow at their origin and symmetrical and low in momentum (i.e. usually have a homogeneous colour without significant aliasing). They are also characterized by the absence of supporting features like increased anterograde velocity, enlargement of cardiac chambers, or pulmonary hypertension. Of note, mild central leakage may be seen in normally functioning bioprosthetic valves.[7,14]

'Caged-ball mechanical prostheses' have a small amount of normal regurgitant flow (closing volume of 2–6 mL per beat).

'Monoleaflet mechanical' valves have small physiologic regurgitant volume (5–9 mL per beat) that includes the closing volume as well leakage backflow through small gaps around the perimeter of the valve. In the Medtronic-Hall valves, there is also often a small amount of regurgitation around the central strut.

'Bileaflet mechanical valves' typically have a small amount (5–10 mL per beat) of normal regurgitation. On Doppler colour flow imaging, two main regurgitant jets originating from the pivot points of the valve disks which may break into one or more 'plumes' and a smaller central jet are often seen (*Figure 2*, *Panel G* and *I*). Smaller jets around the closure rim of the leaflets may also be seen.

Table 9 Definitions of morbidity after heart valve replacement surgery[a]

Complication	Definition	Examples or notes
Structural valve deterioration	Deterioration or dysfunction of the operated valve caused by changes intrinsic to the valve	(1) Mechanical valve—wear, fracture, poppet escape (2) Biological valve—calcification, leaflet tear, stent creep (3) Both—disruption of components of a prosthetic valve
Non-structural dysfunction	Any abnormality not intrinsic to the valve that results in stenosis or regurgitation of the valve or haemolysis	(1) Entrapment by pannus, tissue, or suture (2) Paravalvular leak (3) Inappropriate sizing or positioning (4) Residual leak or obstruction after valve implantation (5) Clinically important intravascular haemolysis (6) Dilatation of aorta or aortic annulus causing aortic regurgitation (for stentless valves)
Valve thrombosis	Any thrombosis not caused by infection that occludes part of the blood flow path, interferes with valve function, or is sufficiently large to warrant treatment	
Embolism	An embolic event that occurs in the absence of infection after the immediate perioperative period	(1) Stroke (>72 h neurological deficit) or non-specific symptoms with brain imaging demonstrating an acute ischaemic event (2) TIA (fully reversible symptoms of short duration with no abnormality on brain imaging) (3) Non-cerebral embolic event (not perioperative myocardial infarct)
Bleeding event	Any episode of major internal or external bleeding that causes death, hospitalization, permanent injury, or blood transfusion	Exclude bleeding associated with major trauma or an operation. Include major unexpected bleeding associated with minor trauma.
Endocarditis	Proved infection of the replacement heart valve	Proof by: (1) Reoperation with evidence of abscess or other local complication (2) Autopsy evidence of abscess, pus, or vegetation (3) Duke criteria positive

[a]Based on definitions in Akins *et al.*[119]

A small degree of central (at the point of apposition or close to the commissures) regurgitation (<1 mL) is also often observed in 'bioprosthetic valves' and more frequently in bovine pericardial valves. Stentless valves, including homografts and autografts, are more likely than stented valves to have minor regurgitant jets.

Key points

All normal functioning mechanical PHVs cause some degree of obstruction to blood flow, closure backflow (necessary to close the valve), and leakage backflow (after valve closure). Quantitative parameters of PHV function include transprosthetic flow velocity and pressure gradients, EOA and DVI. Although good correlation exists between Doppler and invasive measurements, overestimation of pressure gradients by Doppler is frequent in mechanical PHVs. Comparison of the haemodynamic function of different designs of valve cannot be made using label size. The label size cannot be used as surrogate for LVOT diameter in the calculation of the EOA using the continuity equation.

PHV dysfunction

Structural valve dysfunction

Structural valve deterioration results in stenosis or regurgitation through the valve.[7,118,119]

For 'mechanical valves', haemodynamic dysfunction can occur as a result of strut fracture, occluder fracture or escape, loss of leaflet mobility (not due to thrombus, pannus, or vegetation) or ball variance (due to lipid adsorption on the ball of old model Starr-Edwards valves), sewing cuff separation from housing.[7,118]

For 'bioprosthetic valves', haemodynamic dysfunction (stenosis or regurgitation) usually occurs with calcification or tearing of the cusps but occasionally fracture of the stent sewing cuff separation from stent, or valve deformation.

Non-structural and other causes of valve dysfunction

Non-structural dysfunction is any abnormality not intrinsic to the valve itself and includes dehiscence or entrapment of the occluder by pannus, tissue, or suture (*Table 9*).[17,120]

Thrombus formation is the most common cause of obstruction of mechanical prostheses (~0.3 to 8% per patient-year). Although less frequent and more insidious, it can also be observed in bioprosthesis. The incidence of pannus formation causing prosthesis obstruction is similar in biological and mechanical prosthesis. Mitral and tricuspid prostheses are associated with, respective, 7.5 and 11.7 times higher hazard risk of thrombosis and the risk of pannus formation is three times larger in the mitral position. Large prosthesis size (>27 mm), tilting disk, and bileaflet prostheses

are associated with, respective, 67, 69, and 83% risk reduction of thrombosis.[120]

Differentiation between thrombosis and pannus overgrowth remains challenging. Recent onset of dyspnoea or of an embolic event and a history of subtherapeutic anticoagulation are suggestive of obstructive valve thrombosis. The thrombus tends to be mobile and globular with a soft echo density (similar to that of the myocardium) and may be attached to the valve occluder or sewing ring or both (*Figure 9*). Pannus is firmly fixed, has a bright echo density (small dense mass with the same echo intensity as the valve housing), and is attached to the valve apparatus (valve housing and pivot guards) (*Figure 10*).[121] The situation is further complicated, because pannus may induce thrombus formation. On cardiac CT, thrombus has lower measured CT attenuation values than pannus, with a suggested threshold of 200 HU to distinguish either (*Table 10*).[53,61]

Pathologic PHV regurgitation

Pathologic regurgitation is either central or paravalvular.[11,16,20,21] Most pathologic central regurgitations are seen with biologic valves as a sign of structural valve degeneration. A pathological jet is often first seen close to the commissure at a site of an early tear in the leaflet. This may then progress on serial studies. Regurgitation through a mechanical valve may be seen with mechanical interference with closure, for example, by pannus, thrombus, vegetation, or more rarely a chordae. Disappearance of physiological regurgitation and the presence of a new central regurgitation are typically observed in acute thrombosis of mechanical valves.

The incidence of paravalvular regurgitation is similar in mechanical and biological valves. Paravalvular regurgitation depends on numerous factors including surgical technique, the size and composition of the sewing ring and the position of the valve (annular vs. supra-annular), and the quality of the patient's tissues. In the mitral position, it occurs mainly in the posterior and anterior regions. Most are apparent in the immediate postoperative study and occur because of technical problems at the time of surgery including the presence of friable tissue. Late dehiscence is often a sign of infective endocarditis. Less commonly, the integrity of the original suture line could be compromised by usual wear- or age-related deterioration of the surrounding tissue.

Localization of paravalvular regurgitation may be difficult and is only possible with confidence if a trail of flow can be visualized around the outside of the sewing ring. Although paraprosthetic regurgitation is abnormal, small jets are not uncommon especially during perioperative examination early after surgery. Immediately following implantation, the prevalence of paravalvular regurgitation ranges between 5 and 20%.[122] However, the majority of these leaks

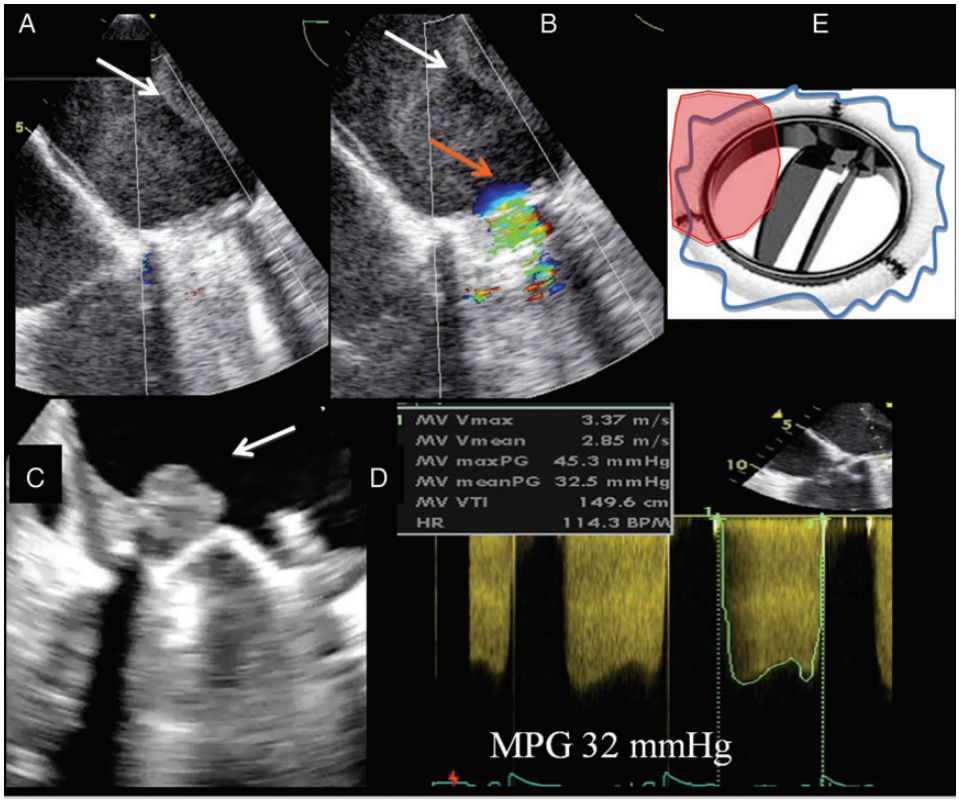

Figure 9 Mechanical valve in mitral position and thrombus obstruction. Increased transprosthetic mean pressure gradient (MPG) over a mechanical valve in mitral position (*D*), as assessed from the transoesophageal view and related to the presence of a thrombus (*A* and *B*, white arrows). Flow acceleration due to the obstruction at the level of the prosthesis is seen by colour flow imaging (orange arrow, *B*). Another example of a thrombotic mass on the atrial side of the prosthesis blocking its medial orifice (*C*, white arrow). A schematic representation is summarized in *E*.

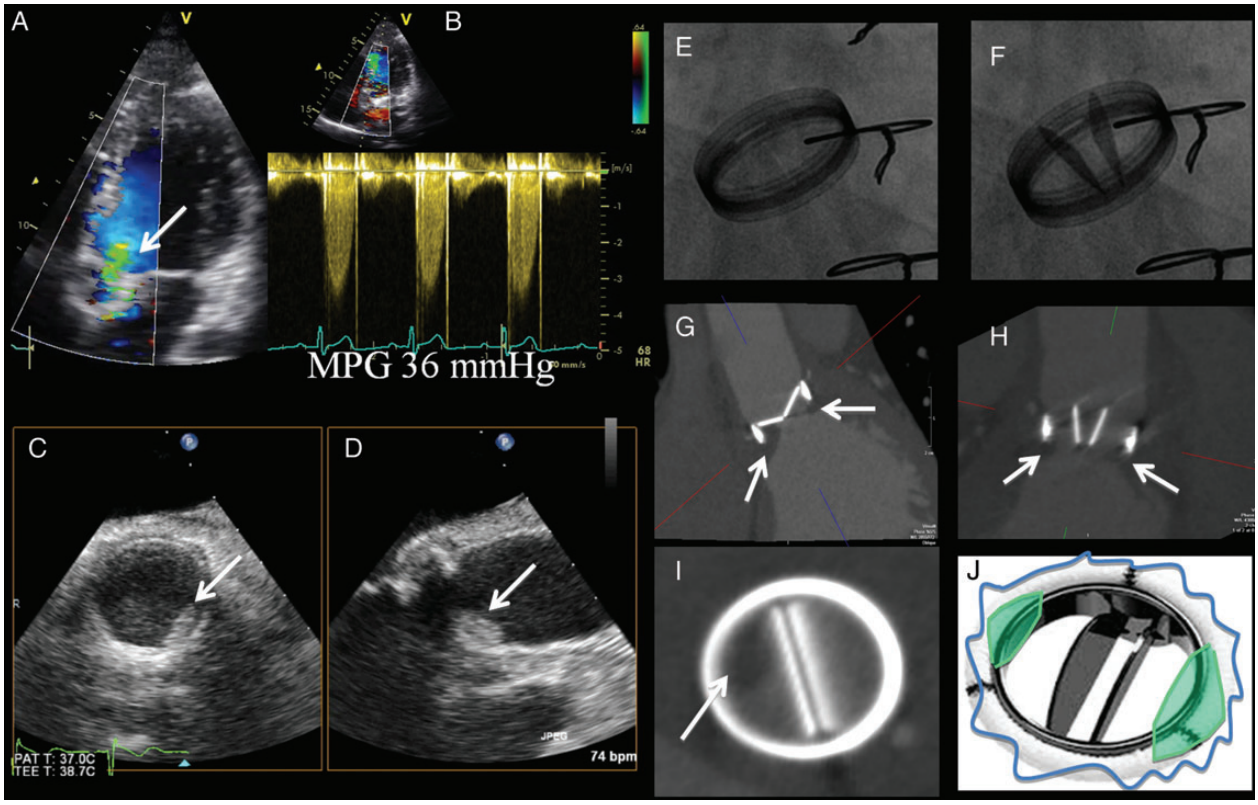

Figure 10 Mechanical valve in aortic position and pannus. Flow acceleration of the anterograde flow is identified with colour flow imaging from the transthoracic apical approach (*A*). High-pressure gradients are documented with continuous wave Doppler from the same approach, mean pressure gradient (MPG) 36 mmHg (*B*). 2D transoesophageal echocardiography enforces the suspicion of prosthesis obstruction by revealing a hyperechogenic mass on the prosthesis (*C* and *D*, white arrows). Cinefluoroscopy shows abnormal opening and closing angle for this type of prosthesis (*E* and *F*). Cardiac computed tomography (CT) scan is in favour of a pannus ingrowth on the prosthesis that blocks the normal movement of the tilting disks (*G*, *H*, and *I*, white arrows). A schematic representation is summarized in *J*.

are clinically and haemodynamically insignificant and, in the absence of endocarditis, have a benign course. There is no evidence that they increase the risk of endocarditis, but on occasion, they may cause haemolytic anaemia due to red cell destruction.[123]

Imaging evaluation of PHV dysfunction

Both qualitative and quantitative assessments are recommended. Excessive motion of the sewing ring may be a clue to valvular dehiscence.[7,122] A rocking motion of $>15^{\circ}$ of sewing ring excursion is abnormal.[14] However, usually rocking in the aortic position implies a large dehiscence, ~40% of the sewing ring. Unlike in the aortic position, rocking of the sewing ring may occur as a result of retention of the native posterior leaflet, but a true dehiscence is obvious from the gap opening between annulus and sewing ring and by the presence of an overlaying jet on colour mapping. Structural deterioration of a bioprosthetic valve should be suspected whenever increased valvular regurgitation or stenosis develops.

When PHV obstruction is suspected, imaging assessment should look for (i) thickening of the leaflets in biological prosthesis, or the presence of a mass limiting the movement of the occluders in mechanical prosthesis; (ii) decreased motion of the disc, ball, or leaflet; (iii) restriction of the colour flow at the PHV orifice; (iv) haemodynamic impairment and ventricular consequences (Doppler echocardiography) (*Table 11*).

Generally, the same principles and methods used for quantification of native valvular regurgitation, detailed in a previous document, can be used for PHVs, but are more challenging (*Figures 11–15*).[20,21] In fact, there are very limited data on the application and validation of these parameters (e.g. vena contracta width, EROA, RVol) in the context of PHVs. Moreover, the frequent eccentricity of regurgitant jets, the presence of multiple jets, and the shadowing effects due to prosthetic materials make detection and quantification more difficult or limited. Indirect clues from various colour Doppler parameters can suggest the presence of significant regurgitation (i.e. turbulent jet at the roof of LA below the acoustic shadow). Transvalvular jets should be distinguished from paravalvular regurgitations (*Figure 16*). At present, integrating multiple qualitative, semi-quantitative, and quantitative findings is the recommended approach for assessing PHV regurgitation.[14]

Patient-prosthesis mismatch

PPM occurs when the EOA of a normally functioning prosthesis is too small in relation to the patient's body size (and thus to cardiac

Table 10 Differential diagnosis: pannus vs. thrombosis

	Pannus	Thrombosis
Chronology	Minimum 12 months, commonly >5 years from surgery date	Occurs at any time (if late usually associated with pannus)
Relation to anticoagulation (low INR)	Poor relationship	Strong relationship
Location	MV > AV	TV >> MV = AV
Morphology	• Small mass • Mostly involve suture line (Ring) • Centripetal growth • Confine to the disk plane • Growth beneath disc	• Larger mass than pannus • Independent motion common • Thin outer ring maybe visible • Project into LA for MV position • Mobile elements
Echo density (video-intensity ratio)	More >0.7 (100% specific)	Less (<0.4)
Cardiac CT: attenuation value	>200 HU	<200 HU
Impact on gradient	AV > MV	MV > AV
Impact on valve orifice	AV > MV	MV > AV
Impact on disc motion	Yes/no	Yes

AV, aortic valve; LA, left atrial; MV, mitral valve; TV, tricuspid valve.

Table 11 Minimum dataset for the echocardiographic assessment of PHVs

Aortic position
- Peak velocity
- Mean gradient
- Velocity time integral (VTI)
- Doppler velocity index (DVI)
- Effective orifice area (EOA) by the continuity equation
- Presence, location, and severity of regurgitation
- +LV size and function, LV hypertrophy (a hyperdynamic LV is a useful indirect sign of severe aortic regurgitation), aorta (most likely to continue to dilate if dilated at the time of surgery)
- + Other valves: appearance, grade of stenosis, and regurgitation

Mitral position
- Peak velocity
- Mean pressure gradient
- Velocity time integral (VTI)
- Doppler velocity index (DVI)
- Effective orifice area (EOA) by the continuity equation
- Pressure half time
- Presence, location, and severity of regurgitation
- +LV size and function, LA size, estimated systolic pulmonary artery pressure (a hyperdynamic LV is a useful indirect sign of severe mitral regurgitation); (pulmonary hypertension may be a sign of mitral dysfunction)
- +Other valves: appearance, grade of stenosis, and regurgitation

Pulmonary position
- Peak velocity
- Peak and mean pressure gradient
- Presence, location, and severity of regurgitation
- +RV size and function, estimated systolic pulmonary artery pressure
- +Other valves: appearance, grade of stenosis, and regurgitation

Tricuspid position
- Peak velocity
- Mean pressure gradient
- Velocity time integral (VTI)
- Doppler velocity index (DVI)
- Pressure half time
- Presence, location, and severity of regurgitation
- +RV size and function, RA size, IVC size, hepatic venous flow, estimated systolic pulmonary artery pressure
- +Other valves: appearance, grade of stenosis, and regurgitation

IVC, inferior vena cava; LV, left ventricle; RA, right atrial; RV, right ventricle.

output requirements), resulting in abnormally high postoperative gradients (i.e. mean gradient >20 mmHg).[103,124] Hence, PPM is not an intrinsic prosthesis dysfunction *per se*. The identification of PPM and its differentiation from dysfunction is achieved by calculating the projected indexed EOA, i.e. the normal reference value of EOA for the model and size of the prosthesis (*Tables 7* and *8*) divided by patient's body surface area. *Table 12* shows the cut-off values of indexed EOA generally used to identify and quantify the severity of PPM.

Moderate PPM may be quite frequent both in the aortic (20–70%) and in the mitral (30–70%) positions, whereas the prevalence of severe PPM ranges from 2 to 10% in both positions.[125] PPM is associated with worse haemodynamics, slower and less complete regression of LV hypertrophy and pulmonary hypertension, worse functional class, exercise capacity, and quality of life, more cardiac events, and lower survival.[126–128] PPM also predispose to faster degeneration of bioprosthetic valves following aortic valve replacement.[129,130]

The other findings supportive of the presence of PPM are (*Table 12*) (i) the measured EOA is within 1 standard deviation or within 0.25 cm^2 of the normal reference EOA; (ii) the measured indexed EOA is lower than the aforementioned cut point values;

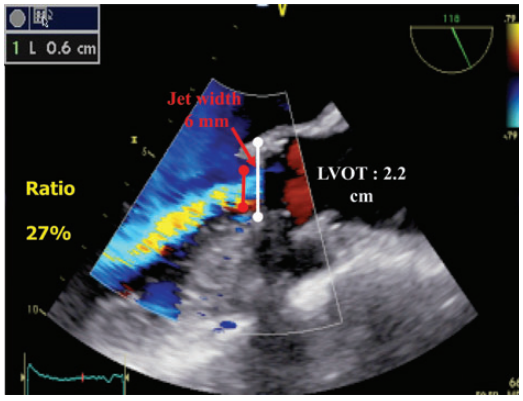

Figure 11 Aortic prosthetic regurgitation. An example of pathological intraprosthetic regurgitation jet from a transoesophageal 120° view. The width of jet expansion into the left ventricular outflow tract (red line) is compared with the width of the outflow tract (white line). Of note, a part of the regurgitant flow is not seen due to the prosthetic valve shadowing effect.

(iii) the valve leaflet morphology and mobility are normal; (iv) the PPM is present early after surgery and on all subsequent echocardiograms.

There are however some specific caveats in the assessment of PPM: (i) the use of the EOA indexed for body surface area may overestimate the severity of PPM in obese patients (body mass index $\geq$30 kg/m^2).[131] It is thus recommended to use lower cut point values of indexed EOA to identify moderate and severe PPM in obese subjects (*Table 12*).[132] Indexing the EOA by the fat free mass measured by a bio-impedance scaler may provide an interesting alternative avenue, but this needs to be validated by further studies; (ii) although PPM is the most frequent cause of high gradients following valve replacement, it is important to highlight that, in the presence of low flow state, PPM may be associated with a normal or low gradient. Indeed as for native valve stenosis, low-flow states are often associated with pseudo-normalization of transvalvular flow velocities and gradients leading to underestimation of PPM or prosthetic valve stenosis. Stress echocardiography may be useful in this context to differentiate a true PPM or stenosis vs. normal valve function; (iii) a large proportion of patients with aortic or mitral prosthetic valves in fact have coexistence of PPM and acquired stenosis or regurgitation. The criteria presented in *Table 12* are

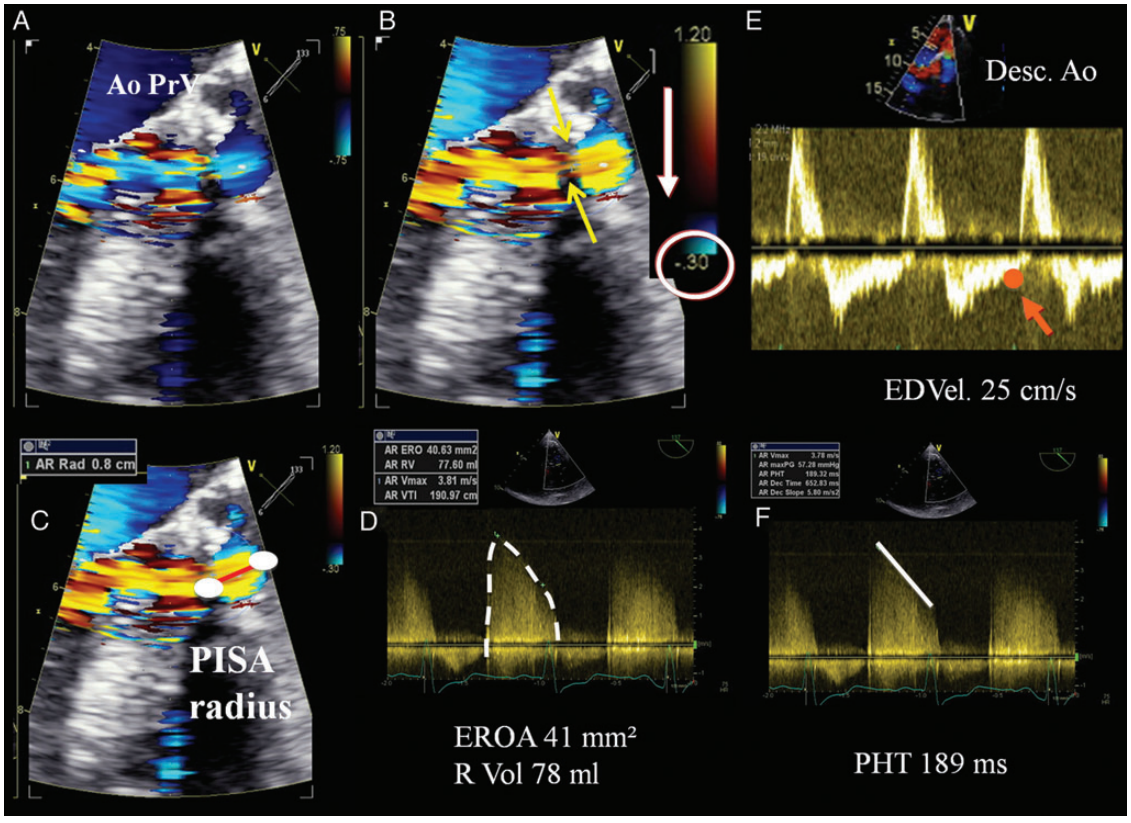

Figure 12 Severe paraprosthetic regurgitation of a mechanical prosthesis in aortic position as assessed by 3D and 2D transoesopgaheal echocardiography (TOE). From a modified 120° approach, the paraprosthetic regurgitant jet can be seen by colour flow imaging (*A*, *B*, and *C*). Note that a clear regurgitant jet convergence zone and a nicely defined vena contracta (*B*, yellow arrows) of the regurgitant jet can be observed. The radius of the proximal isovelocity surface area (PISA) (*C*, red line) can be measured, and with the PISA method, the effective regurgitant orifice area (EROA) and the regurgitant volume (R Vol) can be calculated (*D*). From the transthoracic approach, there is a holodiastolic flow reversal in the descending thoracic aorta (Desc. Ao) with an end-diastolic velocity (EDVel >20 cm/s, *E*). The PHT is shortened (*F*).

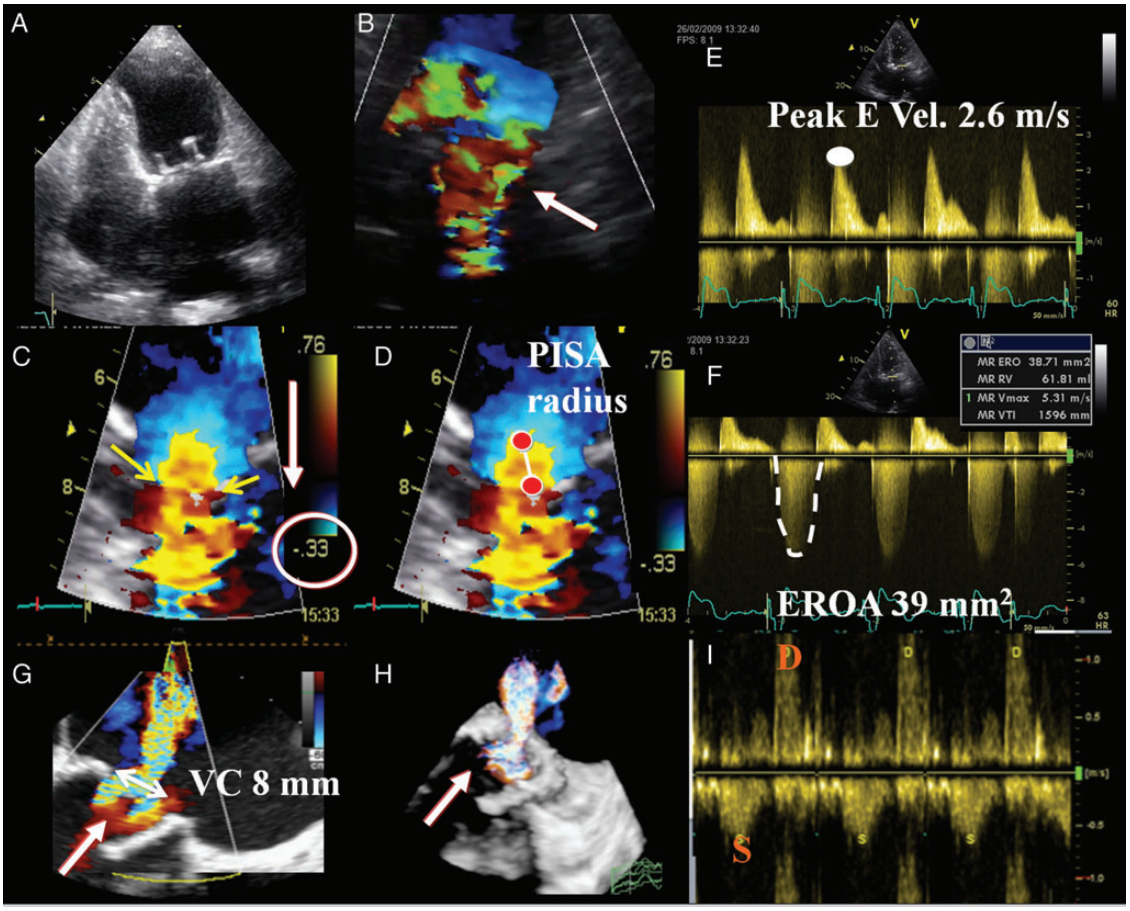

Figure 13 Severe intraprosthetic regurgitation of a bioprosthesis in mitral position (*A*). Note the anterograde turbulent jet (*B*, white arrow) due to the high blood volume (normal anterograde flow + regurgitant volume) passing through the prosthesis. Consequently, the peak velocity of the early diastolic flow is increased ($E = 2.6$ m/s) in relation to the increase in flow (*E*). With colour flow Doppler, and by shifting the baseline into the direction of the regurgitant jet, a clear regurgitant jet convergence zone and a nicely defined vena contracta (*C*, yellow arrows) of the regurgitant jet can be observed. The radius of the proximal isovelocity surface area (PISA) (*D*, white line) can be measured, and with the PISA method the effective regurgitant orifice area (EROA) and the regurgitant volume (R Vol) can be calculated (*F*). Moreover, the analysis of the pulmonary vein flow pattern shows reversal of the systolic S wave (*I*), indicative of severe regurgitation. Same regurgitation from 2D and 3D transoesphageal approach (*G* and *H*).

related to pure PPM with no concomitant dysfunction. In the presence of acquired stenosis, the EOA is significantly below these values and the leaflet morphology/mobility is generally abnormal. The projected indexed EOA is the only parameter that is valid to identify and quantitate PPM in the presence of concomitant stenosis. If there is doubt, CT or cinefluoroscopy can support echocardiography in the diagnosis of pure PPM by showing normal leaflet function, the absence of masses, and small GOA (*Figures 17* and *18*).[130]

Key points

PPM should be distinguished from PHV dysfunction. PPM is present early after surgery and on all subsequent echocardiograms. The echocardiographic diagnosis of pannus formation is often a diagnosis of exclusion but may be detected better by CT. At present, integrating multiple qualitative, semi-quantitative, and quantitative findings is the recommended approach for assessing PHV regurgitation.

Follow-up and monitoring

Patients who have recently undergone valve replacement should not be considered as cured and require careful and, when necessary, frequent follow-up.[133] Ideally, a comprehensive baseline TTE should be obtained at the first postoperative visit usually after 4–6 weeks when the chest wound has healed, chest wall oedema has resolved, and LV systolic function has recovered. However, if the patient is being transferred to another hospital's care and may not return, it may be better to perform the study before discharge. It is then not recommended to perform routine scans in asymptomatic patients with normally functioning mechanical valves or until 5 (ESC) to 10 (ACC/AHA) years after implantation for those with normally functioning biological valves.[4,5] However, it is suggested that routine TTE should still be performed annually for (i) new designs of biological valve for which durability data are not established; (ii) patients with aortic dilatation at the time of surgery; (iii) patients after

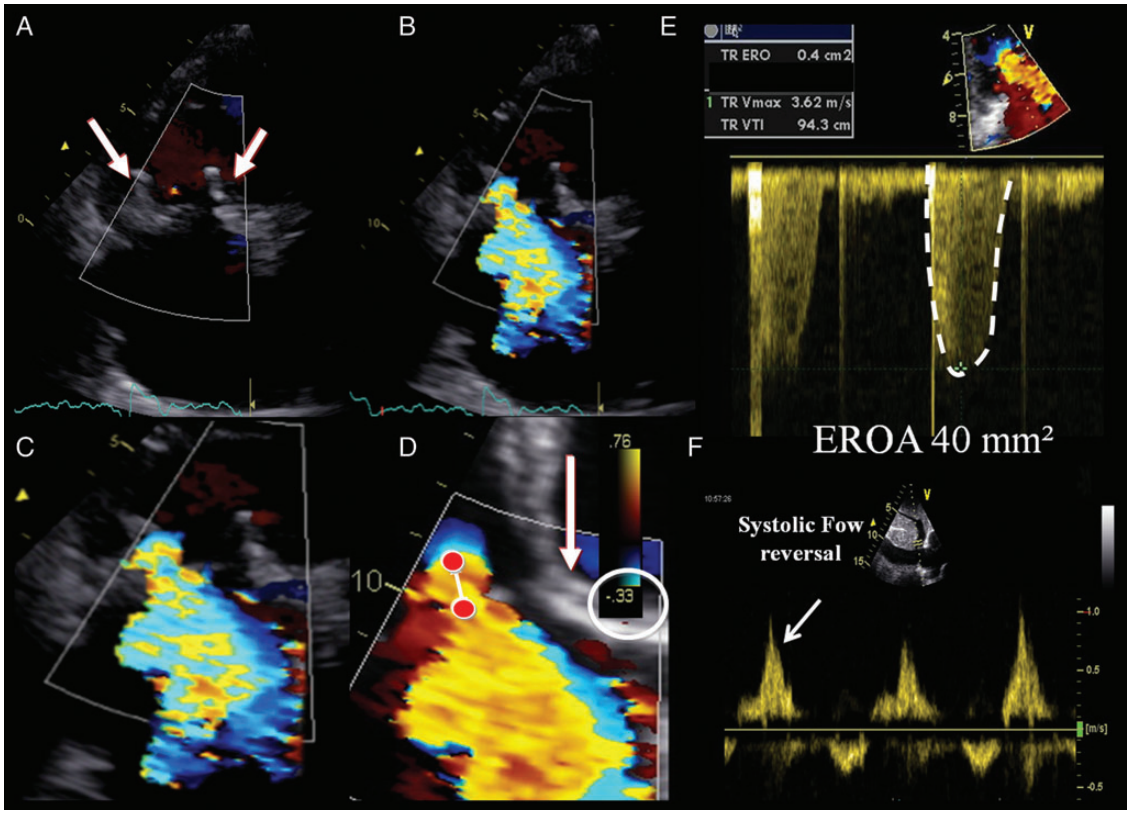

Figure 14 Echocardiographic evaluation of a severe bioprosthesis in tricuspid position (*A*). With colour flow Doppler, and by shifting the baseline into the direction of the regurgitant jet, a clear regurgitant jet convergence zone and a nicely defined vena contracta (*B, C,* and *D*) of the regurgitant jet can be observed. The radius of the proximal isovelocity surface area (PISA) (*D*, white line) can be measured, and with the PISA method the effective regurgitant orifice area (EROA) and the regurgitant volume (R Vol) can be calculated (*E*). Moreover, the analysis of the hepatic vein flow pattern shows reversal of the systolic (S) wave (*F*), indicative of severe regurgitation.

left-sided mitral valve replacement [to check for the development of tricuspid regurgitation (TR) and RV dysfunction]. Echocardiography also becomes indicated if symptoms develop or in case of signs suggesting valve dysfunction or alteration (i.e. thickening of a bioprosthesis, which can represent an early sign of structural valve dysfunction). When TTE/TOE is inconclusive, additional imaging approaches (cinefluoroscopy, cardiac CT, CMR) can be indicated.

Valve-specific approach

Aortic prosthetic valve

Baseline assessment and serial reports

Several clinical and Doppler echocardiographic findings should be reported when assessing aortic PHV function (*Tables 4* and *10*).[7,14] They include (i) measurement of blood pressure; (ii) evaluation of valve morphology and function; (iii) estimation of prosthetic pressure gradients and flow velocities, DVI, EOA; (iv) assessment of regurgitation severity (physiologic/pathologic/central/paravalvular), if present; (v) evaluation of LV size and function; (vi) estimation of pulmonary pressure. The measured value of LVOT and the acoustic window that provides the highest aortic jet velocity are documented. Values should be compared with the normal Doppler data available for each prosthetic valve subtype and size, and the presence of PPM should be noted. The need, the type, and the reason for other imaging approaches required during follow-up should be mentioned. Any changes in aortic PHV morphology and function parameters are documented.

Imaging assessment

Effort should be made to image all portions of the aortic PHV. This involves imaging of the sewing ring, cusps, stents, the occluder(s), and surrounding areas. Echocardiography is the first-line imaging but cinefluoroscopy, cardiac CT, or occasionally CMR can be used when echocardiography is inconclusive (see above).[15,21,29,40,49,63] On TTE, all standard views must be used. Colour Doppler imaging is used to confirm the presence of normal anterograde flow and to demonstrate the expected washing jets.[7,14] Colour Doppler is used to rule out the presence of pathologic valvular or paravalvular jets. The entire circumference of the valve's sewing ring must be assessed. The motion of the cusps or occluder is imaged using parasternal long- and short-axis and the apical three- and five-chamber views. The stents of biological valve are often well seen in the parasternal long-axis view. Careful orientation of the ultrasound beam parallel to the direction of the occluder opening can reduce acoustic shadowing across the plane of the valve and improve occluder visualization. This is

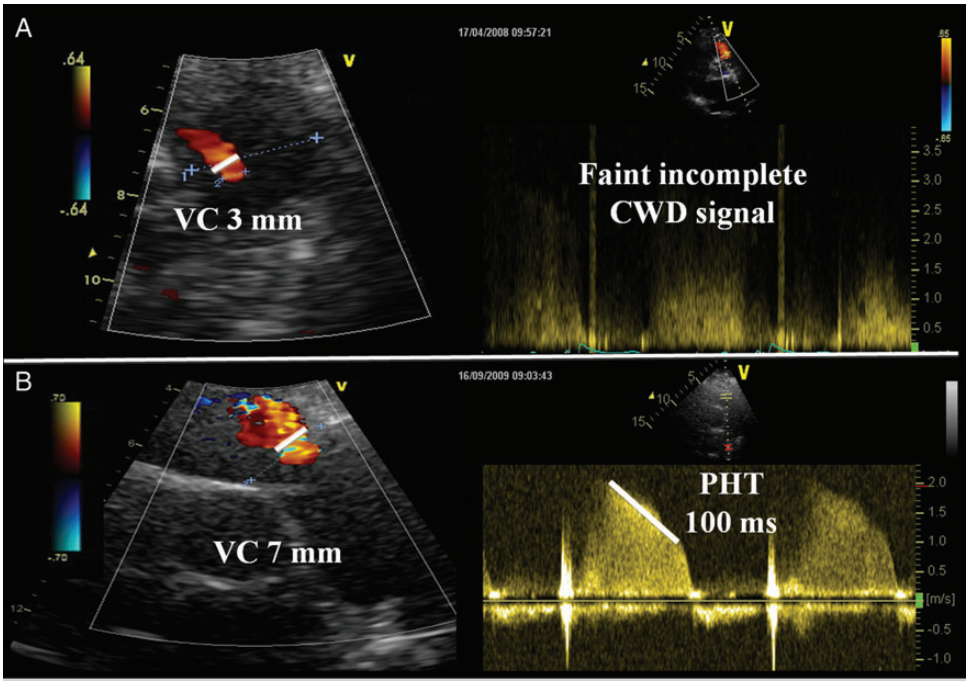

Figure 15 Examples of moderate (*A*) and severe (*B*) intraprosthetic pulmonary regurgitation after a Ross procedure. Colour flow Doppler shows a intraprosthetic central regurgitation jet with a narrow vena contracta width, and continuous wave Doppler (CWD) reveals a faint incomplete signal (*A*), as opposed to a larger vena contracta width and an intense CWD signal and a short PHT in case of severe regurgitation (*B*).

particularly useful for the apical views. Of note, the origin of prosthesis AR (central vs. paravalvular) is best imaged in the parasternal short-axis view. Paravalvular regurgitant jets located posteriorly are however often totally or partially masked in the parasternal long-axis or short-axis views because of the shadowing caused by the prosthetic valve stent. Apical views should thus be carefully examined to properly detect and quantitate these posterior jets. On TOE, the reference view is at mid-oesophageal level usually with a rotation to ~45° and 120° to obtain a short- and long-axis visualization of the valve, showing closure and opening of the aortic cusps or movement of the occluder, and the presence of AR.[15,134] The long-axis view (TTE and TOE) permits visualization of the LVOT, the aortic annulus, the aortic cusps, the sinuses of Valsalva, the sino-tubular junction, and the first centimetres of the tubular aorta. Deep transgastric TOE views at 0° image are also used to evaluate the LVOT, the prosthesis, and the proximal part of the aorta. With TOE, anterior regurgitant jets may be under-detected or underestimated in some views due to the shadowing phenomenon. The jets located on the lateral or medial aspects of the aortic PHVs are often difficult to visualize in the standard TTE and TOE views, and it is necessary to obtain off-axis/intermediary views to reveal these jets. 3D echocardiography, especially during TOE, is ideal for imaging the entire aortic prosthesis, the whole sewing ring, and the extent of any paravalvular leak (*Figure 16*).[22–24]

Valve morphology and function

Aortic PHV dysfunction, stenosis and/or regurgitation, is generally associated with abnormal valve morphology and/or mobility. Imaging may demonstrate the aetiology of dysfunction by showing evidence of leaflet degeneration [thickening (>3 mm), calcification, abnormal mobility] in bioprostheses, abnormal occluder/disc motion in mechanical PHVs, or excessive motion of the sewing ring. If the cusps are thickened or if the occluder has reduced opening, then the valve is likely to be obstructed. Conversely, if the cusps and occluder are thin and open normally, then the valve is likely to be normal provided that pannus can be excluded. The sutures or small fibrin strands may be visible. Early after implantation, an aortic haematoma and oedema can be observed in stentless valve.

Acquired aortic PHV obstruction

Doppler assessment

Doppler ultrasound assessment (CW and pulsed wave) of aortic PHVs is obtained from the apical positions and completed by the interrogation of the right parasternal, suprasternal, and sub-costal views (to measure the highest velocities). CW Doppler signal across the normal aortic PHV usually shows a peak velocity >2 m/s occurring in early systole with a short acceleration time, i.e. the time from the onset of flow to maximal velocity (AT<80 ms), and a triangular envelope.[30,87,111] Increasing grades of obstruction are associated with increasing mean transaortic gradients and peak velocities that occur late in systole with longer AT relative to LV ejection duration and a more rounded Doppler signal (*Figure 19*).

Transaortic gradients and velocities are influenced by prosthesis size, stroke volume, and the presence of PPM or of any obstruction. For example, increased mean transaortic gradients can be observed in small prostheses and in patients with moderate or severe PPM, whereas in patients with severe stenotic aortic PHV, the transaortic

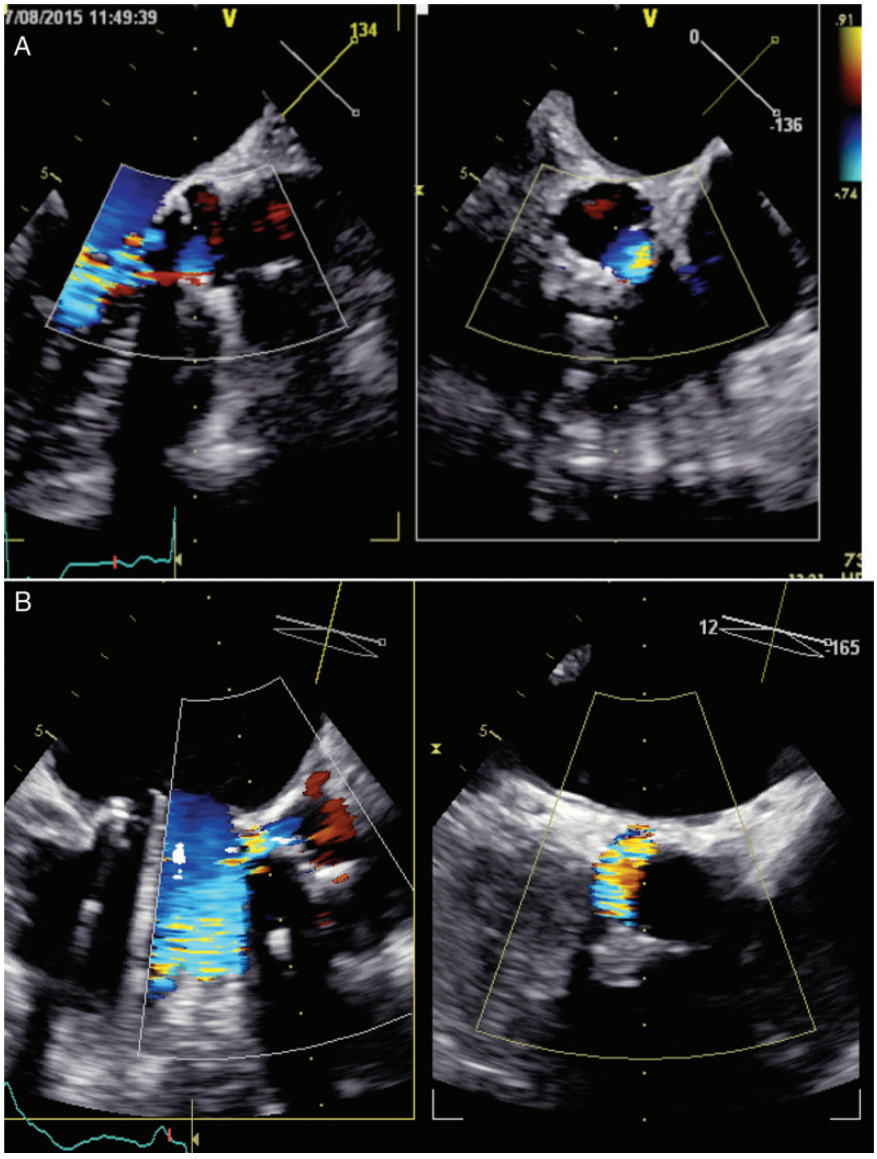

Figure 16 Examples of paraprosthetic aortic regurgitation (*A*, mild regurgitation; *B*, moderate to severe regurgitation) as assessed by multiplane 3D transoesophageal echocardiography.

gradients may be only mildly elevated if concomitant severe LV dysfunction (low flow state) is present. To overcome these limitations, other Doppler-based parameters have been proposed: the AT and the ratio between the AT and the ejection time (ET). An AT >100 ms and an AT/ET ratio >0.37 suggest the presence of aortic PHV stenosis with a good accuracy.[30,111] The advantage of these parameters is that they are independent of Doppler beam angulation in relation to flow direction. On the other hand, the limitation of these parameters is that they are influenced by LV systolic function and chronotropy. Significant aortic PHV stenosis is usually associated with increased transprosthetic peak flow velocity or mean gradient during stress echocardiography ($\geq$3 m/s or $\geq$20 mmHg).[35,135] A change from earlier studies is another specific parameter of PHV stenosis; an increase in mean gradient >10 mmHg or a fall in EOA >25% during follow-up suggests clinically significant obstruction.

The measurement of the EOA and the DVI (VTI_{LVOT}/VTI_{PrV}) provides a less flow-dependent evaluation of the prosthetic aortic valve obstruction.[19] Calculation of the EOA (stroke volume/VTI_{PrV}) by the continuity equation requires accurate estimation of the stroke volume, which depends on precisely recording the LVOT diameter and velocity (both derived from the same anatomical location), and of the aortic jet velocity.[14,25] Although values are to be referenced against normal data for each prosthesis type and size, an EOA <0.8 cm^2 and a DVI <0.25 raise the suspicion of significant aortic PHV stenosis.

Integrative assessment

Echocardiographic detection and grading of aortic PHV obstruction includes integration of data from 2D/3D imaging of the aortic valve as well as qualitative and quantitative Doppler measures of

Table 12 Imaging criteria or the identification and quantitation of prosthesis-patient mismatch

	Mild or not clinically significant	Moderate	Severe
Aortic prosthetic valves			
Indexed EOA (projected or measured)			
BMI <30 kg/m^2	>0.85	0.85–0.66	≤ 0.65
BMI ≥ 30 kg/m^2	>0.70	0.70–0.56	≤ 0.55
Measured EOA vs. normal reference value[a]	Reference $\pm$ 1SD	Reference $\pm$ 1SD	Reference $\pm$ 1SD
Difference (reference EOA − measured EOA) (cm^2)[a]	<0.25	<0.25	<0.25
Valve structure and motion	Usually normal	Usually normal	Usually normal
Mitral prosthetic valves			
Indexed EOA (projected or measured)			
BMI <30 kg/m^2	>1.2	1.2–0.91	≤ 0.90
BMI ≥ 30 kg/m^2	>1.0	1.0–0.76	≤ 0.75
Measured EOA vs. normal reference value[a]	Reference $\pm$ 1SD	Reference $\pm$ 1SD	Reference $\pm$ 1SD
Difference (reference EOA − measured EOA) (cm^2)[a]	<0.25	<0.25	<0.25
Valve structure and motion	Usually normal	Usually normal	Usually normal

See *Tables 7* and *8* to obtain the normal reference values of effective orifice area for the different models and sizes of prostheses.
EOA, effective orifice area; BMI, body mass index; SD, standard deviation.
[a]The criteria proposed for these parameters are valid for near normal or normal stroke volume (50–90 mL).

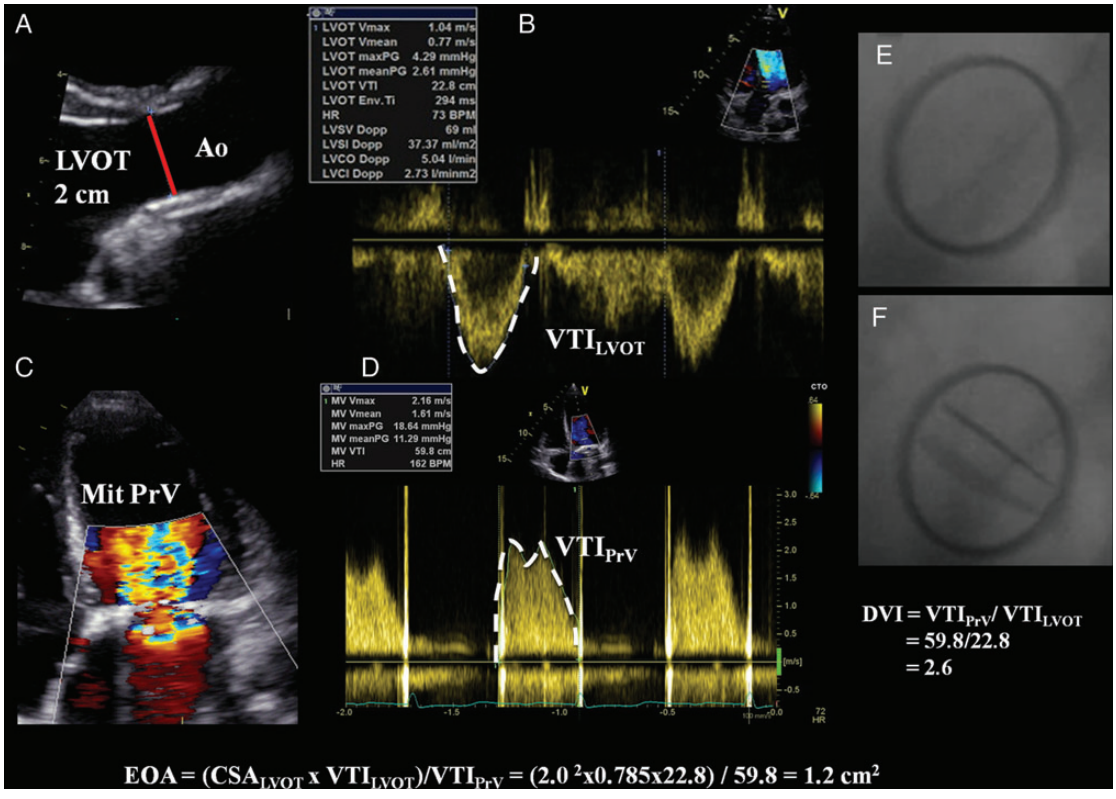

Figure 17 Example of PPM in a patient with a mechanical valve in mitral position. There is an anterograde flow acceleration through the prosthesis as seen with colour flow imaging in *C*. The transprosthetic pressure gradients are high (mean pressure gradient of 11 mmHg, *D*). By applying the continuity equation (*A*, *B*, and *D*), as explained in *Figure 7*, the EOA of this prosthesis is 1.2 cm^2 (0.64 cm^2/m^2), suggesting together with the high-pressure gradient and the increased DVI, either a valve obstruction or a PPM. However, cinefluoroscopy (*E* and *F*) shows normal closing and opening angles, confirming the presence of a PPM.

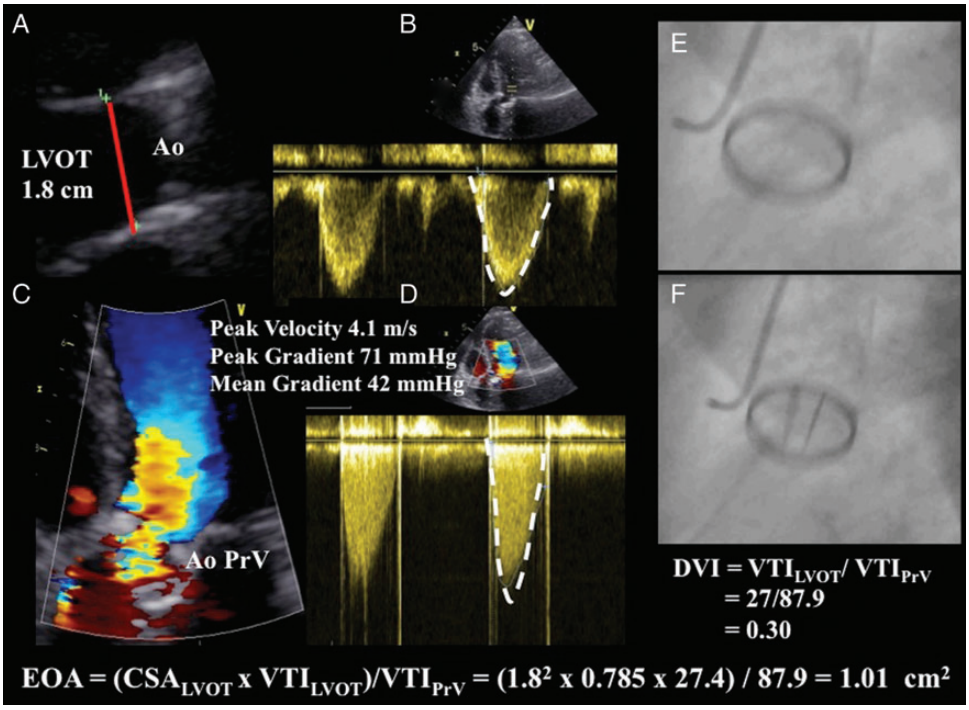

Figure 18 Example of PPM in a patient with a mechanical valve in aortic position. There is an anterograde flow acceleration through the prosthesis as seen with colour flow imaging in *C*. The transprosthetic pressure gradient is high (mean pressure gradient of 42 mmHg, *D*). By applying the continuity equation (*A*, *B*, and *D*) as explained in *Figure 1*, the EOA of this prosthesis is found to be 1.01 cm^2 (0.52 cm^2/m^2), suggesting together with the high-pressure gradient and the low DVI, either a valve obstruction or a PPM. However, cinefluoroscopy (*E* and *F*) shows normal closing and opening angles, confirming the presence of a PPM.

obstruction severity. Other imaging modalities can also be used to assess valve motion, structure, and function. Interpretation of the data should be performed according to the date of valve replacement, the prosthesis' characteristics, and the haemodynamic conditions. *Table 13* lists the imaging parameters used to assess aortic PHV function. When all parameters are normal, the likelihood of valve dysfunction is very low. Conversely, when the majority of the parameters are abnormal, the certainty of aortic PHV obstruction increases.

Differential diagnosis of high-pressure gradients

A high transprosthetic velocity or gradient alone is not a proof of PHV obstruction and may be secondary to PPM, high flow conditions (e.g., post-op period, anaemia, sepsis), occult mitral prosthesis regurgitation, aortic PHV regurgitation, the phenomenon of rapid pressure recovery, technical errors, or localized high central jet velocity in bileaflet mechanical valves.[7] The flow dependency of pressure gradients highlights the need for a stepwise approach including EOA and DVI estimation. The retain algorithm for interpreting these high gradients is derived from a compilation of previously suggested approaches (*Figure 20*).[7,14,102,122,136] After having excluded possible technical errors, the first step is to compare the EOA with the normal reference value of EOA for the type and size of prosthesis implanted. If the EOA is lower than the normal reference value, and especially when there is a decrease in EOA and DVI or an increase in mean gradient over serial studies, the presence of an abnormal prosthesis motion in the context of a DVI <0.25 and AT/ET >0.37 suggests prosthetic valve obstruction. If the measured EOA is close to the normal reference value, one can then calculate the indexed EOA (EOA/BSA) using the measured EOA or alternatively the normal reference value of EOA for the implanted valve (i.e. projected indexed EOA). If the result is <0.85 cm^2/m^2, one can then surmise that PPM is present and that depending on its degree of severity, it may be partially or totally responsible for the high gradient. In this context, it is important to keep in mind that both phenomenon, i.e. PPM and intrinsic dysfunction, may coexist. Of note, PPM is present early after surgery and on all subsequent echocardiograms, so further changes in pressure gradients often account for additional intrinsic dysfunction.

Pathological aortic regurgitation

Colour Doppler evaluation

Using colour flow Doppler, the regurgitant jet into the LV during diastole can be visualized from multiple views. Initial studies that defined AR severity focused on characterization of the colour flow jet.[14,20] Methods that measured jet area or jet length have significant limitations because of variations in haemodynamics, instrument settings, receiving chamber characteristics, jet eccentricity, jet impingement on chamber walls, and variability in perception by readers.[137] The colour jet area and length, which are weakly correlated to the

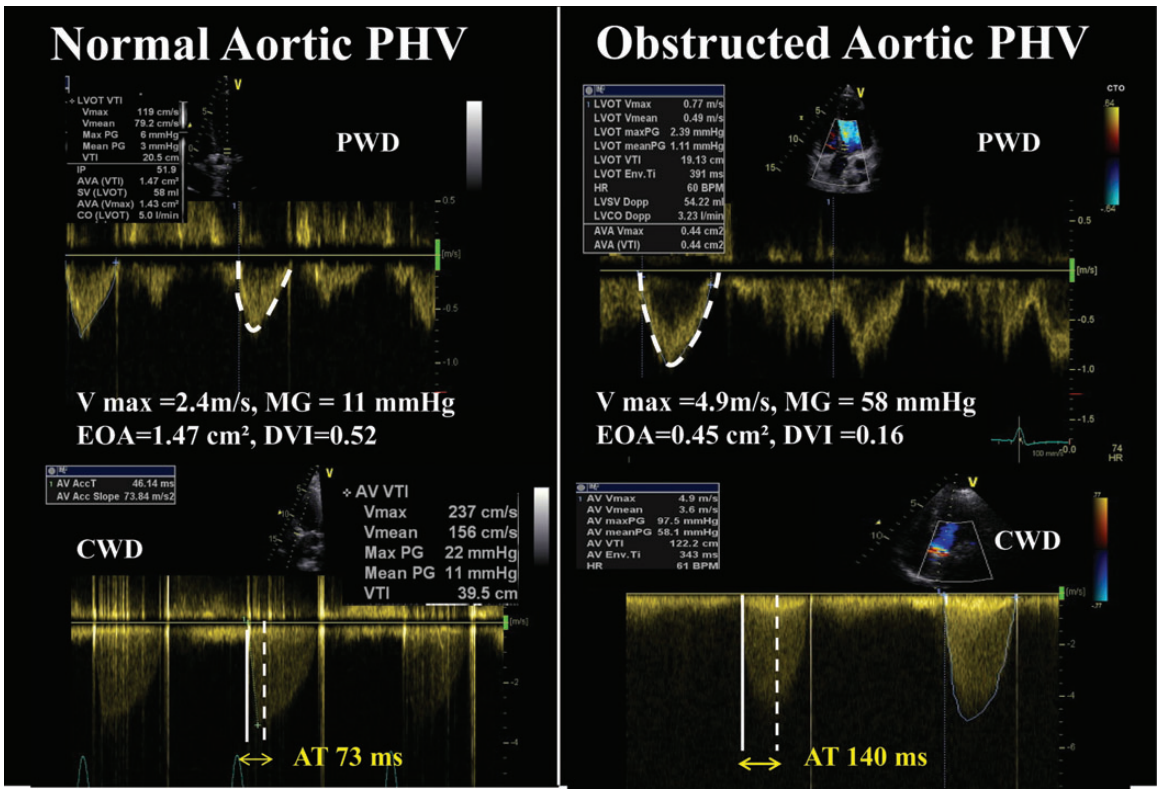

Figure 19 Aortic prosthetic valve obstruction. Haemodynamic profiles of a normally functioning (left panel) vs. obstructed (right panel) prosthesis in aortic position. The normally functioning valve shows low transprosthetic peak flow velocity, low-pressure gradients, a large EOA, and a short acceleration time (time from onset of aortic flow to peak velocity, AT<100 ms), while the obstructed prosthesis shows a high mean pressure gradient, a high peak velocity, a small EOA, and an increased AT (AT>100 ms).

degree of prosthetic AR, are thus not recommended to quantify prosthetic AR.[20] The ratios of regurgitant jet diameter/LVOT diameter from parasternal long-axis view and jet area/LVOT area from parasternal short-axis view just below the prosthesis can be used to estimate the severity of central regurgitation (*Figure 11*). A ratio of jet diameter/LVOT diameter >65% suggests severe regurgitation.[138] However, using this approach, regurgitation severity may be overestimated in the case of eccentric or crescent-shaped jets and underestimated in the case of jets impinging the LVOT wall or the anterior mitral valve.

For semi-quantitative evaluation of paravalvular AR, careful imaging of the neck of the jet in a short-axis view, at the level of the sewing ring, is required to accurately define its circumferential extent, which can be expressed as a percentage of the total sewing ring circumference (<10% = mild; 10–29% = moderate; ≥30% severe) (*Figure 16*).[14,122,139] This method is however limited by the eccentric direction and irregular shape of the defects. Rocking of the prosthesis is usually associated with >40% dehiscence and thus severe regurgitation.[140] The width of the paravalvular jet(s) at origin in multiple views is also helpful to assess severity.

Due to the shadowing caused by the prosthesis ring or stent, the vena contracta width (the regurgitant jet as it traverses the aortic orifice or the effective regurgitant area) may be difficult to measure correctly in the long-axis view and is inaccurate in case of multiple jets, irregular orifice shape, or radial extent of paravalvular jets.[63] When feasible, the measurement of the vena contracta width is useful to distinguish mild from severe prosthetic AR. Using a Nyquist limit of 50–60 cm/s, a vena contracta width of <3 mm correlates with mild AR, whereas a width >6 mm indicates severe AR.

Quantitative assessments based on the proximal isovelocity surface area (PISA) are generally difficult to apply to mechanical aortic prostheses.[141,142] When assessable, especially in bioprostheses with central valvular regurgitation, imaging of the flow convergence zone is usually obtained from the apical three- or five-chamber or parasternal long-axis views. The radius of the PISA is measured at diastole using the first aliasing shell.[20] R Vol and EROA are obtained using the standard formulas. An EROA ≥30 mm^2 or an R Vol ≥60 mL indicates severe prosthetic AR.

Spectral Doppler parameters are useful to assess prosthetic AR, because they are less sensitive to the prosthesis position and the associated shadowing and artefacts. CW Doppler of the AR jet is classically best obtained from the apical five-chamber view. Effort should be made to obtain correct Doppler angle to minimize errors related to possible ultrasound beam misalignment. For eccentric jets, better signals may be obtained from the right parasternal window. The PHT of the CW regurgitant jet signal is useful when the

Table 13 Grading aortic prosthetic valve obstruction

	Normal	Possible obstruction	Significant obstruction
Qualitative			
Valve structure and motion	Normal	Often abnormal[a]	Abnormal[a]
Transvalvular flow envelope[b]	Triangular, early peaking	Triangular to intermediate	Rounded, symmetrical
Semi-quantitative			
Acceleration time (ms)[b]	<80	80–100	>100
Acceleration time/LV ejection time ratio	<0.32	0.32–0.37	>0.37
Quantitative			
Flow dependent			
Peak velocity (m/s)[c,d]	<3	3–3.9	≥4
Mean gradient (mmHg)[c,d]	<20	20–34	≥35
Increase in mean gradient during stress echo	<10	10–19	≥20
Increase in mean gradient during follow-up	<10	10–19	≥20
Flow independent			
Effective orifice area (cm^2)[c,e]	>1.1	0.8–1.1	<0.8
Measured EOA vs. normal reference value[c]	Reference ± 1SD	<Reference −1SD	<Reference −2SD
Difference (reference EOA − measured EOA) (cm^2)[c]	<0.25	0.25–0.35	>0.35
Doppler velocity index[c,e]	≥0.35	0.25–0.34	<0.25

See *Table 7* to obtain the normal reference values of effective orifice area for the different models and sizes of prostheses.
SD, standard deviation.
[a]Abnormal mechanical valves: occluder that is immobile or with restricted mobility, thrombus, or pannus; abnormal biologic valves: leaflet thickening/calcification, thrombus, or pannus.
[b]These parameters are affected by LV function and heart rate.
[c]The criteria proposed for these parameters are valid for near normal or normal stroke volume (50–90 mL) and flow rate (200–300 mL/s).
[d]These parameters are more affected by low or high flow states including low LV output and concomitant aortic regurgitation.
[e]This parameter is dependent on the size of the LV outflow tract.

value is <200 ms, suggesting severe AR, or >500 ms, consistent with mild AR. However, intermediate values of PHT (200–500 ms) are less specific as they are influenced by other variables such as heart rate, LV compliance and pressures, and the acuteness of AR (i.e. in acute AR, the PHT is generally short, regardless of the severity of AR).[143,144] For imaging the diastolic flow reversal in the descending aorta, (i) the sample volume is placed just distal to the origin of the left subclavian artery; (ii) the pulsed wave Doppler is aligned along the major axis of the aorta; (iii) the Doppler filter is decreased to its lowest setting to allow detection of low velocities (<10 cm/s) and the magnitude of the velocity scale is set to 60–80 cm/s for more accurate measurement of end-diastolic flow velocity. With milder degrees of regurgitation, there is a brief reversal of flow limited to early diastole. As the degree of the regurgitation increases, the duration and the velocity of the reversal flow during diastole increase. The presence of holodiastolic flow reversal in the descending thoracic aorta is indicative of at least moderate AR; severe AR is suspected when the end-diastolic velocity is >20 cm/s.[145] The main limitation of this parameter is that it is highly influenced by aorta and LV compliance. Elderly patients with stiff aorta may have holodiastolic flow reversal with trivial or mild AR.

Regurgitant volume can be estimated as the difference between stroke volume at the LVOT (or 2D/3D-derived total LV stroke volume) and the flow at the mitral annulus or at the RVOT. This method cannot be used if there is concomitant >mild mitral or pulmonary regurgitation, respectively. This approach is time consuming and is associated with several pitfalls, the most important being the accurate measure of mitral annulus or RVOT diameter. In general, a regurgitant fraction (RVol divided by the LVOT stroke volume) >50% indicates severe prosthetic AR.[16,20]

The impact of prosthetic AR on the LV depends on the chronicity and severity of the regurgitation as well as on any pre-existing LV dysfunction. In the absence of other conditions, LV dilatation is sensitive for chronic significant AR while a normal LV size almost excludes severe chronic AR. Similarly, if LV volumes fail to decrease after valve replacement for AR or tend to increase after valve replacement for AS and in particular if the LV is hyperdynamic, a haemodynamically significant leak should be suspected. Conversely, LV dilatation may be absent in acute severe AR.[16,20]

Integrative assessment

Echocardiographic assessment of prosthetic AR includes integration of data from 2D/3D imaging of the aortic root, aortic valve, and ventricle as well as Doppler measures of regurgitation severity (*Table 14*). Effort should be made to quantify the degree of regurgitation, except in the presence of mild or less prosthetic AR. The measurement of the vena contracta width and the calculation of the EROA, RVol, and regurgitant fraction are recommended, when feasible. Adjunctive parameters help to consolidate the severity of AR and should be widely used particularly when there is discordance between the quantified degree of prosthetic AR and the clinical context. These parameters should be interpreted according

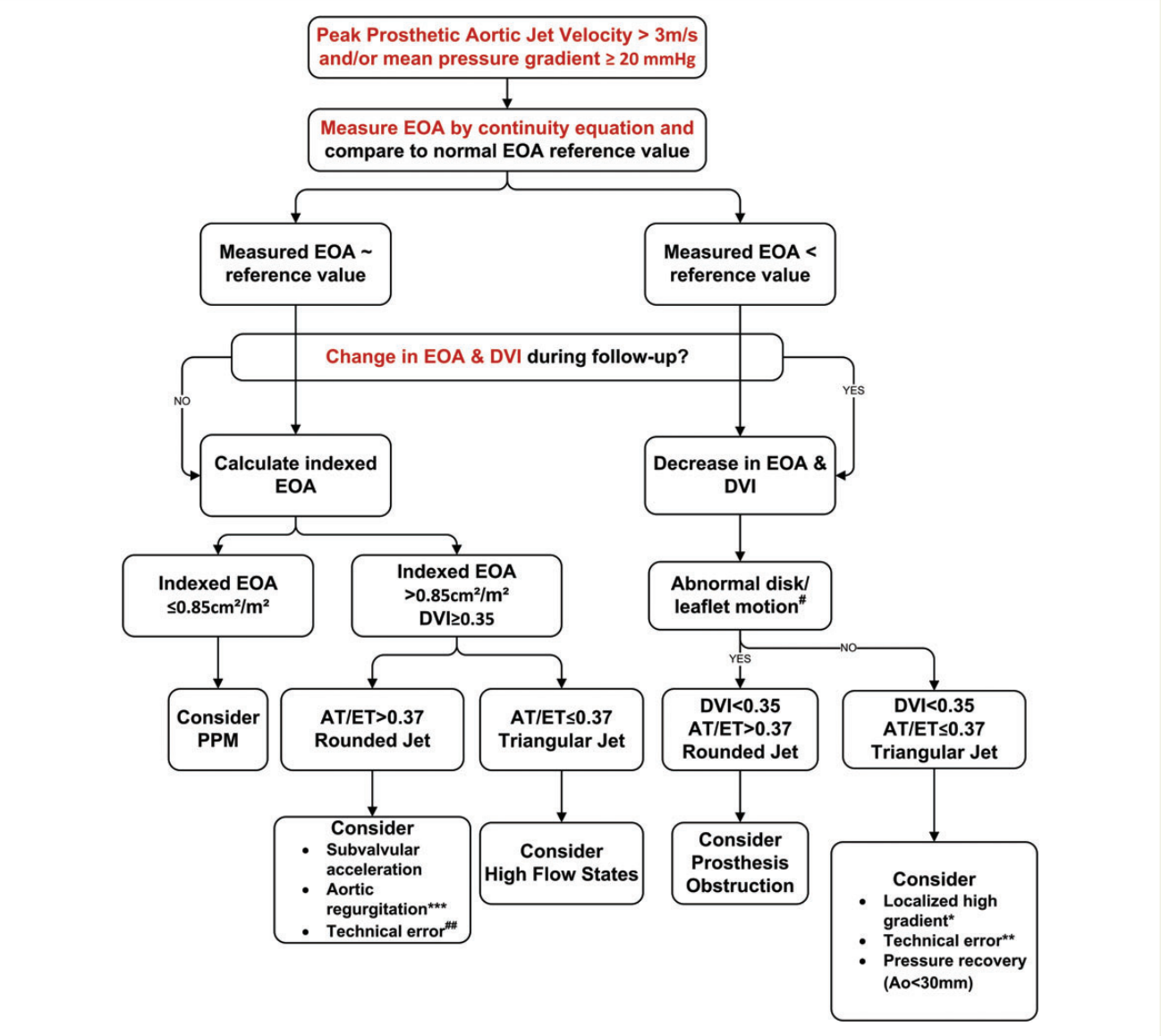

Figure 20 Algorithm for evaluation of high transvalvular aortic gradient. Ao, ascending aorta diameter; AT/ET, acceleration time/ejection time ratio; DVI, Doppler velocity index; EOA, effective orifice area; PPM, patient-prosthesis mismatch. *Bileaflet valves only, small aortic PHV size (19–21 mm). **Consider underestimation of LVOT diameter and/or LVOT VTI. ***Recalculate EOA using RVOT stroke volume. #If leaflet/disc motion unclear by TTE, consider cinefluoroscopy or cardiac CT. ##Consider overestimation of LVOT diameter and/or LVOT VTI.

to the chronicity of prosthetic AR and the LV remodelling. In case of persistent discrepant results and after elimination of technical errors, or when echocardiography is inconclusive, other imaging modalities can be used in experienced centres.

Mitral prosthetic valve

Baseline assessment and serial reports

As for aortic PHV, the echocardiographic report should be comprehensive (*Tables 4* and *10*), including the documentation of (i) the type and size of the prosthetic valve, (ii) blood pressure, (iii) valve morphology and function (including the measure of closing angle for bileaflet mechanical valves when possible), (iv) prosthetic pressure gradients and flow velocities (PHT, DVI, EOA), (v) the heart rate at which gradients are measured, (vi) the presence of regurgitation (location, severity), (vii) LV size and function, (viii) LA size, and (ix) pulmonary pressure.[7,14] Calculated EOA should be compared with reference values for the prosthetic valve type. The presence of any PPM should be reported. When needed, the type and reason for the use of other imaging approaches are to be acknowledged. Any changes in mitral PHV characteristics are documented.

Imaging assessment

All the components of the mitral PHV should be evaluated (sewing ring, cusps, occluder(s), surrounding areas). TTE is the first-line imaging, while TOE is recommended in case of suspected or confirmed dysfunction.[15,21,27,29,134] Cinefluoroscopy, cardiac CT, or

Table 14 Grading the severity of aortic prosthetic valve regurgitation

	Mild	Moderate	Severe
Qualitative			
Valve structure and motion	Usually normal	Usually abnormal[a]	Usually abnormal[a]
Colour flow AR jet width[b]	Small	Intermediate	Large (>65% of LVOT diameter)
CW signal of AR jet	Incomplete or faint	Dense	Dense
Diastolic flow reversal in the descending aorta	Brief, protodiastolic flow reversal	Intermediate	Holodiastolic flow reversal (end-diastolic velocity >20 cm/s)
Semi-quantitative			
Pressure half time (ms)[c]	>500	200–500	<200
Circumferencial extent of paravalvular regurgitation (%)[d]	<10	10–29	≥30
VC width (mm)	<3	3–6	>6
Quantitative			
EROA (mm^2)	<10	10–29	≥30
RVol (mL)[e]	<30	30–59	≥60
Regurgitant fraction (%)	<30	30–50	>50
+LV size[f]			

AR, aortic regurgitation; EROA, effective regurgitant orifice; RVol, regurgitant volume; PHT, pressure half time.
[a]Abnormal mechanical valves: immobile occluder, dehiscence, or rocking (paravalvular regurgitation); abnormal biologic valves: cusps thickening/calcification or prolapse, dehiscence, or rocking (paravalvular regurgitation).
[b]Parameter applicable to central jets and is less accurate in eccentric jets.
[c]This parameter is influenced by left ventricular compliance.
[d]Applies only to paravalvular regurgitation.
[e]Can be estimated by the difference of stroke volume in LVOT minus stroke volume in RV outflow tract (if no >mild pulmonary regurgitation) or at the mitral annulus (if no >mild mitral regurgitation).
[f]Applies to chronic, late post-operative prosthetic aortic valve regurgitation in the absence of other aetiologies.

CMR can be used as complementary tools, if needed (see above).[39,42,64] On TTE, parasternal long- and short-axis views, and all apical views with multiple angulation and off-axis cuts are needed to scan the whole sewing ring, the mitral subvalvular apparatus, and the leaflet/occluder(s) motion. The stents of biological valve are often well seen in the apical four-chamber view. Colour Doppler imaging is used to demonstrate normal forward flow, the expected washing jets, and when present pathologic regurgitation. Acoustic shadowing effects may result in inability to adequately image the LA side of the mitral PHVs, particularly in mechanical prostheses (*Figure 5 Panel A* and *B*).[85,86] Visualization can be improved when the ultrasound beam is oriented parallel to the direction of the occluder opening. The sub-costal view can be helpful to show paraprosthetic jets since the effect of shielding is minimized. TOE is often superior to TTE in detecting and determining the localization and mechanism of prosthetic MR.[146–148] TOE provides better visualization of the LA and mitral regurgitant jet, but acoustic shadowing limits visualization of the LV (*Figure 5*, *Panel C* and *D*). The regurgitant jets are best visualized in the low-oesophageal four-chamber view with rotation of the probe to two- and three-chamber views together with anteflexion and retroflexion. If properly aligned in the centre of the sector, transverse transgastric short-axis view is useful for imaging the entire circumference of the valve/sewing ring. The long-axis view (TTE/TOE) is used to measure the LVOT (see above), while the short-axis view allows determining the circumferential extent of any paravalvular leak. 3D echocardiography, especially during TOE, is ideal for imaging the entire mitral prosthesis, the whole sewing ring, and the extent of paravalvular regurgitation (*Figure 21*).

Valve morphology and function

Imaging may determine the aetiology of obstruction or regurgitation by showing evidence of leaflet degeneration (thickening, calcification, abnormal mobility) in bioprostheses, a rocking motion of the sewing ring or abnormal occluder motion in mechanical PHVs. The occluder in mechanical valves should open quickly and fully and reduced opening is a reliable sign of obstruction provided that LV function is good. In normal bileaflet valves, there might be a slight oscillation of the leaflets during diastole and slight temporal asymmetry of closure. Mitral valve dehiscence occurs mainly in the posterior or lateral region and is only very rarely located anteriorly. The anatomic orientation of the occluders should normally mimic native valve opening; this preserves the inflow pattern and intraventricular LV vortices that are important for LV filling. This is of particular importance for single tilting disk prostheses where the major orifice directs the flow anteriorly as opposed to posteriorly. In a bioprosthesis, the cusps should be thin and fully mobile, with no prolapse. As for aortic position, it is normal to see stitches, fibrin strands, or echoes resembling bubbles in the LV. Heavily calcified cusps (*Figure 22*) and reduced occluder motion are the most reliable signs of obstruction. In a bileaflet mechanical valve, partial obstruction may be obvious when one leaflet clearly moves less than the

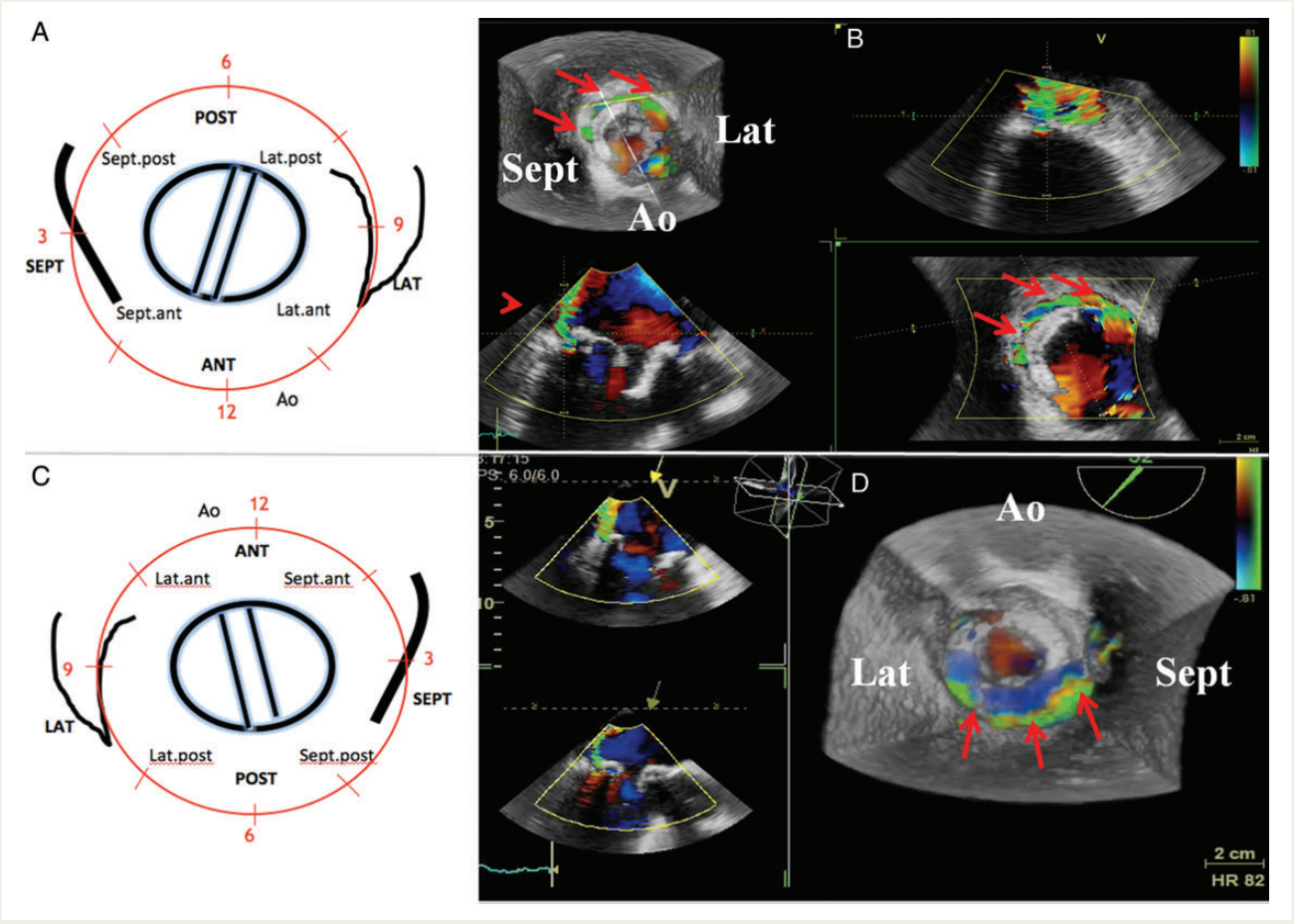

Figure 21 Paravalvular leak due to mitral valve prosthesis dehiscence. Slit-like dehiscence of a bioprosthesis in mitral position from transoesophageal approach, with 3D colour flow Doppler showing the presence of a severe paravalvular regurgitation located posteriorly and involving >25% of the prosthesis circumference from anterior septum to posterior wall of the left atrium (LA) (*B* and *D*). The schematic representation of the prosthesis orientation as seen from the 3D left atrial perspective in *A* and *C* (after reorientation with the aorta up).

other. If the occluder cannot be imaged, obstruction can be suspected when there is a failure of the colour map to fill (narrow high-velocity inflow jet wrap-around aliasing) the PHV orifice in all views. In bioprostheses, the jet can be narrow at the level of the immobile cusps, but can expand rapidly to fill the orifice towards the tips of the stents. Severe impairment in LV function may also cause reduced valve opening, but this will be associated with a thin, low-velocity inflow signal on colour imaging.

Acquired mitral PHV obstruction

Doppler assessment

Doppler ultrasound assessment (CW and pulsed wave) of mitral PHVs is obtained from the apical positions with TTE and low-oesophageal four-chamber view with TOE. Off-axis views may be necessary to correctly align the beam parallel to flow.

Mitral inflow peak early diastolic velocity (*E* velocity) in most normally functioning bileaflet mechanical PHVs is <1.9 m/s but can be as high as 2.4 m/s in small mismatched prostheses.[87,149–151] The normal mean transmitral gradient is generally <5–6 mmHg.[152] Increasing grades of stenosis are associated with increasing transmitral velocities and gradients. However, prosthesis size, ventricular and atrial function, chamber compliances, relative chamber pressures, and the presence of PPM or of any obstruction can influence transmitral velocities. The presence of tachycardia leads to a shortening of the diastolic filling and increased in the peak early mitral velocity.[19] Similarly, significant MR, which leads to a volume overload state, increases transmitral flow velocities. All this highlights the need for comparing serial values in the same patient over time.[14] In the absence of any these conditions, an early mitral peak velocity ≥2.5 m/s and a mean transmitral pressure gradient ≥10 mmHg suggest the presence of severe mitral prosthetic obstruction.[14] Significant mitral PHV obstruction is usually associated with increased transprosthetic [mean gradient (≥12 mmHg) during stress echocardiography (*Figure 23*)].[35,135] A change from immediate post-operative values is also supportive of acquired PHV obstruction. An increase in mean gradient >5 mmHg with similar heart rates is suggestive of the occurrence of valve obstruction.

A PHT <130 ms is often consistent with normal mitral PHV function, whereas a PHT >200 ms on sequential echocardiograms suggests the presence of significant stenosis. As PHT is influenced by

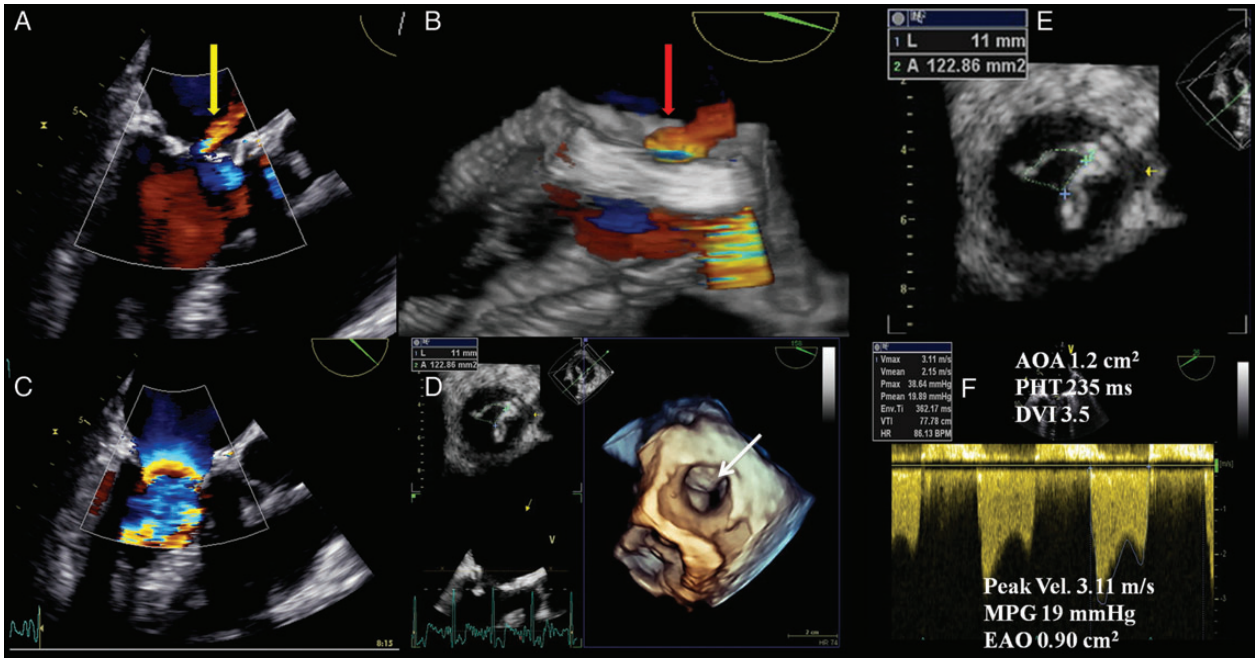

Figure 22 Degenerative mitral bioprosthesis and high gradient. Dysfunctional bioprosthesis as seen with 2D and 3D transoesophageal echocardiography (TOE). 2D (*A*) and 3D (*B*) colour flow imaging of the prosthesis show an abnormal intraprosthetic regurgitation (yellow arrow in 2D TOE and red arrow in 3D TOE). 2D colour flow imaging of the anterograde flow shows a significant aliasing at the level of the prosthesis indicative of a high-velocity flow profile (*C*). Incomplete opening of one of the cusps (anterior) is seen from the 3D dataset (*D*, white arrow). *E* and *F* showing the anatomic orifice area (AOA) obtained by planimetry and the EOA obtained by the continuity equation. Both confirm significant obstruction.

heart rate, LA, and LV compliance, patients with tachycardia or reduced atrioventricular compliance may exhibit a normal PHT despite the presence of significant prosthetic valve stenosis. PHT should not be obtained in case of first-degree atrioventricular block when *E* and *A* velocities are merged or the diastolic filling period is short. Slight increments in PHT (130–200 ms) are to be interpreted with caution.[149,151]

The EOA and the DVI (VTI_{PrV}/VTI_{LVOT}) are less flow-dependent parameters. The EOA is calculated using the continuity equation (stroke volume/VTI_{PrV}), which is not valid in case of >mild MR or AR. In case of AR, the RVOT stroke volume can be used as an alternative approach. Conversely, the PHT-derived EOA is not valid in prosthetic mitral valve.[103,108] The correct interpretation of DVI requires the absence of significant AR. Although values are to be referenced against normal data for each prosthesis type and size, an EOA <1 cm^2 and a DVI >2.5 raise suspicion for significant mitral PHV obstruction.[14]

Integrative assessment

Echocardiographic assessment of mitral PHV obstruction includes integration of data from 2D/3D imaging of the mitral valve as well as qualitative and quantitative Doppler measures of obstruction severity (*Figure 24*). Other imaging modalities, when indicated, can be used to alternatively assess valve motion, structure, and function. For instance, in case of Doppler silent prosthetic valve thrombosis, which is characterized by normal or slightly elevated Doppler gradients, identification of abnormal disk motion of the bileaflet mitral PHV can require the use of cinefluoroscopy or cardiac CT.[45]

Interpretation of the data should be performed according to the date of valve replacement, the prosthesis' characteristics, and the haemodynamic conditions. *Table 15* lists the imaging parameters used to assess mitral PHV function. When all parameters are normal, the probability of valve dysfunction is very low while PHV dysfunction is likely if the majority of them are abnormal.[149]

Differential diagnosis of high-pressure gradients

In a mitral prosthesis, a mean gradient of 6 mmHg or more may indicate pathologic obstruction, the presence of hyperdynamic states (e.g. post-op period, anaemia, sepsis), tachycardia, PPM, regurgitation, technical errors, or localized high central jet velocity in bileaflet mechanical valves.[7,14,102,122,136] To overcome the flow dependency of pressure gradients, a stepwise approach including EOA and DVI estimation is required (*Figure 24*). After having excluded possible technical errors, the EOA is compared with the normal reference value of EOA for the type and size of prosthesis implanted. If the EOA is lower than the normal reference value, and especially when there is a decrease in EOA and DVI during follow-up, the presence of an abnormal prosthetic motion (or suspected by abnormal colour flow) in the context of a DVI >2.2 and PHT ≥ 130 ms suggests prosthetic valve obstruction. A PHT <130–200 ms in a patient with a high transprosthetic gradient is not a sign of pathologic obstruction but rather is a sign of a high transprosthetic flow rate, especially when the leaflet/disc mobility is normal. In this situation, lower velocities can be obtained by careful Doppler beam orientation to avoid this central acceleration. If the EOA is close to the

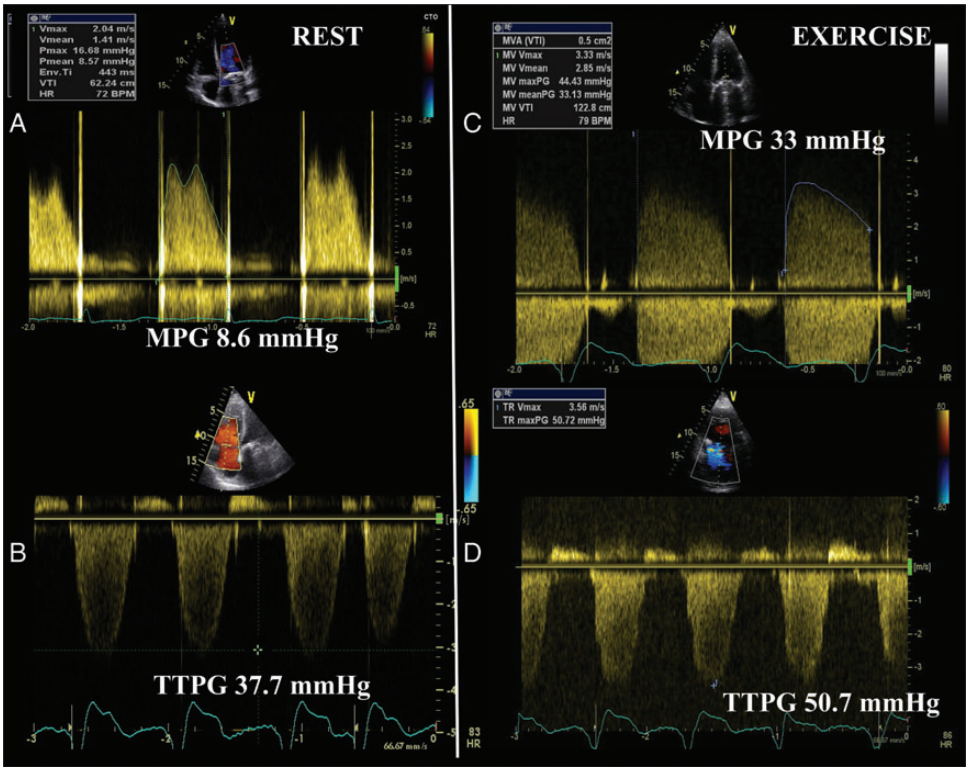

Figure 23 Mitral valve prosthesis dysfunction and exercise echocardiography. Significant increase in mean pressure gradient (MPG) during exercise echocardiography over a prosthetic mechanical valve in mitral position (*C*) in a patient with mildly elevated resting gradients (*A*), complaining of exercise-induced dyspnoea. During exercise (*D*), there is a significant increase in transtricuspid pressure gradient (TTPG) compared with rest (*B*) that parallels the increase in pressure gradients across the mitral prosthesis.

reference value, one can calculate the indexed EOA (EOA/BSA) with measured or projected (normal reference value) EOA. If the indexed is $\leq$1.2 cm^2/m^2, one can assume that PPM is present and that depending on its degree of severity, it may be partially or totally responsible for the high gradient. In this context, it is important to keep in mind that both phenomenon, i.e. PPM and intrinsic dysfunction, may coexist. Of note, PPM is present early after surgery and on all subsequent echocardiograms, so further changes in pressure gradients often account for additional intrinsic dysfunction. In the other case (indexed EOA $>$1.2 cm^2/m^2), if the leaflet mobility is considered to be normal or is undetermined and the DVI is $<$2.2, one should suspect occult mitral trans- or paravalvular regurgitation or high flow states.

Pathological mitral regurgitation

Colour Doppler evaluation

Rating the severity of prosthetic MR is also a considerable challenge. The volume of the regurgitant flow jet is determined by the size of the regurgitant orifice, the driving force from the pressure gradient across the orifice, and the duration of systole.[20]

Colour flow imaging is the most common way to assess MR severity. The general assumption is that as the severity of the MR increases, the size and the extent of the jet into the LA also increase.[153] However, the relation between jet area and MR severity presents a large range of variability. So, this approach is a source of many errors and is not recommended to assess MR severity.[20] Nevertheless, the detection of a large eccentric jet adhering, swirling, and reaching the posterior wall of the LA is in favour of significant prosthetic MR. Conversely, small thin jets that appear just beyond the mitral leaflets usually indicate mild MR.[154]

On colour Doppler, paravalvular leaks have a typical appearance of a jet that passes from the LA into the LA outside the prosthesis ring and often projects into the atrium in an eccentric direction. For semi-quantitative evaluation of paravalvular MR, careful imaging of the neck of the jet in a short-axis view, at the level of the sewing ring, is required to accurately define its circumferential extent, which can be expressed as a percentage of the total sewing ring circumference ($<$10% = mild; 10–29% = moderate; $\geq$30% severe).[155] Rocking of the prosthesis is usually associated with $>$40% dehiscence and thus severe regurgitation.

The vena contracta is the area of the jet as it leaves the regurgitant orifice; it reflects thus the regurgitant orifice area. The vena contracta width is useful to distinguish mild from severe prosthetic MR. It is measure from the parasternal long-axis or apical four-chamber views. A vena contracta $<$3 mm indicates mild prosthetic MR while a width $\geq$7 mm defines severe MR.[151] Due to the shadowing caused by the prosthetic material, the vena contracta width may be difficult to assess. It is inaccurate in case of multiple jets or irregular orifice shape.[14,20]

The PISA method is feasible, especially in bioprosthetic valves (*Figure 13*). Imaging of the flow convergence zone is usually obtained from the apical four-chamber view, though other views can be used if parallel to regurgitant flow direction.[153,156] The area of interest is optimized by lowering imaging depth and reducing the Nyquist limit to ~15–40 cm/s. The radius of the PISA is measured at mid-systole

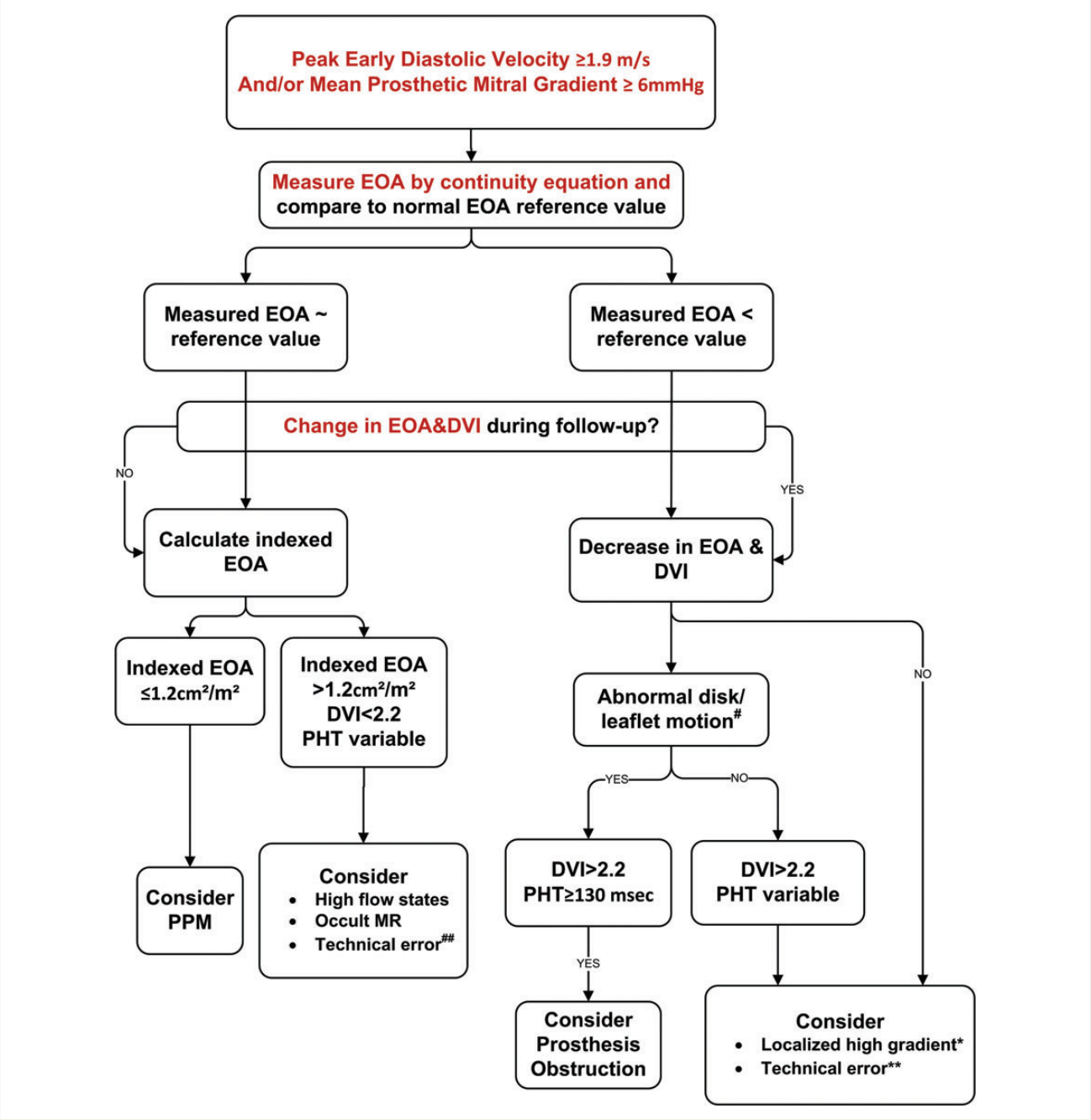

Figure 24 Algorithm for evaluation of high transvalvular mitral gradient. DVI, Doppler velocity index; EOA, effective orifice area; PPM, patient-prosthesis mismatch. *Bileaflet valves only. **Consider underestimation of LVOT diameter and/or LVOT VTI. #If leaflet/disc motion unclear by TTE, consider cinefluoroscopy or cardiac CT. ##Consider overestimation of LVOT diameter and/or LVOT VTI.

using the first aliasing. R Vol and EROA are obtained using the standard formulas. Qualitatively, the presence of flow convergence at a Nyquist limit of 50–60 cm/s should alert to the presence of severe MR. Grading of severity of MR classifies regurgitation as mild, moderate, or severe, and sub-classifies the moderate regurgitation group into 'mild-to-moderate' (EROA of 20–29 mm^2 or a R Vol of 30–44 mL) and 'moderate-to-severe' (EROA of 30–39 mm^2 or a R Vol of 45–59 mL). Quantitatively, prosthetic MR is considered severe if EROA is $\geq$40 mm^2 and R Vol $\geq$60 mL. The PISA method faces several advantages and limitations, which have been addressed elsewhere. Briefly, the PISA method is based on the assumption of hemispheric symmetry of the velocity distribution proximal to the circular regurgitant lesion, which may not hold for eccentric jets, multiple jets, or complex or elliptical regurgitant orifices.[20] Also the acoustic shadowing may hamper the proper visualization of the PISA.

Spectral Doppler parameters can be used as additive or alternative features to corroborate severity of regurgitation. In the absence

Table 15 Grading mitral prosthetic valve obstruction

	Normal	Possible obstruction	Significant obstruction
Qualitative			
Valve structure and motion	Normal	Often abnormal[a]	Abnormal[a]
Semi-quantitative			
Pressure half time (ms)[b]	<130	130–200	>200
Quantitative			
Flow dependent			
Peak velocity (m/s)[c,d,f]	<1.9	1.9–2.5	≥2.5
Mean gradient (mmHg)[c,d,f]	≤5	6–10	≥10
Increase in mean gradient during stress echo	<5	5–12	>12
Follow-up increase in mean gradient	<3	3–5	>5
Flow independent			
Effective orifice area (cm^2)[c,g]	≥2	1–2	<1
Effective orifice area vs. normal reference value[c,g]	Reference ± 1SD	<Reference −1SD	<Reference −2SD
Difference (reference EOA − measured EOA) (cm^2)[c]	<0.25	0.25–0.35	>0.35
Doppler velocity index[c,d,e,g]	<2.2	2.2–2.5	>2.5

See *Table 8* to obtain the normal reference values of effective orifice area for the different models and sizes of prostheses.
PHT, pressure half time; SD, standard deviation.
[a]Abnormal mechanical valves: occluder that is immobile or with restricted mobility, thrombus or pannus; abnormal biologic valves: cusps thickening/calcification, thrombus, or pannus.
[b]This parameter is influenced by heart rate, left atrial compliance, and left ventricular compliance. This parameter should not be measured during tachycardia, first atrioventricular block, or circumstances that cause fusion between the *E* and *A* velocities or shorten the diastolic filling period.
[c]The criteria proposed for these parameters are valid for near normal or normal diastolic volume (i.e. stroke volume: 50–90 mL) and heart rate (50–80 bpm).
[d]These parameters are also abnormal in the presence of significant mitral prosthesis regurgitation.
[e]This parameter is dependent on the size of the LV outflow tract. In atrial fibrillation, the VTI_{PrMV} and the VTI_{LVOT} should be measured in matched cardiac cycles.
[f]These parameters are more affected by flow and heart rate.
[g]These parameters are not valid when >mild concomitant aortic or mitral regurgitation is present.

of prosthetic mitral obstruction, the increase in transprosthetic mitral flow that occurs with increasing MR severity can be detected as higher flow velocities during early diastolic filling (increased *E* velocity). In the absence of mitral stenosis, a peak *E* velocity >1.5 m/s at PW Doppler suggests severe prosthetic MR. Conversely, a dominant A wave (atrial contraction) basically excludes severe MR. The presence of a retrograde systolic flow (PW Doppler 1 cm deep into the pulmonary vein) in one or more of the pulmonary veins is another specific parameter for significant MR (*Figure 13*).[157] A dense MR signal with a full CW Doppler envelope also indicates more severe MR than a faint signal. When truncated (notched) with a triangular contour and an early peak velocity (blunt), it indicates elevated LA pressure or a prominent regurgitant pressure wave in the LA due to severe MR. In eccentric MR, it may be difficult to record the full CW envelope of the jet because of its eccentricity.

Regurgitant volume can be calculated by subtracting the forward stroke volume at the LVOT (or RV stroke volume if >mild AR) from the total transmitral stroke volume (or 2D/3D-derived total LV stroke volume). This approach is time consuming and is associated with several drawbacks. In general, a regurgitant fraction >50% indicates severe prosthetic MR.

The impact of prosthetic MR on LV, LA, and pulmonary pressures depends on the chronicity and severity of the regurgitation as well as on the pre-existing cardiomyopathy. In the absence of other conditions, LV and LA dilatation are sensitive for chronic significant MR, while normal size almost excludes severe chronic MR. Similarly, if LV volumes fail to decrease after valve replacement for MR or tend to increase after valve replacement for mitral stenosis, and in particular if the LV is hyperdynamic, a haemodynamically significant leak should be suspected among other factors. Conversely, LV or LA dilatation may be absent in acute severe MR.

Given that direct detection of prosthetic MR is often not possible with TTE, the presence of occult prosthetic MR should be suspected when the following signs are present: (i) the presence of flow convergence on the LV side of the prosthesis during systole; (ii) the presence of a turbulent colour flow within the LA distal to the acoustic shadow; (iii) increased mitral peak *E* wave velocity, gradient, and/or DVI; (iv) unexplained or new worsening of pulmonary arterial hypertension; and a dilated and hyperkinetic LV. PHT is often normal in prosthetic MR unless there is concomitant stenosis.[149,158] TOE should be systematically performed when there is a clinical or TTE suspicion of occult MR.[134]

Integrative assessment

Echocardiographic assessment of prosthetic MR includes integration of data from 2D/3D imaging of the valve and ventricle as well as Doppler measures of regurgitation severity (*Table 16*). An effort should be made to quantify the degree of regurgitation, except in the presence of mild or less prosthetic MR. The measurement of the vena contracta width and the calculation of the EROA, RVol, and regurgitant fraction is recommended, when feasible. Adjunctive parameters help to consolidate the severity of MR and should be widely used particularly when there is discordance between the

Table 16 Imaging criteria for grading the severity of prosthetic mitral valve regurgitation

	Mild	Moderate	Severe
Qualitative			
Valve structure and motion	Usually normal	Usually abnormal[a]	Usually abnormal[a]
Colour flow MR jet[b]	Small	Intermediate	Large central jet or eccentric jet adhering, swirling, and reaching the posterior LA wall
Flow convergence[c]	No or small	Intermediate	Large[d]
CW signal of MR jet	Faint/Parabolic	Dense/Parabolic	Dense/triangular
Semi-quantitative			
Pulmonary vein flow	Systolic dominance	Systolic blunting[e]	Systolic flow reversal[f]
Mitral inflow	Variable	Variable	Peak velocity $\geq$1.9 m/s; Mean gradient $\geq$5 mmHg
Doppler velocity index (VTI_{PrMV}/VTI_{LVOT})	$<$2.2	2.2–2.5	$>$2.5
VC width (mm)	$<$3	3–5.9	$\geq$6
Circumferential extent of paravalvular regurgitation (%)[g]	$<$10%	10–29%	$\geq$30%
Quantitative[h]			
EROA (mm^2)	$<$20	20–39	$\geq$40
RVol (mL)[i]	$<$30	30–59	$\geq$60
Regurgitant fraction (%)	$<$30	30–50	$>$50
+LV and LA size[j] and the systolic pulmonary arterial pressure			

[a]Abnormal mechanical valves: immobile occluder, dehiscence, or rocking (paravalvular regurgitation); abnormal biologic valves: cusps thickening/calcification, dehiscence, or rocking (paravalvular regurgitation).
[b]Parameter applicable to central jets and is less accurate in eccentric jets.
[c]At a Nyquist limit of 50–60 cm/s.
[d]PISA radius $<$0.4 and $\geq$0.9 cm for central jets, respectively, with a baseline shift at a Nyquist limit of 40 cm/s.
[e]Unless other reasons of systolic blunting (atrial fibrillation, elevated LA pressure).
[f]Pulmonary venous systolic flow reversal is specific but not sensitive for severe MR.
[g]Applies only to paravalvular regurgitation.
[h]These quantitative parameters are less well validated than in native MR.
[i]Can be estimated by the PISA method if feasible or by calculating the difference between stroke volume measured at the mitral annulus and stroke volume measured in the LVOT (if no $>$mild aortic regurgitation).
[j]Applies to chronic, late post-operative prosthetic mitral valve regurgitation in the absence of other aetiologies and acute MR.

quantified degree of prosthetic MR and the clinical context. These parameters should be interpreted according to the chronicity of prosthetic MR and the LV remodelling. If results are still discrepant and after elimination of technical errors, or when echocardiography is inconclusive, other imaging modalities can be used in experienced centres to assess valve motion, structure, and function.

Tricuspid prosthetic valve

Baseline assessment and serial reports

The echocardiographic report includes the documentation of (i) the type and size of the prosthetic valve, (ii) blood pressure, (iii) valve morphology and function, (iv) prosthetic pressure gradients and flow velocities (EOA, DVI), (v) the heart rate at which gradients are measured, (vi) the presence of regurgitation (location, severity), (vii) RV size and function, (viii) RA size, (ix) inferior vena cava dimensions and respiratory changes, and (x) pulmonary pressure (*Tables 4* and *10*).[7,14] Calculated EOA should be compared with reference values for the prosthetic valve type. When needed, the type and reason for the use of other imaging approaches are to be acknowledged. Any changes in tricuspid PHV characteristics are documented.

Imaging assessment

Because of the anterior position of the tricuspid PHV, assessment of tricuspid valve by TTE is generally superior to imaging by TOE.[81] The three main TTE views allowing the tricuspid valve visualization are the parasternal (long-axis view of RV inflow, short-axis view at the level of the aortic valve), the apical four-chamber, and the sub-costal views. All views, particularly from the apex, will need multiple tilting to obtain optimal views of the RV and tricuspid valve. The RV inflow and sub-costal views are very useful for assessing colour flow through tricuspid prosthesis, because the acoustic shadowing interference is less than in apical views.[14,20] With TOE standard views of the tricuspid prosthesis include mid-oesophageal four-chamber and modified bicaval views, the mid-oesophageal inflow–outflow view, and the transgastric RV inflow–outflow view.

Valve morphology and function

Imaging may identify the aetiology of PHV dysfunction including obstruction or regurgitation due to bioprosthesis degeneration (thickening, calcification, abnormal mobility), rocking motion of the sewing ring, or abnormal occluder motion in mechanical PHVs.

Acquired tricuspid PHV obstruction

Doppler assessment

Doppler ultrasound assessment (CW and pulsed wave) of tricuspid PHVs is obtained from multiple views. Various transducer positions and off-axis views are used to correctly align the ultrasound beam as much as parallel to flow. Determination of the severity of tricuspid PHV stenosis has been validated in a limited number of patients.

Tricuspid inflow peak early diastolic velocity (*E* velocity) in most normally functioning tricuspid PHVs is $<$1.9 to 2 m/s.[159,160] The normal mean transtricuspid gradient is often $<$6 to 9 mmHg, depending on the prosthesis type. Increasing grades of obstruction are associated with increasing transmitral velocities and gradients. However, velocities vary with respiration, heart rate, chamber compliances and pressures, and the presence of any obstruction. To minimize the respiratory flow variations, averaging a minimum of 5 cycles (during end-expiratory or quiet respiration) is recommended whether the patient is in sinus rhythm or in atrial fibrillation. In the absence of tachycardia or significant TR, an early tricuspid peak velocity $\geq$1.9–2 m/s and a mean transtricuspid pressure gradient $\geq$6–9 mmHg are suggestive of possible tricuspid prosthetic obstruction.[161–163]

A short PHT is often consistent with normal tricuspid PHV function, whereas a significantly prolonged PHT on sequential echocardiograms suggests possible stenosis. As this parameter is influenced by heart rate and right chambers compliance, PHT should be interpreted with caution.[161,162]

The EOA and the DVI (VTI_{PrV}/VTI_{LVOT}) are less flow-dependent parameters. The DVI can be used to distinguish stenosis from regurgitation, because in both cases the gradient is increased. A DVI $\geq$3.2 for tricuspid biosprosthetic valves or $\geq$2 for mechanical bileaflet valve in the absence of significant AR suggests possible tricuspid stenosis.[81,163] The EOA derived by PHT has not been validated in tricuspid PHV. The EOA is thus calculated using the continuity equation (stroke volume/VTI_{PrV}), which is not valid in case of $>$mild AR. In case of AR, the RVOT can be used as an alternative approach. Of note, no cut-off value of EOA has been validated.

Integrative assessment

Echocardiographic assessment of tricuspid PHV obstruction includes integration of data from 2D/3D imaging of the tricuspid valve as well as Doppler measures of stenosis severity (*Figure 25*). Other imaging modalities, when indicated, can be used to alternatively assess valve motion, structure, and function. Interpretation of the data should be performed according to the date of valve replacement, the prosthesis' characteristics, and the haemodynamic conditions. *Table 17* lists the imaging parameters used to assess tricuspid PHV function. More parameters are abnormal, the higher the likelihood of possible PHV dysfunction.

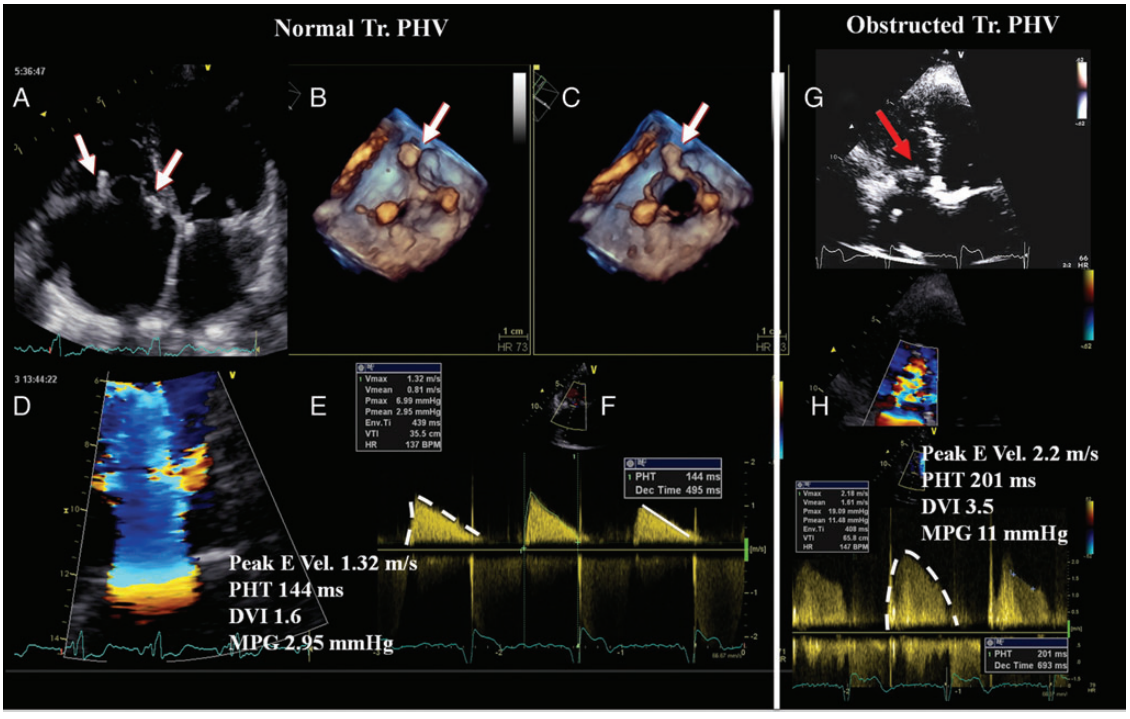

Figure 25 Echocardiographic evaluation of bioprostheses in tricuspid position. Normally functioning prosthesis in *A–F*. Dysfunctional prosthesis with signs of severe stenosis in *G* and *H*. The white arrows in *A–C* indicate the pillars of the prosthesis's frame as seen in 2D transthoracic echocardiography (*A*) and 3D transoesophageal echocardiography (*B*, closed position; *C*, opened position). The haemodynamic parameters [peak early diastolic velocity, pressure half time (PHT), Doppler velocity index (DVI), and mean pressure gradient (MPG)] are all normal (*E* and *F*). Pathologic increased echogenicity of the bioprosthesis (red arrow, *G*), suggestive of prosthesis dysfunction and abnormal haemodynamic parameters, confirming prosthesis dysfunction (*H*).

Table 17 Grading tricuspid prosthetic valve obstruction

	Normal	Possible obstruction[a]
Qualitative		
Valve structure and motion	Normal	Often abnormal[b]
Semi-quantitative		
Pressure half time (ms)	<130	≥130
Doppler velocity index	<2	≥2
Quantitative		
Flow dependent		
Peak velocity (m/s)[c]	<1.9	≥1.9
Mean gradient (mmHg)[c]	<6	≥6

[a]Because of respiratory variation, average 3–5 cycles in sinus rhythm.
[b]Cusps thickening or immobility.
[c]May be increased also with valvular regurgitation.

Differential diagnosis of high-pressure gradients

In a tricuspid prosthesis, a mean gradient of >6 mmHg may denote pathologic obstruction, the presence of hyperdynamic states (e.g., post-op period, anaemia, sepsis), tachycardia, PPM, regurgitation, technical errors, or localized high central jet velocity (only for bileaflet mechanical valves).[122,124] In the presence of normal leaflet/disc mobility, normal or mildly prolonged PHT, and normal DVI, one should suspect PPM, localized high gradient in bileaflet mechanical valves (redo the Doppler recording avoiding central jet velocities), PHV regurgitation or high flow states. Conversely, the presence of an abnormal PHV motion in the context of a high DVI, prolonged PHT, and progressive increase in mean gradient during follow-up suggests prosthetic valve obstruction.

Pathological tricuspid regurgitation

Colour Doppler evaluation

Grading the severity of prosthetic TR is in principle similar to prosthetic MR. However, because standards for determining the TR severity are less robust than for MR, the algorithms for relating colour flow-derived parameters to TR severity are less well developed.

Colour flow imaging is useful for screening the presence of TR. The general assumption is that larger colour jets that extend deep into the RA represent more TR than smaller thin jets that are seen just beyond the tricuspid valve. As for MR, this method is a source of many errors and is limited by several technical and haemodynamic factors.[163,164] Colour flow imaging is not recommended for assessing TR severity. Nevertheless, the detection of a large eccentric jet adhering, swirling, and reaching the posterior wall of the RA is in favour of severe TR.[14,20] Conversely, small thin central jets usually indicate mild TR. It should be noted that normal bioprosthetic valve might have mild TR in the early post-operative period.

The vena contracta width of the TR is typically imaged in the apical four-chamber view using the same settings as for MR. Averaging measurements over at least two to three beats are recommended. A vena contracta ≥7 mm is in favour of severe while a diameter <6 mm may be either mild or moderate TR.[165] Due to the shadowing caused by the prosthetic material, the vena contracta width may be difficult to assess. It is inaccurate in case of multiple jets or irregular orifice shape.

Although providing quantitative assessment, the PISA method has not been validated in the setting of tricuspid PHV. However, in the absence of distortion of the flow convergence zone, the PISA method can be applied to grade severe prosthetic TR.[14,20]

Spectral Doppler parameters can be used as additive or alternative features to corroborate severity of regurgitation. Similar to MR, the severity of TR will affect the early tricuspid diastolic filling (*E* velocity). In the absence of tricuspid stenosis, an elevated tricuspid peak *E* velocity (1.9–2.1 cm/s or greater), although not specific, is a common finding in severe TR. The presence of a holosystolic reversal flow (PW Doppler) in the hepatic vein is another specific parameter for significant TR.[164,166] A dense TR signal with a full CW Doppler envelope also indicates more severe TR than a faint signal. When truncated (notched) with a triangular contour and an early peak velocity (blunt), it indicates a prominent regurgitant pressure wave in the RA due to severe TR. In eccentric TR, it may be difficult to record the full CW envelope of the jet.

Quantitative PW Doppler method has not been validated to quantify the prosthetic TR severity.

The impact of prosthetic TR on right heart chambers depends on the chronicity and severity of the regurgitation as well as on the pre-existing conditions. In the absence of other conditions, RV and RA enlargement (with diastolic septal flattening) and inferior vena cava dilatation with minimal change on respiration are sensitive for chronic significant TR while normal size almost excludes severe chronic TR. When these findings are absent, the presence of significant TR should be questioned.

Integrative assessment

Echocardiographic assessment of prosthetic TR includes integration of data from 2D/3D imaging of the valve, right heart chambers, septal motion and inferior vena cava, as well as Doppler measures of regurgitant severity (*Table 18*). The consensus of the experts is to advocate grading the severity of TR by using the vena contracta width, except in the presence of mild or trivial TR. Adjunctive parameters help to consolidate about the severity of TR. These parameters should be interpreted according to the chronicity of prosthetic TR and the RV remodelling. In case of discrepant/inconclusive echo results, other imaging modalities imaging can be used in experienced centres to assess valve motion, structure, and function.

Pulmonary prosthetic valve

Baseline assessment and serial reports

The echocardiographic report includes the documentation of (i) the type and size of the prosthetic valve, (ii) valve morphology and function, (iii) prosthetic pressure gradients and flow velocities, (iv) the presence of regurgitation (location, severity), (v) RV size and function, (vi) pulmonary pressure, (vii) pulmonary artery dimension (*Tables 4* and *10*).[7,14] When needed, the type and reason for the use of other imaging approaches are to be acknowledged. Any changes in pulmonic PHV characteristics are reported.

Imaging assessment

Because the pulmonary valve is located anteriorly and superiorly, it is often difficult to fully visualize by either TTE or TOE.[20] With TTE,

Table 18 Grading the severity of tricuspid prosthetic valve regurgitation

	Mild	Moderate	Severe
Qualitative			
Valve structure and motion	Usually normal	Usually abnormal[a]	Usually abnormal[a]
Colour flow TR jet[b]	Small	Intermediate	Very large central jet or eccentric wall impinging jet
Flow convergence[c]	No or small	Intermediate	Large[d]
CW signal of TR jet	Faint/Parabolic	Dense/Parabolic	Dense/Early peaking
Semi-quantitative			
Hepatic vein flow	Systolic dominance	Systolic blunting[e]	Systolic flow reversal[f]
Tricuspid inflow	Variable	Variable	Elevated pressure gradient
VC width (mm)	ND	<7	>7
Quantitative			
EROA (mm^2)	ND	ND	ND
R Vol (mL)	ND	ND	ND
Regurgitant fraction (%)	ND	ND	ND
+RA-RV-IVC dimensions[g]			

[a]Dehiscence (paravalvular regurgitation), leaflet thickening/calcification (paravalvular regurgitation); abnormal biologic valves: cusps thickening/calcification.
[b]Parameter applicable to central jets and is less accurate in eccentric jets.
[c]At a Nyquist limit of 50–60 cm/s.
[d]Baseline Nyquist limit shift of 28 cm/s.
[e]Unless other reasons of systolic blunting (atrial fibrillation, elevated RA pressure).
[f]Pulmonary venous systolic flow reversal is specific but not sensitive for severe MR.
[g]Applies to chronic, late post-operative prosthetic tricuspid valve regurgitation.

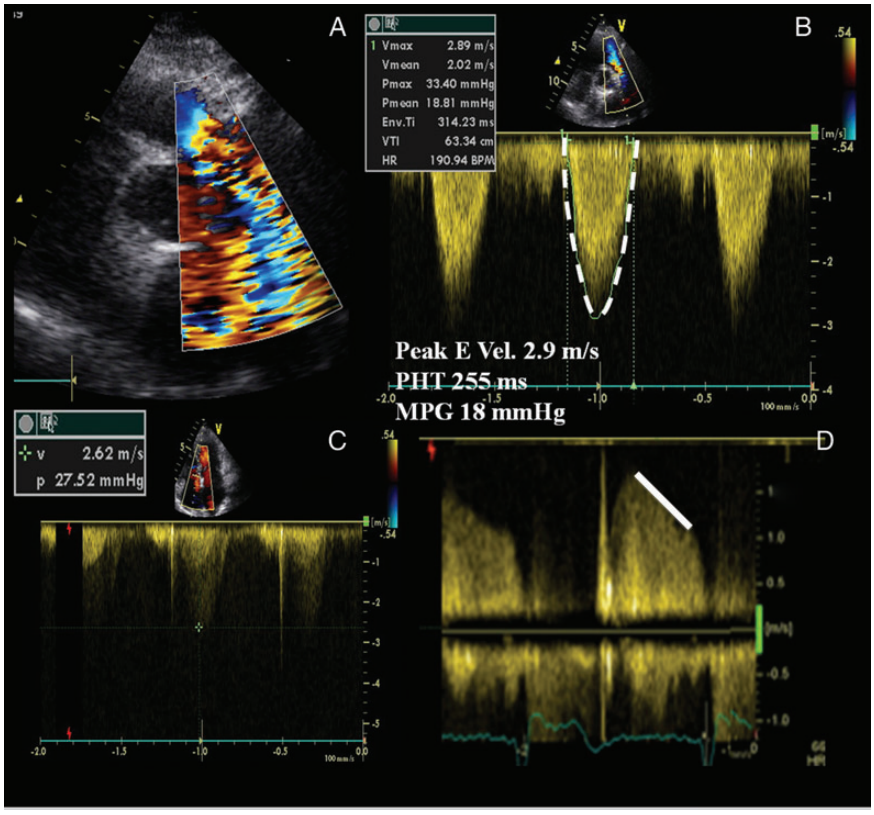

Figure 26 Degenerative bioprosthesis in pulmonary position. Highly turbulent anterograde flow related both to the presence of stenosis and significant prosthesis regurgitation (*A*). The anterograde flow velocity and mean pressure gradient (MPG) are increased (*B*). An intense continuous wave Doppler signal and a short PHT are seen, related to the presence of a concomitant intraprosthetic regurgitation (*D*). The transtricuspid systolic gradient is measured in *C*.

the pulmonic valve is imaged from the parasternal short-axis view at the level of the aortic valve, the RVOT view, and the sub-costal view. Tilting the probe in a slight cranial direction gives a clearer view of both the pulmonic valve and the proximal pulmonary artery. On TOE, the pulmonic valve is imaged from the high oesophageal view at 50°–90° near the level of the short-axis view of the aortic valve (usually found at ~30°). Slight withdrawal of the probe from the level of the aortic valve at 50°–90° may facilitate visualization of the pulmonic valve, main pulmonary artery, and its bifurcation. It can also be imaged from a deep transgastric view in a 120° imaging plane. Colour flow Doppler is used to detect any flow acceleration or regurgitation. 3D TOE allows for accurate evaluation of bioprosthetic pulmonary valve structure and function, and enhances the precision and monitoring of percutaneous valvuloplasty.[167]

Table 19 Grading pulmonary prosthetic valve obstruction

	Normal	Possible obstruction
Qualitative		
Valve structure and motion	Normal	Often abnormal[a]
Colour flow	Normal	Narrowing of forward colour map
Semi-quantitative		
Pressure half time (ms)	<230	≥230
Quantitative		
Flow dependent		
Peak velocity (m/s)[b,c]	<3.2 Bioprosthesis, <2.5 Homograft	≥3.2 Bioprosthesis, ≥2.5 Homograft
Mean gradient (mmHg)	<20 Bioprosthesis, <15 Homograft	≥20 Bioprosthesis ≥15 Homograft

[a]Cusps thickening or immobility.
[b]The criterion is valid for near normal or normal stroke volume (50–90 mL) and flow rate (200–300 mL/s).
[c]Increase in peak velocity on serial studies is the more reliable parameter.

Valve morphology and function

Pulmonic PHV dysfunction, stenosis and/or regurgitation, is generally associated with abnormal valve morphology (calcifications, pannus, thrombus) and/or mobility (rocking motion of the sewing ring, abnormal occluder motion).

Acquired pulmonary PHV obstruction

Doppler assessment

Using both CW and PW Doppler at the level of the pulmonary valve, velocities across the pulmonary valve are measured. Several cycles should be recorded to account for small variations in velocities during the respiratory cycle. The funnel shape of the RVOT and the potential concomitant stenosis of the pulmonary branches limit the accuracy of the continuity equation to calculate the EOA. Currently, pulmonary valve conduits are commonly used, and it is important to know the type of degeneration that these devices may show (edge stenosis), which may cause increased gradients.[14,22]

Current evidence on the determination of the prosthetic pulmonary obstruction is limited. Doppler findings suspicious of prosthetic pulmonary valve stenosis include: narrowing of forward colour flow map, single transvalvular peak velocity >3.2 m/s for bioprostheses (mean gradient ≥20 mmHg) or >2.5 m/s for homografts (mean gradient ≥15 mmHg), increase in peak velocity on serial studies, elevated RV systolic pressure, and new impairment of RV function (*Figure 26*). When stenosis of the pulmonary branches co-exists, PW Doppler may be preferred over CW Doppler to measure the transprosthetic gradient (provided that there is not aliasing).[168,169]

Table 20 Grading the severity of pulmonary prosthetic valve regurgitation

	Mild	Moderate	Severe
Qualitative			
Valve structure and motion	Usually normal	Usually abnormal[a]	Usually abnormal[a]
Colour flow PR jet width[b,c]	Small	Intermediate	Large (>50–65% of RVOT diameter)
CW signal of PR jet	Incomplete or faint	Dense	Dense
CW Jet deceleration rate	Slow	Variable	Steep, early termination of diastolic flow[d]
Diastolic flow reversal in the pulmonary artery	None	Present	Present
Pulmonary vs. Systemic flow by PW Doppler	Slightly increased	Intermediate	Greatly increased
Semi-quantitative			
Pressure half time (ms)[e]	ND	ND	<100 ms
Quantitative	ND	ND	ND
+RV size[f]			

[a]Abnormal mechanical valves: immobile occluder, dehiscence, or rocking (paravalvular regurgitation); abnormal biologic valves: leaflet thickening/calcification or prolapse, dehiscence, or rocking (paravalvular regurgitation).
[b]Parameter applicable to central jets and is less accurate in eccentric jets.
[c]At a Nyquist limit of 50–60 cm/s; parameter applies to central jets and not eccentric jets.
[d]Steep deceleration is not specific for severe PR.
[e]Pressure half time is shortened with increasing RV diastolic pressure.
[f]Applies to chronic, unless other cause of RV dilatation exists, including residual postsurgical dilatation.

Integrative assessment

Echocardiographic assessment of pulmonary PHV obstruction includes integration of data from 2D/3D imaging of the pulmonic valve as well as Doppler measures of stenosis severity. Other imaging modalities, when indicated, can be used to alternatively assess valve structure, motion, and function. *Table 19* lists the imaging parameters used to assess pulmonary PHV function.

Pathological pulmonary regurgitation

Colour Doppler evaluation

There is a paucity of data regarding the imaging assessment of prosthetic pulmonary regurgitation (PR). Detection of prosthetic PR relies almost exclusively on colour flow imaging. PR is diagnosed by documenting a diastolic jet in the RVOT directed towards the RV.

Significant prosthetic PR is distinguished from mild PR by a longer duration of flow (holodiastolic) and a wider jet as the regurgitant jet crosses the pulmonic valve.[170] However, in severe PR, where equalization of diastolic pulmonary artery and RV pressures occurs earlier in diastole, the colour jet area can be brief and inaccurate (dependency on the driving pressure).[171] The assessment of prosthetic PR severity is usually estimated by the diameter of the jet at its origin.[172–174] The maximum colour jet diameter (width) is measured in diastole immediately below the pulmonic valve (at the junction of the RVOT and pulmonary annulus) in the parasternal short-axis view or from the sub-costal view. Although this measurement suffers from a high inter-observer variability, a jet width that occupies >50–65% of the RV outflow tract width measured in the same frame suggests severe PR.

Detection of reversal colour Doppler flow in pulmonary arteries is a specific sign of at least moderate to severe PR.[14,20]

Although the vena contracta width is probably a more accurate method than the jet width to evaluate PR severity by colour Doppler, it lacks validation studies. In some patients, the flow convergence zone can be assessed. However, no studies have examined the clinical accuracy of this method in quantifying the severity of PR.

A short PHT (<100 ms) (sine wave shape of the CW Doppler signal due to rapid deceleration rate with termination of flow in mid to late diastole) and a dense CW PR jet are not specific but compatible with severe prosthetic PR.[175,176] The PHT is dependant not only on PR severity but also on diastolic intrapulmonary pressures and on diastolic properties of the RV, with shorter PHT when RV physiology is restrictive.

Theoretically, PW Doppler assessment of the forward and reverse flows at the pulmonary annulus and in the pulmonary artery can been used to calculate R Vol and regurgitant fraction. The pulmonary annulus should be measured carefully during early ejection (2–3 frames after the R wave on the ECG), just below the valve. This technique is subject to errors in measurement and is not validated for this purpose. A regurgitant fraction <30% is suggestive of mild PR, whereas a regurgitant fraction >50% can be consistent with severe PR.[174]

Evidence of RV dilatation with flattening of the interventricular septum in diastole and resultant paradoxical motion is suggestive but not specific for severe PR. Nevertheless, its absence suggests milder degree of PR or acute PR. Of note, dilatation can be observed in other conditions (non-specific) or may be absent in acute severe PR.

Integrative assessment

Echocardiographic assessment of prosthetic PR includes integration of data from 2D/3D imaging of the pulmonary valve and RV as well as Doppler measures of regurgitation severity (*Table 20*). As for all regurgitant lesions, all modalities should be used. In case of discrepant/ inconclusive echo results, CMR can be used in experienced centres.

Conflict of interest: None declared.

References

1. Nkomo VT, Gardin JM, Skelton TN, Gottdiener JS, Scott CG, Enriquez-Sarano M. Burden of valvular heart diseases: a population-based study. *Lancet* 2006;**368**:1005–11.
2. Dunning J, Gao H, Chambers J, Moat N, Murphy G, Pagano D *et al.* Aortic valve surgery: marked increases in volume and significant decreases in mechanical valve use—an analysis of 41227 patients over 5 years from the Society for Cardiothoracic Surgery in Great Britain and Ireland National database. *J Thorac Cardiovasc Surg* 2011;**142**:776–82.
3. Go AS, Mozaffarian D, Roger VL, Benjamin EJ, Berry JD, Blaha MJ *et al.* Executive summary: heart disease and stroke statistics-2014 update: a report from the American Heart Association. *Circulation* 2014;**129**:399–410.
4. Vahanian A, Alfieri O, Andreotti F, Antunes MJ, Baron-Esquivias G, Baumgartner H *et al.* Guidelines on the management of valvular heart disease (version 2012). *Eur Heart J* 2012;**33**:2451–96.
5. Nishimura RA, Otto CM, Bonow RO, Carabello BA, Erwin JP, Guyton RA *et al.* AHA/ACC Guideline for the management of patients with valvular heart disease. *J Am Coll Cardiol* 2014;**63**:2438–88.
6. Jamieson WR. Update on technologies for cardiac valvular replacement, transcatheter innovations, and reconstructive surgery. *Surg Technol Int* 2010;**20**:255–81.
7. Pibarot P, Dumesnil JG. Prosthetic heart valves: selection of the optimal prosthesis and long-term management. *Circulation* 2009;**119**:1034–48.
8. Nappi F, Spadaccio C, Chello M, Acar C. The Ross procedure: underuse or undercomprehension? *J Thorac Cardiovasc Surg* 2015;**149**:1463–4.
9. Phan K, Tsai Y-C, Niranjan N, Bouchard D, Carrel TP, Dapunt OE *et al.* Sutureless aortic valve replacement: a systematic review and meta-analysis. *Ann Cardiothorac Surg* 2015;**4**:100–11.
10. Kodali SK, Williams MR, Smith CR, Svensson LG, Webb JG, Makkar RR *et al.* Two-year outcomes after transcatheter or surgical aortic-valve replacement. *N Engl J Med* 2012;**366**:1686–95.
11. Zamorano JL, Badano LP, Bruce C, Chan KL, Gonçalves A, Hahn RT *et al.* EAE/ASE recommendations for the use of echocardiography in new transcatheter interventions for valvular heart disease. *Eur Heart J* 2011;**32**:2189–214.
12. Christakis GT, Buth KJ, Goldman BS, Fremes SE, Rao V, Cohan G *et al.* Inaccurate and misleading valve sizing: a proposed standard for valve size nomenclature. *Ann Thorac Surg* 1998;**66**:1198–203.
13. Chambers JB, Oo L, Narracott A, Lawford PM, Blauth CI. Manufacturer's labelled size in six bileaflet mechanical aortic valves: a comparison of orifice size and biological equivalence. *J Thorac Cardiovasc Surg* 2003;**125**:1388–93.
14. Zoghbi WA, Chambers JB, Dumesnil JG, Foster E, Gottdiener JS, Grayburn PA *et al.* Recommendations for evaluation of prosthetic valves with echocardiography and Doppler ultrasound. *J Am Soc Echocardiogr* 2009;**22**:975–1014.
15. Flaschkampf FA, Wouters PF, Edvardsen T, Evangelista A, Habib G, Hoffman P *et al.* Recommendations for transoesophageal echocardiography: EACVI update 2014. *Eur Heart J Cardiovasc Imaging* 2014;**15**:353–65.
16. Lancellotti P, Price S, Edvardsen T, Cosyns B, Neskovic AN, Dulgheru R *et al.* The use of echocardiography in acute cardiovascular care: recommendations of the European Association of Cardiovascular Imaging and the Acute Cardiovascular Care Association. *Eur Heart J Cardiovasc Imaging* 2015;**16**:119–46.
17. Habib G, Lancellotti P, Antunes MJ, Bongiorni MG, Casalta JP, Del Zotti F *et al.* ESC 2015 guidelines on management of infective endocarditis. *Eur Heart J* 2015;**36**:3075–128.
18. Muratori M, Montorsi P, Teruzzi G, Celeste F, Doria E, Alamanni F *et al.* Feasibility and diagnostic accuracy of quantitative assessment of mechanical prostheses leaflet motion by transthoracic and transesophageal echocardiography in suspected prosthetic valve dysfunction. *Am J Cardiol* 2006;**97**:94–100.
19. Baumgartner H, Hung J, Bermejo J, Chambers JB, Evangelista A, Griffin BP *et al.* Echocardiographic assessment of valve stenosis: EAE/ASE recommendations for clinical practice. *Eur J Echocardiogr* 2009;**10**:1–25.
20. Lancellotti P, Tribouilloy C, Hagendorff A, Popescu BA, Edvardsen T, Pierard LA *et al.* Recommendations for the echocardiographic assessment of native valvular

regurgitation: an executive summary from the European Association of Cardiovascular Imaging. *Eur Heart J Cardiovasc Imaging* 2013;**14**:611–44.
21. Cosyns B, Garbi M, Separovic J, Pasquet A, Lancellotti P, Education Committee of the European Association of Cardiovascular Imaging Association (EACVI). Update of the Echocardiography Core Syllabus of the European Association of Cardiovascular Imaging (EACVI). *Eur Heart J Cardiovasc Imaging* 2013;**14**:837–9.
22. Lang RM, Badano LP, Tsang W, Adams DH, Agricola E, Buck T *et al.* EAE/ASE recommendations for image acquisition and display using three-dimensional echocardiography. *Eur Heart J Cardiovasc Imag* 2012;**13**:1–46.
23. Sugeng L, Shernan SK, Weinert L, Shook D, Raman J, Jeevanandam V *et al.* Real-time three-dimensional transesophageal echocardiography in valve disease: comparison with surgical findings and evaluation of prosthetic valves. *J Am Soc Echocardiogr* 2008;**21**:1347–54.
24. Ansingkar K, Nanda NC, Aaluri SR, Mukhtar O, Puri VK, Kirklin JT *et al.* Transesophageal three-dimensional color Doppler echocardiographic assessment of valvular and paravalvular mitral prosthetic regurgitation. *Echocardiography* 2000; **17**:579–83.
25. Anwar AM, Nosir YF, Alasnag M, Chamsi-Pasha H. Real time three-dimensional transesophageal echocardiography: a novel approach for the assessment of prosthetic heart valves. *Echocardiography* 2014;**31**:188–96.
26. Tsang W, Weinert L, Kronzon I, Lang RM. Three-dimensional echocardiography in the assessment of prosthetic valves. *Rev Esp Cardiol* 2011;**64**:1–7.
27. Singh P, Manda J, Hsiung MC, Mehta A, Kesanolla SK, Nanda NC *et al.* Live/real time three-dimensional transesophageal echocardiographic evaluation of mitral and aortic valve prosthetic paravalvular regurgitation. *Echocardiography* 2009;**26**: 980–7.
28. Kronzon I, Sugeng L, Perk G, Hirsh D, Weinert L, Garcia Fernandez MA *et al.* Real-time 3-dimensional transesophageal echocardiography in the evaluation of postoperative mitral annuloplasty ring and prosthetic valve dehiscence. *J Am Coll Cardiol* 2009;**53**:1543–7.
29. Mukhtari O, Horton CJ Jr, Nanda NC, Aaluri SR, Pacifico A. Transesophageal color Doppler three-dimensional echocardiographic detection of prosthetic aortic valve dehiscence: correlation with surgical findings. *Echocardiography* 2001;**18**: 393–7.
30. Faletra FF, Moschovitis G, Auricchio A. Visualisation of thrombus formation on prosthetic valve by real-time three-dimensional transoesophageal echocardiography. *Heart* 2009;**95**:482.
31. Goldstein SA, Taylor AJ, Wang Z, Weigold WG. Prosthetic mitral valve thrombosis: cardiac CT, 3-dimensional transesophageal echocardiogram, and pathology correlation. *J Cardiovasc Comput Tomogr* 2010;**4**:221–3.
32. Ozkan M, Gürsoy OM, Astarcıoğlu MA, Gündüz S, Cakal B, Karakoyun S *et al.* Real-time three-dimensional transesophageal echocardiography in the assessment of mechanical prosthetic mitral valve ring thrombosis. *Am J Cardiol* 2013; **112**:977–83.
33. Gürsoy OM, Karakoyun S, Kalçık M, Özkan M. The incremental value of RT three-dimensional TEE in the evaluation of prosthetic mitral valve ring thrombosis complicated with thromboembolism. *Echocardiography* 2013;**30**:198–201.
34. De Cicco G, Lorusso R, Colli A, Nicolini F, Fragnito C, Grimaldi T *et al.* Aortic valve periprosthetic leakage: anatomic observations and surgical results. *Ann Thorac Surg* 2005;**79**:1480–5.
35. Pibarot P, Dumesnil JG, Jobin J, Lemieux M, Honos G, Durand LG. Usefulness of the indexed effective orifice area at rest in predicting an increase in gradient during maximum exercise in patients with a bioprosthesis in the aortic valve position. *Am J Cardiol* 1999;**83**:542–6.
36. Garbi M, Chambers J, Vannan MA, Lancellotti P. Valve stress echocardiography: a practical guide for referral, procedure, reporting, and clinical implementation of results from the HAVEC group. *JACC Cardiovasc Imaging* 2015;**8**:724–36.
37. Lancellotti P, Pellika P, Budts W, Chaudhry F, Donal E, Dulgheru R *et al.* Recommendations for the clinical use of stress echocardiography in non-ischemic heart disease: Joint Document of the European Association of Cardiovascular Imaging (EACVI) and the American Society of Echocardiography (ASE). *Eur Heart J Cardiovasc Imaging* 2016; in press.
38. Cianciulli T, Lax J, Beck M, Cerruti F, Gigena G, Saccheri M *et al.* Cinefluoroscopic assessment of mechanical disc prostheses: its value as a complementary method to echocardiography. *J Heart Valve Dis* 2005;**14**:664–73.
39. Montorsi P, Cavoretto D, Repossini A, Bartorelli A, Guazzi M. Valve design characteristics and cine-fluoroscopic appearance of five currently available bileaflet prosthetic heart valves. *Am J Cardiac Imaging* 1996;**10**:29–41.
40. Montorsi P, Cavoretto D, Parolari A, Muratori M, Alimento M, Pepi M. Diagnosing prosthetic mitral valve thrombosis and the effect of the type of prosthesis. *Am J Cardiol* 2002;**90**:73–6.
41. Muratori M, Montorsi P, Maffessanti F, Teruzzi G, Zoghbi WA, Gripari P *et al.* Dysfunction of bileaflet aortic prosthesis: accuracy of echocardiography versus fluoroscopy. *JACC Cardiovasc Imaging* 2013;**6**:196–205.
42. Habets J, Symersky P, van Herwerden LA, de Mol B, Spijkerboer AM, Mali WT *et al.* Prosthetic heart valve assessment with multidetector-row CT: imaging characteristics of 91 valves in 83 patients. *Eur Radiol* 2011;**21**:1390–6.
43. von Knobelsdorff-Brenkenhoff F, Röttgen R, Schulz-Menger J. Complementary assessment of aortic bioprosthetic dysfunction using cardiac magnetic resonance imaging and computed tomography. *J Heart Valve Dis* 2012;**21**:20–2.
44. Manghat NE, Rachapalli V, Van LR, Veitch AM, Roobottom CA, Morgan-Hughes GJ. Imaging the heart valves using ECG-gated 64-detector row cardiac CT. *Br J Radiol* 2008;**81**:275–90.
45. Chenot F, Montant P, Goffinet C, Pasquet A, Vancraeynest D, Coche E *et al.* Evaluation of anatomic valve opening and leaflet morphology in aortic valve bioprosthesis by using multidetector CT: comparison with transthoracic echocardiography. *Radiology* 2010;**255**:377–85.
46. Suchá D, Symersky P, Vonken EJ, Provoost E, Chamuleau SA, Budde RP. Multidetector-row computed tomography allows accurate measurement of mechanical prosthetic heart valve leaflet closing angles compared with fluoroscopy. *J Comput Assist Tomogr* 2014;**38**:451–6.
47. Tarzia V, Bortolussi G, Rubino M, Gallo M, Bottio T, Gerosa G. Evaluation of prosthetic valve thrombosis by 64-row multi-detector computed tomography. *J Heart Valve Dis* 2015;**24**:210–3.
48. O'Neill AC, Martos R, Murtagh G, Ryan ER, McCreery C, Keane D *et al.* Practical tips and tricks for assessing prosthetic valves and detecting paravalvular regurgitation using cardiac CT. *J Cardiovasc Comput Tomogr* 2014;**8**:323–7.
49. Hara M, Nishino M, Taniike M, Makino N, Kato H, Egami Y *et al.* Impact of 64 multidetector computed tomography for the evaluation of aortic paraprosthetic regurgitation. *J Cardiol* 2011;**58**:294–9.
50. Teshima H, Hayashida N, Fukunaga S, Tayama E, Kawara T, Aoyagi S *et al.* Usefulness of a multidetector-row computed tomography scanner for detecting pannus formation. *Ann Thorac Surg* 2004;**77**:523–6.
51. Habets J, Tanis W, Mali WT, Chamuleau SA, Budde RP. Imaging of prosthetic heart valve dysfunction. Complementary diagnostic value of TEE and MDCT? *JACC Cardiovasc Imaging* 2012;**5**:956–61.
52. O'Neill AC, Kelly RM, McCarthy CJ, Martos R, McCreery C, Dodd JD. Thrombosed prosthetic valve in Ebstein's anomaly: Evaluation with echocardiography and 64-slice cardiac computed tomography. *World J Cardiol* 2012;**4**:240–1.
53. Tanis W, Habets J, van den Brink RB, Symersky P, Budde RP, Chamuleau SA. Differentiation of thrombus from pannus as the cause of acquired mechanical prosthetic heart valve obstruction by non-invasive imaging: a review of the literature. *Eur Heart J Cardiovasc Imaging* 2014;**15**:119–29.
54. Chung MS, Yang DH, Kim DH, Kang JW, Lim TH. Subvalvular pannus formation causing aortic stenosis in patients with a normal prosthetic aortic valve: computed tomography finding. *Eur Heart J Cardiovasc Imaging* 2015;**16**:458.
55. Tanis W, Suchá D, Laufer W, Habets J, van Herwerden LA, Symersky P *et al.* Multidetector-row computed tomography for prosthetic heart valve dysfunction: is concomitant non-invasive coronary angiography possible before redo-surgery? *Eur Radiol* 2015;**25**:1623–30.
56. Habets J, van den Brink RB, Uijlings R, Spijkerboer AM, Mali WP, Chamuleau SA *et al.* Coronary artery assessment by multidetector computed tomography in patients with prosthetic heart valves. *Eur Radiol* 2012;**22**:1278–86.
57. Girard SE, Miller FA Jr, Orszulak TA, Mullany CJ, Montgomery S, Edwards WD *et al.* Reoperation for prosthetic aortic valve obstruction in the era of echocardiography: trends in diagnostic testing and comparison with surgical findings. *J Am Coll Cardiol* 2001;**37**:579–84.
58. Hoffmann MH, Shi H, Manzke R, Schmid FT, De Vries L, Grass M *et al.* Noninvasive coronary angiography with 16-detector row CT: effect of heart rate. *Radiology* 2005;**234**:86–97.
59. Konen E, Goitein O, Feinberg MS, Eshet Y, Raanani E, Rimon U *et al.* The role of ECG-gated MDCT in the evaluation of aortic and mitral mechanical valves: initial experience. *Am J Roentgenol* 2008;**191**:26–31.
60. Picano E, Vañó E, Rehani MM, Cuocolo A, Mont L, Bodi V *et al.* The appropriate and justified use of medical radiation in cardiovascular imaging: a position document of the ESC Associations of Cardiovascular Imaging, Percutaneous Cardiovascular Interventions and Electrophysiology. *Eur Heart J* 2014;**35**:665–72.
61. Habets J, Meijer TS, Meijer RC, Mali WP, Vonken EJ, Budde RP. CT attenuation measurements are valuable to discriminate pledgets used in prosthetic heart valve implantation from paravalvular leakage. *Br J Radiol* 2012;**85**:e616–21.
62. Raman SV, Cook SC. Cardiovascular computed tomography and MRI in clinical practice: aortopathy. *J Cardiovasc Med* 2007;**8**:35–540.
63. Ribeiro HB, Le Ven F, Larose E, Dahou A, Nombela-Franco L, Urena M *et al.* Cardiac magnetic resonance versus transthoracic echocardiography for the assessment and quantification of aortic regurgitation in patients undergoing transcatheter aortic valve implantation. *Heart* 2014;**100**:1924–32.
64. Simprini LA, Afroz A, Cooper MA, Klem I, Jensen C, Kim RJ *et al.* Routine cine-CMR for prosthesis-associated mitral regurgitation: a multicenter comparison to echocardiography. *J Heart Valve Dis* 2014;**23**:575–82.

65. von Knobelsdorff-Brenkenhoff F, Rudolph A, Wassmuth R, Schulz-Menger J. Assessment of mitral bioprostheses using cardiovascular magnetic resonance. *J Cardiovasc Magn Reson* 2010;**12**:36.
66. Suchá D, Symersky P, Tanis W, Mali WP, Leiner T, van Herwerden LA *et al.* Multimodality imaging assessment of prosthetic heart valves. *Circ Cardiovasc Imaging* 2015;**8**:e003703.
67. Fujita N, Chazouilleres AF, Hartiala JJ, O'Sullivan M, Heidenreich P, Kaplan JD *et al.* Quantification of mitral regurgitation by velocity-encoded cine nuclear magnetic resonance imaging. *J Am Coll Cardiol* 1994;**23**:951–8.
68. Han Y, Peters DC, Salton CJ, Bzymek D, Nezafat R, Goddu B *et al.* Cardiovascular magnetic resonance characterization of mitral valve prolapse. *JACC Cardiovasc Imaging* 2008;**1**:294–303.
69. von Knobelsdorff-Brenkenhoff F, Rudolph A, Wassmuth R, Bohl S, Buschmann EE, Abdel-Aty H *et al.* Feasibility of cardiovascular magnetic resonance to assess the orifice area of aortic bioprostheses. *Circ Cardiovasc Imaging* 2009;**2**:397–404.
70. Buchner S, Debl K, Poschenrieder F, Feuerbach S, Riegger GA, Luchner A *et al.* Cardiovascular magnetic resonance for direct assessment of anatomic regurgitant orifice in mitral regurgitation. *Circ Cardiovasc Imaging* 2008;**1**:148–55.
71. Pennekamp W, Geyhan N, Soeren P, Volkmar N. Determination of flow profiles of different mechanical aortic valve prostheses using phase-contrast MRI. *J Cardiovasc Surg* 2011;**52**:277–84.
72. Adegbite O, Kadem L, Newling B. Purely phase-encoded MRI of turbulent flow through a dysfunctional bileaflet mechanical heart valve. *MAGMA* 2014;**27**: 227–35.
73. Houlind K, Eschen O, Pedersen EM, Jensen T, Hasenkam JM, Paulsen PK. Magnetic resonance imaging of blood velocity distribution around St. Jude medical aortic valves in patients. *J Heart Valve Dis* 1996;**5**:511–7.
74. Clavel MA, Pibarot P. Assessment of low-flow, low-gradient aortic stenosis: multimodality imaging is the key to success. *EuroIntervention* 2014;**10**(Suppl. U): U52–60.
75. Hendel RC, Patel MR, Kramer CM, Poon M, Hendel RC, Carr JC *et al.* ACCF/ACR/SCCT/SCMR/ASNC/ NASCI/SCAI/SIR 2006 appropriateness criteria for cardiac computed tomography and cardiac magnetic resonance imaging. *J Am Coll Cardiol Radiol* 2006;**48**:1475–97.
76. Baikoussis NG, Apostolakis E, Papakonstantinou NA, Sarantitis I, Dougenis D. Safety of magnetic resonance imaging in patients with implanted cardiac prostheses and metallic cardiovascular electronic devices. *Ann Thorac Surg* 2011;**91**: 2006–11.
77. Shellock FG. Prosthetic heart valves and annuloplasty rings: assessment of magnetic field interactions, heating, and artifacts at 1.5 Tesla. *J Cardiovasc Magn Reson* 2001;**3**:317–24.
78. Pizzi MN, Roque A, Fernández-Hidalgo N, Cuéllar-Calabria H, Ferreira-González I, Gonzàlez-Alujas MT *et al.* Improving the diagnosis of infective endocarditis in prosthetic valves and intracardiac devices with 18F-FDG-PET/CT-Angiography: initial results at an infective endocarditis referral center. *Circulation* 2015;**132**:1113–26.
79. Dweck MR, Jones C, Joshi NV, Fletcher AM, Richardson H, White A *et al.* Assessment of valvular calcification and inflammation by positron emission tomography in patients with aortic stenosis. *Circulation* 2012;**125**:76–86.
80. Blauwet LA, Malouf JF, Connolly HM, Hodge DO, Evans KN, Herges RM *et al.* Comprehensive echocardiographic assessment of normal mitral Medtronic Hancock II, Medtronic Mosaic, and Carpentier-Edwards Perimount bioprostheses early after implantation. *J Am Soc Echocardiogr* 2010;**23**:656–66.
81. Blauwet LA, Burkhart HM, Dearani JA, Malouf JF, Connolly HM, Hodge DO *et al.* Comprehensive echocardiographic assessment of mechanical tricuspid valve prostheses based on early postimplantation echocardiographic studies. *J Am Soc Echocardiogr* 2011;**24**:414–24.
82. Badano L, Mocchegiani R, Bertoli D, DeGaetano G, Carratino L, Pasetti L *et al.* Normal echocardiographic characteristics of the Sorin-Bicarbon bileaflets prosthetic heart valve in mitral and aortic position. *J Am Soc Echocardiogr* 1997;**10**: 632–43.
83. David TE, Armstrong S, Sun Z. Clinical and haemodynamic assessment of the Hancock II bioprosthesis. *Ann Thorac Surg* 1992;**54**:661–7.
84. Van den Brink RBA. Evaluation of prosthetic heart valves by transoesophageal echocardiography: problems, pitfalls, and timing of echocardiography. *Semin Sardiothorac Vasc Anesth* 2006;**10**:89–100.
85. Alton M, Pasierski TJ, Orsinelli DA, Eaton GM, Pearson AC. Comparison of transthoracic and transesophageal echocardiography in evaluation of 47 Starr-Edwards prosthetic valves. *J Am Coll Cardiol* 1992;**20**:1503–11.
86. Daniel WG, Mugge A, Grote J, Hausmann D, Nikutta P, Laas J *et al.* Comparison of transthoracic and transesophageal echocardiography for detection of abnormalities of prosthetic and bioprosthetic valves in the mitral and aortic positions. *Am J Cardiol* 1993;**71**:210–5.
87. Rosenhek R, Binder T, Maurer G, Baumgartner H. Normal values for Doppler echocardiographic assessment of heart valve prostheses. *J Am Soc Echo* 2003; **16**:1116–27.
88. Orsinelli D, Pasierski TJ, Pearson A. Spontaneously appearing microbubbles associated with prosthetic cardiac valves detected by transesophageal echocardiography. *Am Heart J* 1994;**128**:990–6.
89. Johansen P, Manning K, Tarbell J, Fontaine A, Deutsch S, Nygaard H. A new method for evaluation of cavitation near mechanical heart valves. *J Biomech Eng* 2003; **125**:663–70.
90. Rodriguez RA, Nathan HJ, Ruel M, Rubens F, Dafoe D, Mesana T. A method to distinguish between gaseous and solid cerebral emboli in patients with prosthetic heart valves. *Eur J Cardiothorac Surg* 2009;**35**:89–95.
91. Hutchinson K, Hafeez F, Woods TD, Chopra PS, Warner TF, Levine RL *et al.* Recurrent ischemic strokes in a patient with Medtronic-Hall prosthetic aortic valve and valve strands. *J Am Soc Echocardiogr* 1998;**11**:755–7.
92. Ionescu AA, Newman GR, Butchart EG, Fraser AG. Morphologic analysis of a strand recovered from a prosthetic mitral valve: no evidence of fibrin. *J Am Soc Echocardiogr* 1999;**12**:766–8.
93. Rozich JD, Edwards WD, Hanna RD, Laffey DM, Johnson GH, Klarich KW. Mechanical prosthetic valve-associated strands: pathologic correlates to transesophageal echocardiography. *J Am Soc Echocardiogr* 2003;**16**:97–100.
94. Hixson CS, Smith MD, Mattson MD, Morris EJ, Lenhoff SJ, Salley RK. Comparison of transesophageal color flow Doppler imaging of normal mitral regurgitant jets in St. Jude Medical and Medtronic Hall cardiac prostheses. *J Am Soc Echocardiogr* 1992;**5**:57–62.
95. Mohr-Kahaly S, Kupferwasser I, Erbel R, Oelert H, Meyer J. Refurgitant flow in apparently normal valve prosthesis: improved detection and semi-quantitative analysis by transesophageal two-dimensional color-coded Doppler echocardiography. *J Am Soc Echocardiogr* 1990;**3**:187–95.
96. Yoganathan AP, Reamer HH, Corcoran WH, Harrison EC, Shulman IA, Parnassus W. The Starr-Edwards aortic ball: flow characteristics, thrombus formation, and tissue overgrowth. *Artif Organs* 1981;**6**:6–17.
97. Pibarot P, Dumesnil JG, Briand M, Laforest I, Cartier P. Hemodynamic performance during maximum exercise in adult patients with the ross operation and comparison with normal controls and patients with aortic bioprostheses. *Am J Cardiol* 2000;**86**:982–8.
98. Quinones MA, Otto CM, Stoddard M, Waggoner A, Zoghbi WA. Recommendations for quantification of Doppler echocardiography: a report from the Doppler Quantification Task Force of the Nomenclature and Standards Committee of the American Society of Echocardiography. *J Am Soc Echocardiogr* 2002;**15**:167–84.
99. Badano L, Zamorano JL, Pavoni D, Tosoratti E, Baldassi M, Zakja E *et al.* Clinical and haemodynamic implications of supra-annular implant of biological aortic valves. *J Cardiovasc Med* 2006;**7**:524–32.
100. Baumgartner H, Khan S, DeRobertis M, Czer L, Maurer G. Discrepancies between Doppler and catheter gradients in aortic prosthetic valves in vitro. A manifestation of localized gradients and pressure recovery. *Circulation* 1990;**82**:1467–75.
101. Bech-Hanssen O, Caidahl K, Wallentin I, Brandberg J, Wranne B, Ask P. Aortic prosthetic valve design and size: relation to Doppler echocardiographic findings and pressure recovery an in vitro study. *J Am Soc Echocardiogr* 2000;**13**:39–50.
102. Bach DS. Echo/Doppler evaluation of hemodynamics after aortic valve replacement. Principles of interrogation and evaluation of high gradients. *J Am Coll Cardiol Imag* 2010;**3**:296–304.
103. Dumesnil JG, Honos GN, Lemieux M, Beauchemin J. Validation and applications of mitral prosthetic valvular areas calculated by Doppler echocardiography. *Am J Cardiol* 1990;**65**:1443–8.
104. Garcia D, Pibarot P, Landry C, Allard A, Chayer B, Dumesnil JG *et al.* Estimation of aortic valve effective orifice area by Doppler echocardiography: effects of valve inflow shape and flow rate. *J Am Soc Echocardiogr* 2004;**17**:756–65.
105. Flaschkampf FA, Weyman AE, Guerrero JL. Influence of orifice geometry and flow rate on effective valve area: an in vitro study. *J Am Coll Cardiol* 1991;**15**:1173–80.
106. Gilon D, Cape EG, Handschumacher MD, Song JK, Solheim J, VanAuker M *et al.* Effect of three-dimensional valve shape on the hemodynamics of aortic stenosis: three-dimensional echocardiographic stereolithography and patient studies. *J Am Coll Cardiol* 2002;**40**:1479–86.
107. Pibarot P, Dumesnil JG, Cartier PC, Métras J, Lemieux MD. Patient prosthesis mismatch can be predicted at the time of operation. *Ann Thorac Surg* 2001;**71**:S265–8.
108. Bitar JN, Lechin ME, Salazar G, Zoghbi WA. Doppler echocardiographic assessment with the continuity equation of St. Jude medical mechanical prostheses in the mitral valve position. *Am J Cardiol* 1995;**76**:287–93.
109. Pibarot P, Honos GN, Durand LG, Dumesnil JG. Substitution of left ventricular outflow tract diameter with prosthesis size is inadequate for calculation of the aortic prosthetic valve area by the continuity equation. *J Am Soc Echocardiogr* 1995;**8**:511–7.

110. Smadi O, Garcia J, Pibarot P, Gaillard E, Hassan I, Kadem L. Accuracy of Doppler-echocardiographic parameters for the detection of aortic bileaflet mechanical prosthetic valve dysfunction. *Eur Heart J Cardiovasc Imaging* 2014;**15**:142–51.
111. Zekry SB, Saad RM, Ozkan M, Al Shahid MS, Pepi M, Muratori M *et al.* Flow acceleration time and ratio of acceleration time to ejection time for prosthetic aortic valve function. *JACC Cardiovasc Imaging* 2011;**4**:1161–70.
112. Garcia D, Dumesnil JG, Durand LG, Kadem L, Pibarot P. Discrepancies between catheter and Doppler estimates of valve effective orifice area can be predicted from the pressure recovery phenomenon: practical implications with regard to quantification of aortic stenosis severity. *J Am Coll Cardiol* 2003;**41**:435–42.
113. Vandervoort PM, Greenberg NL, Pu M, Powell KA, Cosgrove DM, Thomas JD. Pressure recovery in bileaflet heart valve prostheses. Localized high velocities and gradients in central and side orifices with implications for Doppler-catheter gradient relation in aortic and mitral position. *Circulation* 1995;**92**:3464–72.
114. Aljassim O, Svensson G, Houltz E, Bech-Hanssen O. Doppler-catheter discrepancies in patients with bileaflet mechanical prostheses or bioprostheses in the aortic valve position. *Am J Cardiol* 2008;**102**:1383–9.
115. Bach DS, Schmitz C, Dohmen G, Aaronson KD, Steinseifer U, Kleine P. In vitro assessment of prosthesis type and pressure recovery characteristics: Doppler echocardiography overestimation of bileaflet mechanical and bioprosthetic aortic valve gradients. *J Thorac Cardiovasc Surg* 2012;**144**:453–8.
116. Bech-Hanssen O, Caidahl K, Wallentin I, Brandberg J, Wranne B, Ask P. Aortic prosthetic valve design and size: relation to Doppler echocardiographic findings and pressure recovery - an in vitro study. *J Am Soc Echocardiogr* 2000;**13**:39–50.
117. Evin M, Pibarot P, Guivier-Curien C, Tanne D, Kadem L, Rieu R. Localized transvalvular pressure gradients in mitral bileaflet mechanical heart valves and impact on gradient overestimation by Doppler. *J Am Soc Echocardiogr* 2013;**26**:791–800.
118. Ye Z, Shiono M, Sezai A, Inoue T, Hata M, Niino T *et al.* Reoperation for a patient 25 Years after a Starr-Edwards ball mitral valve was installed. *Ann Thorac Cardiovasc Surg* 2002;**8**:311–5.
119. Akins CW, Miller DC, Turina MI, Kouchoukos NT, Blackstone EH, Grunkemeier GL *et al.* Guidelines for reporting mortality and morbidity after cardiac valve interventions. *J Thorac Cardiovasc Surg* 2008;**135**:732–8.
120. Rizzoli G, Guglielmi C, Toscano G, Pistorio V, Vendramin I, Bottio T *et al.* Reoperations for acute prosthetic thrombosis and pannus: an assessment of rates, relationship and risk. *Eur J Cardiothorac Surg* 1999;**16**:74–80.
121. Roudaut R, Serri K, Lafitte S. Thrombosis of prosthetic heart valves: diagnosis and therapeutic considerations. *Heart* 2007;**93**:137–42.
122. Pibarot P, Dumesnil JG. Doppler echocardiographic evaluation of prosthetic valve function. *Heart* 2012;**98**:69–78.
123. Genoni M, Franzen D, Tavakoli R, Seiffert B, Graves K, Jenni R *et al.* Does the morphology of mitral paravalvular leaks influence symptoms and hemolysis? *J Heart Valve Dis* 2001;**10**:426–30.
124. Pibarot P, Dumesnil JG. Hemodynamic and clinical impact of prosthesis-patient mismatch in the aortic valve position and its prevention. *J Am Coll Cardiol* 2000;**36**:1131–41.
125. Pibarot P, Dumesnil JG. Valve prosthesis-patient mismatch, 1978 to 2011: from original concept to compelling evidence. *J Am Coll Cardiol* 2012;**60**:1136–9.
126. Head S, Mokhles M, Osnabrugge R, Pibarot P, Mack MJ, Takkenberg J *et al.* The impact of prosthesis-patient mismatch on long-term survival after aortic valve replacement: a systematic review and meta-analysis of 34 observational studies comprising 27,186 patients with 133,141 patient-years. *Eur Heart J* 2012;**33**:1518–29.
127. Takagi H, Yamamoto H, Iwata K, Goto SN, Umemoto T. A meta-analysis of effects of prosthesis-patient mismatch after aortic valve replacement on late mortality. *Int J Cardiol* 2012;**159**:150–4.
128. Pibarot P, Weissman NJ, Stewart WJ, Hahn RT, Lindman BR, McAndrew T *et al.* Incidence and sequelae of prosthesis-patient mismatch in transcatheter versus surgical valve replacement in high-risk patients with severe aortic stenosis-A PARTNER trial cohort A analysis. *J Am Coll Cardio* 2014;**64**:1323–34.
129. Flameng W, Herregods MC, Vercalsteren M, Herijgers P, Bogaerts K, Meuris B. Prosthesis-patient mismatch predicts structural valve degeneration in bioprosthetic heart valves. *Circulation* 2010;**121**:2123–9.
130. Mahjoub H, Mathieu P, Larose E, Dahou A, Senechal M, Dumesnil JG *et al.* Determinants of aortic bioprosthetic valve calcification assessed by multidetector CT. *Heart* 2015;**101**:472–7.
131. Mohty D, Dumesnil JG, Echahidi N, Mathieu P, Dagenais F, Voisine P *et al.* Impact of prosthesis-patient mismatch on long-term survival after aortic valve replacement: influence of age, obesity, and left ventricular dysfunction. *J Am Coll Cardiol* 2009;**53**:39–47.
132. Kappetein AP, Head SJ, Genereux P, Piazza N, Van Mieghem NM, Blackstone EH *et al.* Updated standardized endpoint definitions for transcatheter aortic valve implantation: the Valve Academic Research Consortium-2 consensus document. *Eur J Cardiothorac Surg* 2012;**42**:S45–60.
133. Lancellotti P, Rosenhek R, Pibarot P, Iung B, Otto CM, Tornos P *et al.* ESC Working Group on Valvular Heart Disease position paper—heart valve clinics: organization, structure, and experiences. *Eur Heart J* 2013;**34**:1597–606.
134. Bach DS. Transesophageal echocardiographic (TEE) evaluation of prosthetic valves. *Cardiol Clin* 2000;**18**:751–71.
135. Chambers J, Rimington H, Rajani R, Hodson F, Blauth C. Hemodynamic performance on exercise: comparison of a stentless and stented biological aortic valve replacement. *J Heart Valve Dis* 2004;**13**:729–33.
136. Dumesnil JG, Pibarot P. Prosthesis-patient mismatch; an update. *Curr Cardiol Rep* 2011;**13**:250–7.
137. Rallidis LS, Moyssakis IE, Ikonomidis I, Nihoyannopoulos P. Natural history of early aortic paraprosthetic regurgitation: a five-year follow-up. *Am Heart J* 1999;**138**:351–7.
138. Perry GJ, Helmcke F, Nanda NC, Byard C, Soto B. Evaluation of aortic insufficiency by Doppler colour flow mapping. *J Am Coll Cardiol* 1987;**9**:952–9.
139. Leon MB, Smith CR, Mack M, Miller DC, Moses JW, Svensson LG *et al.* Transcatheter aortic-valve implantation for aortic stenosis in patients who cannot undergo surgery. *N Engl J Med* 2010;**363**:1597–607.
140. Effron MK, Popp RL. Two-dimensional echocardiographic assessment of bioprosthetic valve dysfunction and infective endocarditis. *J Am Coll Cardiol* 1983;**2**:597–606.
141. Tribouilloy CM, Enriquez-Sarano M, Fett SL, Bailey KR, Seward JB, Tajik AJ. Application of the proximal flow convergence method to calculate the effective regurgitant orifice area in aortic regurgitation. *J Am Coll Cardiol* 1998;**32**:1032–9.
142. Pouleur AC, de Waroux JB, Goffinet C, Vancraeynest D, Pasquet A, Gerber BL *et al.* Accuracy of the flow convergence method for quantification of aortic regurgitation in patients with central versus eccentric jets. *Am J Cardiol* 2008;**102**:475–80.
143. Samstad SO, Hegrenaes L, Skjaerpe T, Hatle L. Half time of the diastolic aortoventricular pressure difference by continuous wave Doppler ultrasound: a measure of the severity of AR? *Br Heart J* 1989;**61**:336–43.
144. Griffin BP, Flachskampf FA, Siu S, Weyman AE, Thomas JD. The effects of regurgitant orifice size, chamber compliance, and systemic vascular resistance on aortic regurgitant velocity slope and pressure half-time. *Am Heart J* 1991;**122**:1049–56.
145. Tribouilloy C, Avinée P, Shen WF, Rey JL, Slama M, Lesbre JP. End diastolic flow velocity just beneath the aortic isthmus assessed by pulsed Doppler echocardiography: a new predictor of the aortic regurgitant fraction. *Br Heart J* 1991;**65**:37–40.
146. Foster GP, Isselbacher EM, Rose GA, Torchiana DF, Akins CW, Picard MH. Accurate localization of mitral regurgitant defects using multiplane transesophageal echocardiography. *Ann Thorac Surg* 1998;**65**:1025–31.
147. Vitarelli A, Conde Y, Cimino E, Leone T, D'Angeli I, D'Orazio S *et al.* Assessment of severity of mechanical prosthetic mitral regurgitation by transoesophageal echocardiography. *Heart* 2004;**90**:539–44.
148. Sprecher DL, Adamick R, Adams D, Kisslo J. In vitro color flow, pulsed and continuous wave Doppler ultrasound masking of flow by prosthetic valves. *J Am Coll Cardiol* 1987;**9**:1306–10.
149. Fernandes V, Olmos L, Nagueh SF, Quinones MA, Zoghbi WA. Peak early diastolic velocity rather than pressure half-time is the best index of mechanical prosthetic mitral valve function. *Am J Cardiol* 2002;**89**:704–10.
150. Goetze S, Brechtken J, Agler DA, Thomas JD, Sabik JF III, Jaber WA. In vivo short-term Doppler hemodynamic profiles of 189 Carpentier- Edwards Perimount pericardial bioprosthetic valves in the mitral position. *J Am Soc Echocardiogr* 2004;**17**:981–7.
151. Malouf JF, Ballo M, Connolly HM, Hodge DO, Herges RM, Mullany CJ *et al.* Doppler echocardiography of 119 normal-functioning St Jude Medical mitral valve prostheses: a comprehensive assessment including time-velocity integral ratio and prosthesis performance index. *J Am Soc Echocardiogr* 2005;**18**:252–6.
152. Panidis IP, Ross J, Mintz GS. Normal and abnormal prosthetic valve function as assessed by Doppler echocardiography. *J Am Coll Cardiol* 1986;**8**:317–26.
153. Chaliki HP, Nishimura RA, Enriquez-Sarano M, Reeder GS. A simplified, practical approach to assessment of severity of mitral regurgitation by Doppler color flow imaging with proximal convergence: validation with concomitant cardiac catheterization. *Mayo Clin Proc* 1998;**73**:929–35.
154. Flachskampf FA, Hoffmann R, Franke A, Job FP, Schöndube FA, Messmer BJ *et al.* Does multiplane transesophageal echocardiography improve the assessment of prosthetic valve regurgitation? *J Am Soc Echocardiogr* 1995;**8**:70–8.
155. Becerra JM, Almeria C, de Isla LP, Zamorano J. Usefulness of 3D transoesophageal echocardiography for guiding wires and closure devices in mitral perivalvular leaks. *Eur J Echocardiogr* 2009;**10**:979–81.
156. Enriquez-Sarano M, Miller FA, Hayes SN, Bailey KR, Tajik AJ, Seward JB. Effective mitral regurgitant orifice area: clinical use and pitfalls of the proximal isovelocity surface area method. *J Am Coll Cardiol* 1995;**25**:703–9.
157. Enriquez-Sarano M, Dujardin KS, Tribouilloy CM, Seward JB, Yoganathan AP, Bailey KR *et al.* Determinants of pulmonary venous flow reversal in mitral

regurgitation and its usefulness in determining the severity of regurgitation. *Am J Cardiol* 1999;**83**:535–41.
158. Olmos L, Salazar G, Barbetseas J, Quinones MA, Zoghbi WA. Usefulness of transthoracic echocardiography in detecting significant prosthetic mitral valve regurgitation. *Am J Cardiol* 1999;**83**:199–205.
159. Connolly HM, Miller FA, Taylor CL, Naessens JM, Seward JB, Tajik AJ. Doppler hemodynamic profiles of 82 clinically and echocardiographically normal tricuspid valve prostheses. *Circulation* 1993;**88**:2722–7.
160. Kobayashi Y, Nagata S, Ohmori F, Eishi K, Nakano K, Miyatake K. Serial Doppler echocardiographic evaluation of bioprosthetic valves in the tricuspid position. *J Am Coll Cardiol* 1996;**27**:1693–7.
161. Blauwet LA, Miller FA. Echocardiographic assessment of prosthetic heart valves. *Prog Cardiovasc Dis* 2014;**57**:100–10.
162. Aoyagi S, Nishi Y, Kawara T, Oryoji A, Kosuga K, Ohishi K. Doppler echocardiographic evaluation of St. Jude Medical valves in the tricuspid position. *J Heart Valve Dis* 1993;**2**:279–86.
163. Blauwet LA, Danielson GK, Burkhart HM, Dearani JA, Malouf JF, Connolly HM *et al.* Comprehensive echocardiographic assessment of the hemodynamic parameters of 285 tricuspid valve bioprostheses early after implantation. *J Am Soc Echocardiogr* 2010;**23**:1045–59.
164. Gonzalez-Vilchez F, Zarauza J, Vazquez de Prada JA, Martín Durán R, Ruano J, Delgado C *et al.* Assessment of tricuspid regurgitation by Doppler color flow imaging: angiographic correlation. *Int J Cardiol* 1994;**44**:275–83.
165. Tribouilloy CM, Enriquez-Sarano M, Bailey KR, Tajik AJ, Seward JB. Quantification of tricuspid regurgitation by measuring the width of the vena contracta with Doppler color flow imaging: a clinical study. *J Am Coll Cardiol* 2000;**36**:472–8.
166. Nagueh SF, Kopelen HA, Zoghbi WA. Relation of mean right atrial pressure to echocardiographic and Doppler parameters of right atrial and right ventricular function. *Circulation* 1996;**93**:1160–9.
167. Ahmed MI, Escañuela MG, Crosland WA, McMahon WS, Alli OO, Nanda NC. Utility of live/real time three-dimensional transesophageal echocardiography in the assessment and percutaneous intervention of bioprosthetic pulmonary valve stenosis. *Echocardiography* 2014;**31**:531–3.
168. Rosti L, Murzi B, Colli AM, Festa P, Redaelli S, Havelova L *et al.* Mechanical valves in the pulmonary position: a reappraisal. *J Thorac Cardiovasc Surg* 1998;**115**:1074–9.
169. Waterbolk TW, Hoendermis ES, den HI, Ebels T. Pulmonary valve replacement with a mechanical prosthesis. Promising results of 28 procedures in patients with congenital heart disease. *Eur J Cardiothorac Surg* 2006;**30**:28–32.
170. Maciel BC, Simpson IA, Valdes-Cruz LM, Recusani F, Hoit B, Dalton N *et al.* Color flow Doppler mapping studies of 'physiologic' pulmonary and tricuspid regurgitation: evidence for true regurgitation as opposed to a valve closing volume. *J Am Soc Echocardiogr* 1991;**4**:589–97.
171. Kobayashi J, Nakano S, Matsuda H, Arisawa J, Kawashima Y. Quantitative evaluation of pulmonary regurgitation after repair of tetralogy of Fallot using real-time flow imaging system. *Jpn Circ J* 1989;**53**:721–7.
172. Williams RV, Minich LL, Shaddy RE, Pagotto LT, Tani LY. Comparison of Doppler echocardiography with angiography for determining the severity of pulmonary regurgitation. *Am J Cardiol* 2002;**89**:1438–41.
173. Puchalski MD, Askovich B, Sower CT, Williams RV, Minich LL, Tani LY. Pulmonary regurgitation: determining severity by echocardiography and magnetic resonance imaging. *Congenit Heart Dis* 2008;**3**:168–75.
174. Goldberg SJ, Allen HD. Quantitative assessment by Doppler echocardiography of pulmonary or aortic regurgitation. *Am J Cardiol* 1985;**56**:131–5.
175. Lei MH, Chen JJ, Ko YL, Cheng JJ, Kuan P, Lien WP. Reappraisal of quantitative evaluation of pulmonary regurgitation and estimation of pulmonary artery pressure by continuous wave Doppler echocardiography. *Cardiology* 1995;**86**:249–56.
176. Silversides CK, Veldtman GR, Crossin J, Merchant N, Webb GD, McGrindle BW *et al.* Pressure Halftime predicts hemodynamically significant pulmonary regurgitation in adult patients with repaired tetralogy of Fallot. *J Am Soc Echocardiogr* 2003;**16**:1057–62.